TECHNICAL MEMORANDUM ◦ NOVEMBER 2021

Analyses and Preliminary Modeling of Sediment Transport Following the Proposed Scott Dam Removal, Eel River, California

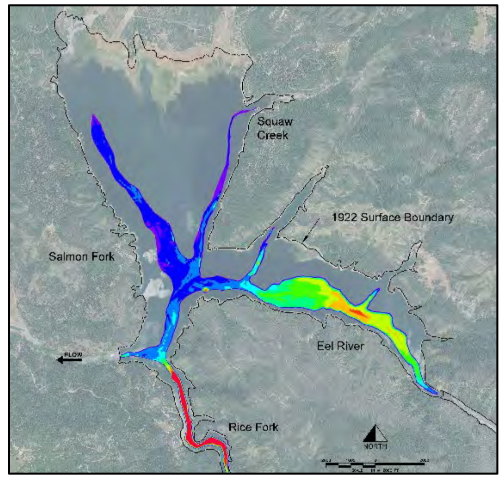

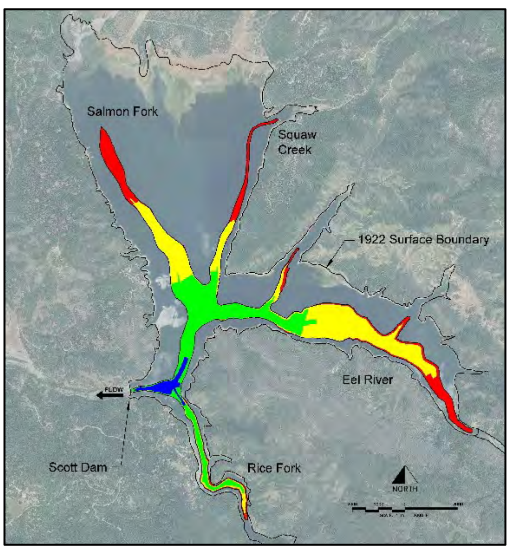

PREPARED FOR

Two-Basin Solution Partners
California Trout
Humboldt County
Mendocino County Inland Water and Power Commission
Round Valley Indian Tribes
Sonoma County Water Agency

PREPARED BY

Stillwater Sciences
850 G Street, Suite K
Arcata, CA 95521

Suggested citation:
Stillwater Sciences. 2021. Analyses and Preliminary Modeling of Sediment Transport Following the Proposed Scott Dam Removal, Eel River, California. Prepared for Two-Basin Solution Partners. November.

Cover photos (clockwise from top left): Scott Dam (credit: McBain Associates), Lake Pillsbury sediment deposit volume estimate (credit: McBain Associates), estimated Lake Pillsbury sediment volume exposure sequencing during four-phased dam removal alternative (credit: McBain Associates), sediment deposit in Lake Pillsbury observed during low water (credit: PG&E).

Table of Contents

Tables

Figures

Appendices

1 INTRODUCTION

1.1 Background

The Potter Valley Project (Project) is an inter-basin hydroelectric project located 15 miles northeast of Ukiah that annually diverts approximately 60,000 acre-feet (ac-ft) of water from the upper Eel River to the upper Russian River. Project features include Scott Dam, a 130-foot-tall concrete gravity dam that impounds Lake Pillsbury, a 2,300-acre storage reservoir; Cape Horn Dam that impounds the 106-acre Van Arsdale Reservoir; and a diversion system that diverts water from the Eel River at Van Arsdale Intake to the Project's powerhouse located in the headwaters of the Russian River watershed. The Project began diverting water in 1908 when Cape Horn Dam and the Van Arsdale Diversion were built. Scott Dam was built in 1921 approximately 12 miles upstream of Cape Horn Dam at river mile (RM) 168.5.

Pacific Gas and Electric Company's (PG&E's) Project license expires in 2022. PG&E filed a Pre-Application Document (PAD) and Notice of Intent (NOI) to formally initiate the relicensing process for the Project in April 2017. PG&E withdrew its NOI and PAD and discontinued its efforts to relicense the Project in January 2019, and in March 2019, the Federal Energy Regulatory Commission (FERC) issued a notice soliciting interested potential applicants other than PG&E to file an NOI and PAD. In May 2019, the Two-Basin Solution Partners (Partners) entered into a Planning Agreement to explore pathways to obtain a new license for the Project. In June 2019, the Partners filed a NOI with FERC stating the intent to undertake a Feasibility Study of a potential licensing proposal for the Project. The Feasibility Study examined the practicability of potential actions in meeting agreed upon common goals and to inform the Partners of cost and performance tradeoffs associated with those actions. Phase 1 of the Feasibility Study, completed and filed with FERC in May 2020, included the following key elements: (1) a Regional Entity that will apply for the new license and assume the new license if issued, (2) a Project Plan, (3) a Fisheries Restoration Plan, (4) an Application Study Plan, and (5) a Financial Plan. Phase 2 of the Feasibility Study was initiated in April 2020 with grant funding from the California Department of Fish and Wildlife to supplement technical analyses conducted during Phase 1, and to conduct new technical analyses.

This Technical Memorandum was prepared for the Partners by the Consultant Team to supplement technical analyses performed during Phase 1 of the Feasibility Study. The information provided in this document is a continuation of work along a path starting with preliminary analyses of feasibility, transitioning towards more refined analyses of a focused project plan and implementation of the best possible project that meets programmatic goals in a cost-effective manner. This Technical Memorandum is informational, is not binding of any of the Partners, and will not be filed with FERC as the basis for compliance under the Integrated License Process or other FERC regulations. While this Technical Memorandum contributes to the information available to the Partners, the Partners have not solely relied on this document for justification for any decision they have made or will make regarding FERC filings or cooperative agreements. More detailed environmental and engineering studies will be conducted during implementation of the FERC study and outside of the FERC process. Accordingly, this Technical Memorandum reflects a step that will be expanded and built upon through additional studies, analysis, synthesis, and ultimately decisions by the Partners on proceeding with a Project Plan.

1.2 Purpose

The potential removal of Scott Dam is being studied because it is the most feasible approach to provide upstream and downstream fish passage and restore anadromous fish access to the 289-square mile (mi^2) watershed upstream of the dam. Scott Dam impounds Lake Pillsbury (Figure 1) with a storage capacity of 94,400 acre-ft at the top of the spillway (i.e., 1,821.12 ft[1]) upon its completion in 1922 (PG&E 2017a). By 2015, the storage capacity of Lake Pillsbury was reduced to 76,876 acre-ft (McBain Associates and Princeton Hydro 2019) due to sedimentation. Although the change in storage capacity by 2015 implies a minimum[2] sediment deposition volume of 17,524 acre-ft, or 28.3 million cubic yards (CY), the most recent, more refined analyses that combined digital elevation model data and thalweg survey data estimate a sediment deposition volume of 13,016 acre-ft (21 million CY; Stillwater Sciences et al. 2021). An order-of-magnitude analysis by Stillwater Sciences (2021a) provided estimates of the magnitude and duration of high suspended sediment concentration due to erosion of fine sediment from the 21 million CY stored in Lake Pillsbury under two possible dam removal alternatives: (1) a four-stage dam removal alternative ("staged dam removal alternative") described in McBain Associates and Princeton Hydro (2019), and (2) a rapid sediment release dam removal alternative ("rapid dam removal alternative") using vertical notching or tunneling proposed in Stillwater Sciences (2021a); these alternatives are described in more detail in Stillwater Sciences (2021a). This technical memorandum provides analyses and modeling of coarse sediment transport following Scott Dam removal, focusing on the potential sediment deposition downstream of Scott Dam. The modeling results are preliminary in that they rely on currently available field data, which is incomplete. Additional field data collection such as reservoir coring to better understand characteristics of reservoir sediments is currently proposed. Once new data become available, evaluations will be performed to inform whether the modeling needs to be updated.

[1] NAVD88 datum throughout the document unless labeled otherwise. Add 78.78 ft to convert to Pacific Gas and Electric Company (PG&E) datum at Scott Dam site. Other related documents may also have used NGVD29 datum. Subtract 2.92 ft from NAVD88 elevation to obtain NGVD29 elevation at Scott Dam site.

[2] The sediment accumulation calculated by differencing storage values at different times is generally less than the actual amount of sediment accumulation because sediment deposition upstream of the storage area, which is generally a small fraction of the overall sediment deposition, is not accounted for.

Figure 1. Scott Dam and Lake Pillsbury, Eel River, California.

2 HYDROLOGY AND GEOMORPHOLOGY

The Eel River watershed has a catchment area of approximately 289 mi2 at the Scott Dam site encompassing two major sub-basins [i.e., Eel River (153 mi^2) and Rice Fork (96 mi^2)], and some smaller sub-basins (e.g., Salmon/Smokehouse Creeks, Squaw Valley Creek, and Horsepasture Gulch) (Figure 1). The maximum peak discharge recorded just downstream of Scott Dam was 56,300 cubic feet per second (cfs) on December 22, 1964 (Figure 2). The estimated 2-, 10-, 50-, and 100-year peak discharges at the same location for the post-dam-construction era are 10,600 cfs, 34,300 cfs, 52,900 cfs, and 59,200 cfs, respectively (Table 1 and Figure 2) (McMillen Jacobs Associates 2018).

Unimpaired annual maximum daily average discharges from the simulated unimpaired series between water year [WY] 1911 and WY 2017 (Addley et al. 2019) show that a daily average discharge of 1,000 cfs is exceeded almost every year (0.99 exceedance probability), and the exceedance probabilities for 2,000 cfs and 5,000 cfs daily average discharges are 0.98 and 0.86, respectively (Figure 3). The unimpaired 2-year annual maximum daily average discharge (0.5 exceedance probability) is slightly over 10,000 cfs (Figure 3).

Several tributaries enter the Eel River downstream of Scott Dam (Figure 1), increasing catchment area to 345 mi^2 at Cape Horn Dam (river mile [RM] 156.8) approximately 11.7 river miles downstream of Scott Dam. This constitutes an increase in catchment area of roughly 1.25% per river mile, or a total of 19% increase from Scott Dam to Cape Horn Dam. Catchment area continues to increase farther downstream, reaching 709 mi^2 just upstream of Middle Fork Eel River confluence at RM 119.4 and 1,463 mi^2 downstream of Middle Fork Eel River confluence (Figure 4).

Figure 5 shows the longitudinal profile of the Eel River between Scott Dam and Middle Fork Eel River confluence, showing three sub-reaches with distinctive average channel gradients upstream of Cape Horn Dam: a 2.5-mile reach immediately downstream of Scott Dam (0.33%), followed by a 4-mile sub-reach (0.80%), and a reach transitioning to an average slope of 0.18% slope approaching Cape Horn Dam. The relatively low channel gradient just upstream of Cape Horn Dam is apparently due to sediment deposition in Van Arsdale Reservoir. Van Arsdale Reservoir is completely filled with sediment, and sediment passes over Cape Horn Dam during high flow events, often resulting in sediment deposition in and impairment of the fish ladder located along the left bank of the river. Occasional mechanical sediment removal from Van Arsdale Reservoir is also needed in order to keep Van Arsdale Diversion functioning properly. The mid-section, with an average gradient of 0.8% is likely close to the channel gradient prior to the construction of Scott Dam. The sub-reach immediately downstream of Scott Dam likely has been degraded due to the trapping of sediment in Lake Pillsbury following dam closure. To what extent this reach has been degraded is unknown, but it has minimal importance in the analysis presented in this document. Between Cape Horn Dam and Middle Fork Eel River the channel has an average channel gradient of 0.29%, which is lower than the average channel gradient between Scott and Cape Horn Dams but higher than the short reach within Van Arsdale Reservoir.

The active channel of the Eel River downstream of Scott Dam is about 170 ft wide, narrows to about 100 ft between 5 and 11 RM downstream, then gradually widens to about 180 ft as the river enters Van Arsdale Reservoir (Figure 6). Active channel width generally varies between 100 and 250 ft downstream of Cape Horn Dam.

Table 1. Eel River typical annual peak discharge below Scott Dam (McMillen Jacobs Associates 2018).

Recurrence Interval (years)	Peak Discharge (cubic feet per second)
1.25	3,360
2	10,600
5	24,500
10	34,300
50	52,900
100	59,200

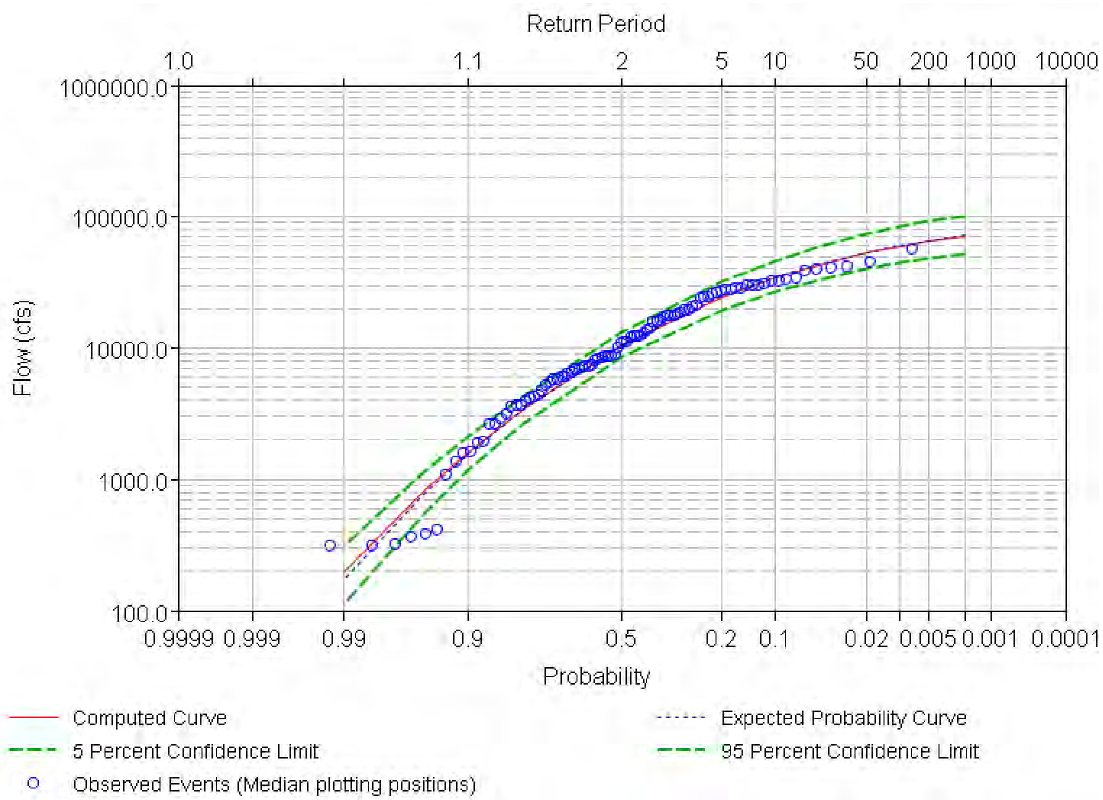

Figure 2. Eel River below Scott Dam peak discharge Log-Pearson type III fitting (McMillen Jacobs Associates 2018).

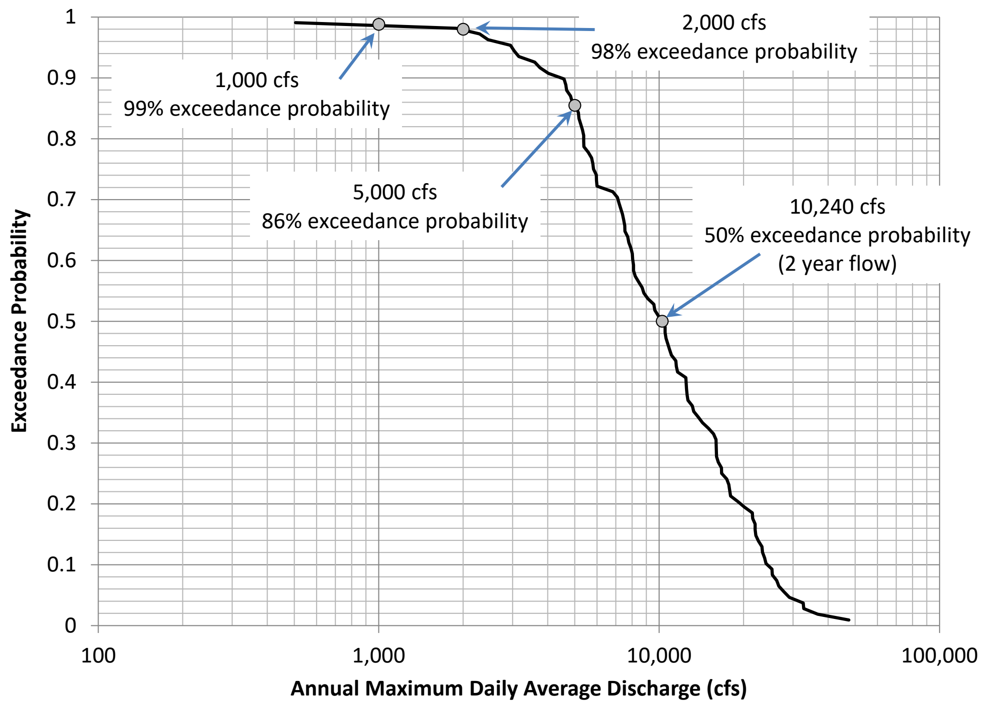

Figure 3. Eel River below Scott Dam flow duration curve based on estimated unimpaired daily average discharge between WY 1911 and 2017 (Addley et al., 2019). The 1,000 cfs, 2,000 cfs, and 5,000 cfs flows are the daily average discharges mentioned in Stillwater Sciences (2021a) as possible target flow for the rapid sediment release dam removal alternative using vertical notching.

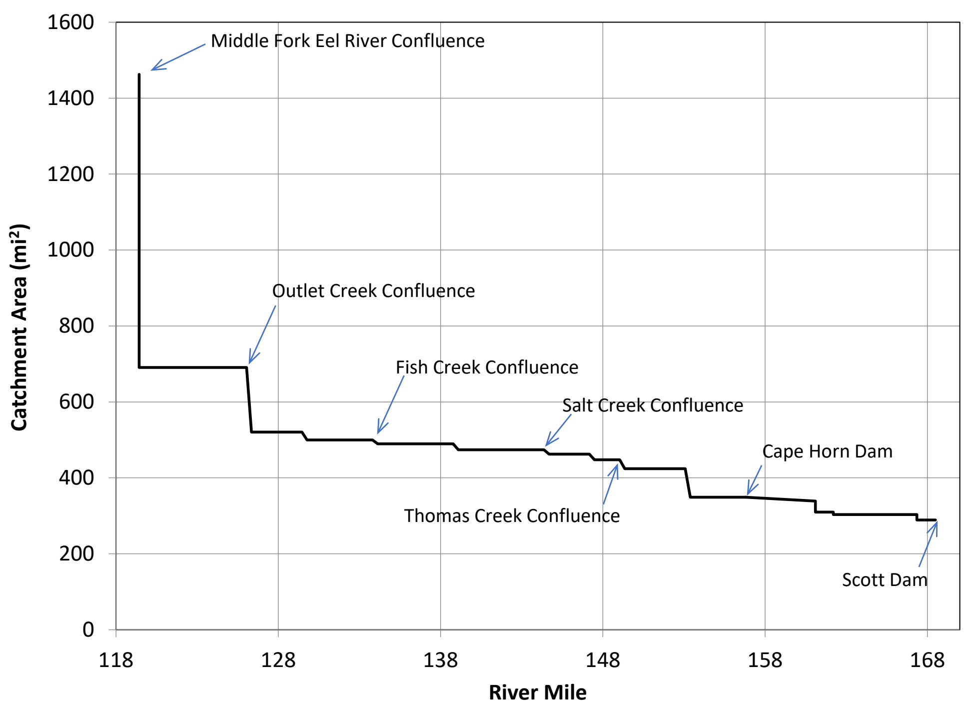

Figure 4. Catchment area of the Eel River between Scott Dam and Middle Fork Eel River confluence.

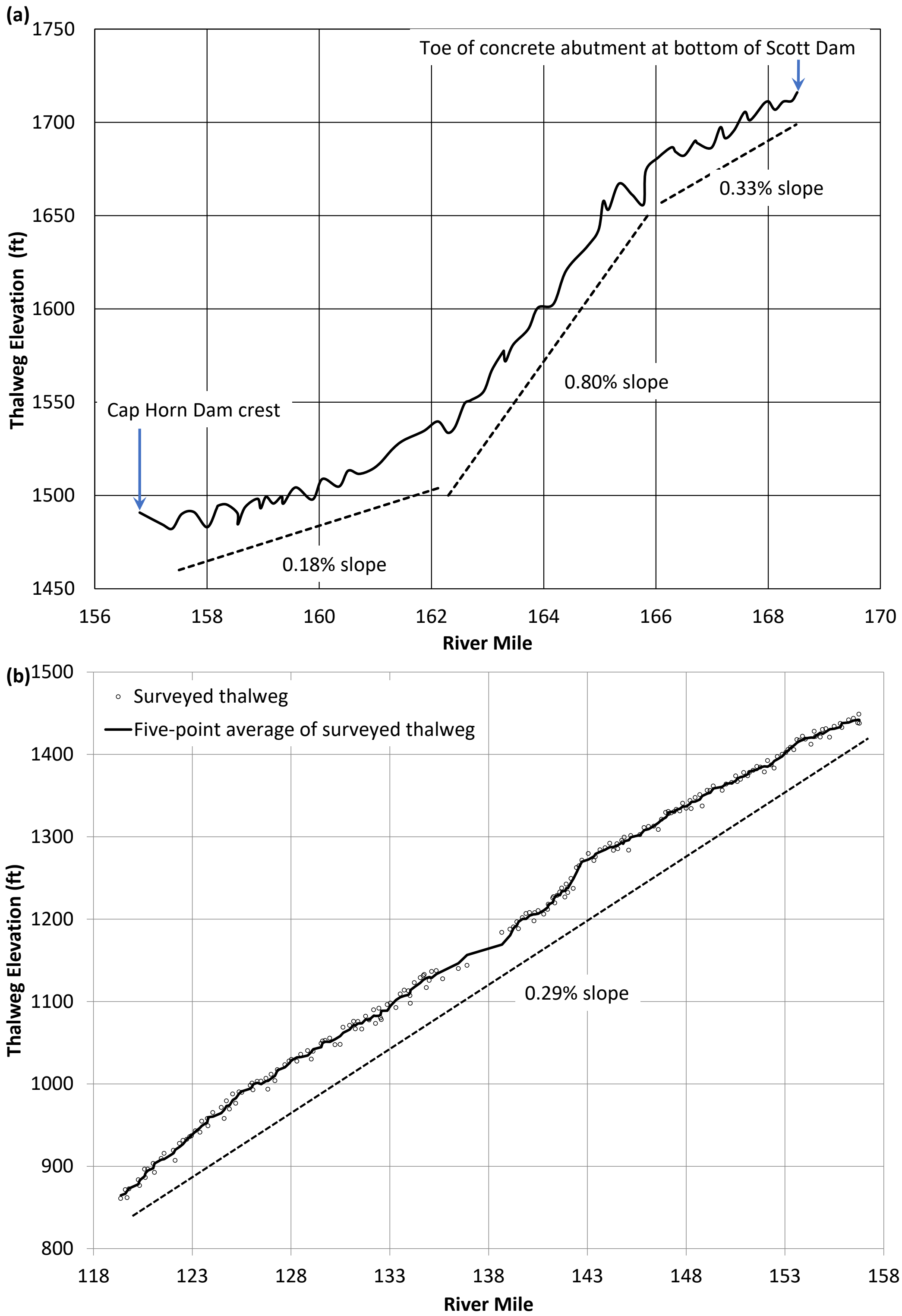

Figure 5. Longitudinal profile of the Eel River. (a) Between Scott and Cape Horn Dams; (b) between Cape Horn Dam and Middle Fork Eel River confluence. Profiles are based on cross section surveys performed by Stillwater Sciences in 2020-2021 (Stillwater Sciences 2021b.

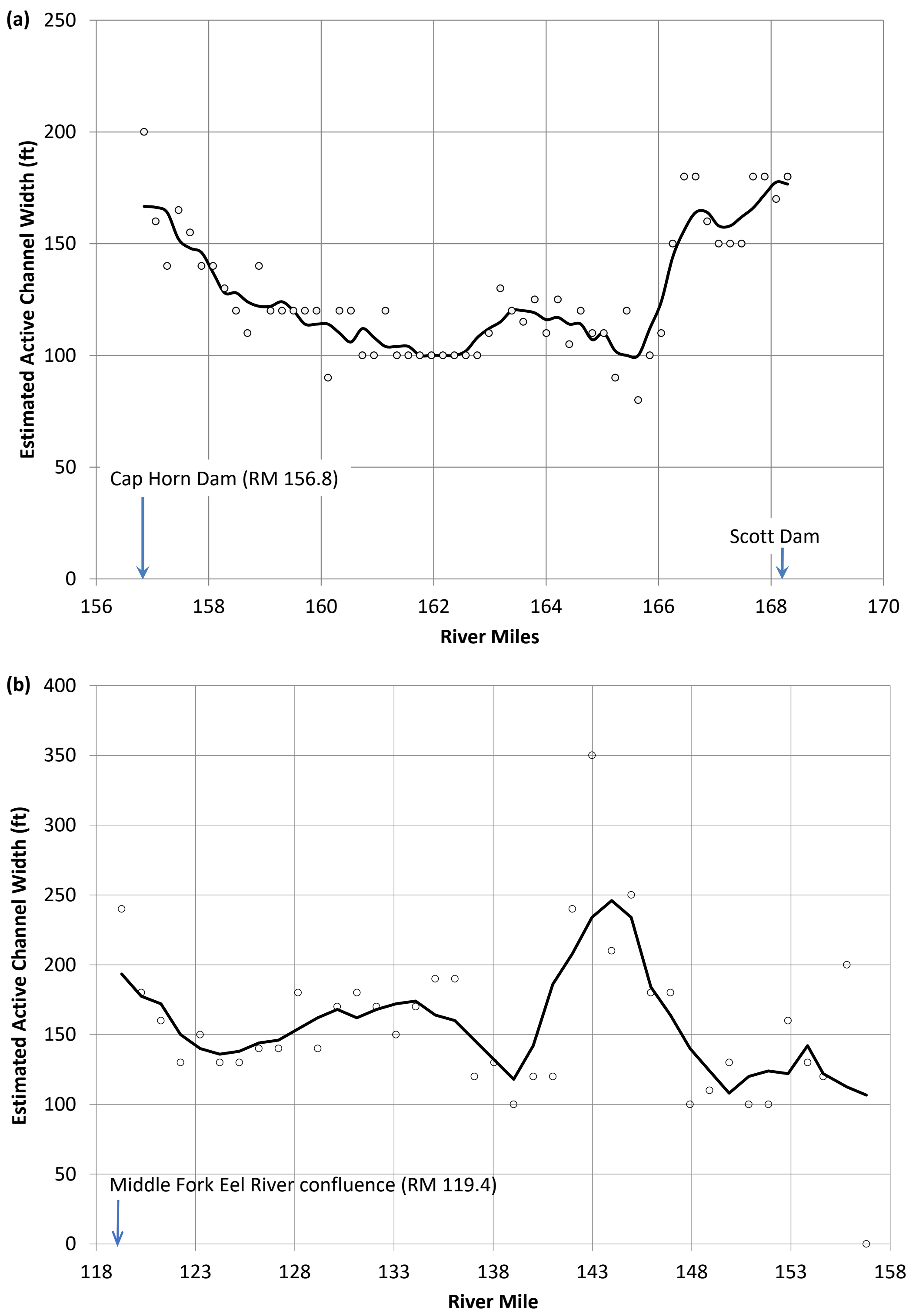

Figure 6. Active channel width of the Eel River (a) between Cape Horn and Scott Dams and (b) between Cape Horn Dam and Middle Fork Eel River. Symbols were estimated using the 2016 and 2017 aerial photos in Google Earth, the line is the 5-point average of the symbols.

3 LAKE PILLSBURY SEDIMENT DEPOSIT

Based on the most recent analyses, 21 million CY of sediment accumulated in Lake Pillsbury between 1922 and 2015, of which 12 million CY would be available for downstream fluvial transport following dam removal (Stillwater Sciences et al. 2021). Although sediment accumulation within Lake Pillsbury continued after 2015 and will continue until the dam is removed, we do not extrapolate sediment volumes past 2015, primarily because the additional deposit is relatively small and well within the expected accuracy of the analyses and modeling.

Two sources exist for grain size distribution of Lake Pillsbury deposit: United States Geological Survey (USGS) (1964) and Geosyntec (2020). Neither is comprehensive, and both sets of samples were collected from shallow cores in the inundated area, representing bottomset deposits. No reliable information of the volume and grain size distribution of topset deposits is available. The USGS (1964) data set includes 26 density samples collected with a calibrated density probe and 26 grain size samples collected with a split-core sampler suspended by boat-mounted streamflow-measuring equipment that likely penetrated only shallow depths into the deposits. The dry density (dry mass per bulk volume) of the USGS samples ranges between 1,096 and 2,349 pounds per cubic yard (lb/CY) (41–87 pounds per cubic feet [lb/ft^3]) with an average density of 1,590 lb/CY (59 lb/ft^3). The median grain size ranges between 0.0031 and 0.32 millimeter (mm) with a median value of 0.011 mm (Figure 7). Approximately 34% of the deposit is sand sized-particles (0.0625–2 mm), and the rest is primarily silt and clay (i.e., those finer than 0.0625 mm). The Geosyntec (2020) sampling does not provide dry-density and grain-size data, but the fractions of silt and clay data from the samples are consistent with the data provided in USGS (1964). With additional sediment sampling still in the planning stage, and under the assumption that sediment accumulation continues with the same-sized sediment, the dry density and grain-size distribution from USGS (1964) were used as input for the analyses and modeling. Future refinements/updates to the analyses and modeling may be required once new information on sediment grainsize characteristics for the reservoir deposit is available.

Figure 9 shows Lake Pillsbury profiles along the Eel River, Rice Fork, Salmon/Smokehouse Creeks, Squaw Valley Creek, and Horsepasture Gulch. The figure shows significant sediment deposition along the Eel River and Rice Fork and less sediment deposition along the other streams.

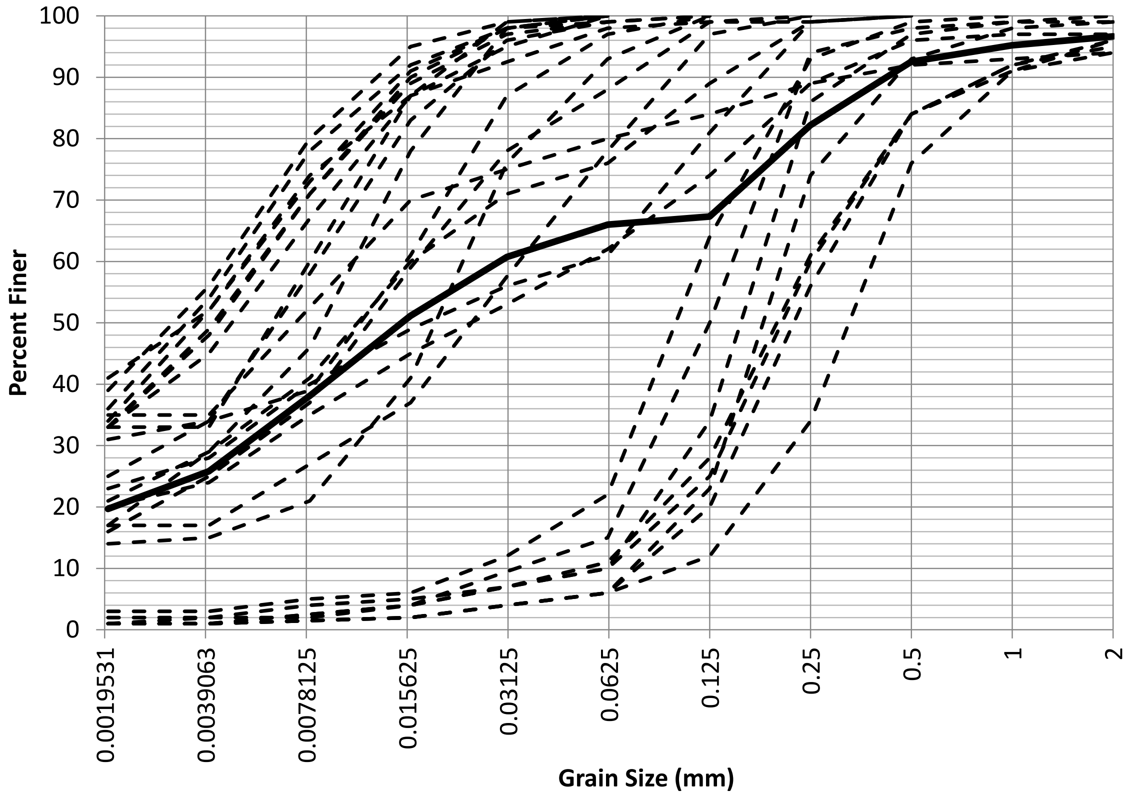

Figure 7. Grain size distributions of the USGS (1964) samples (dashed lines). The solid line is the average of all 26 samples.

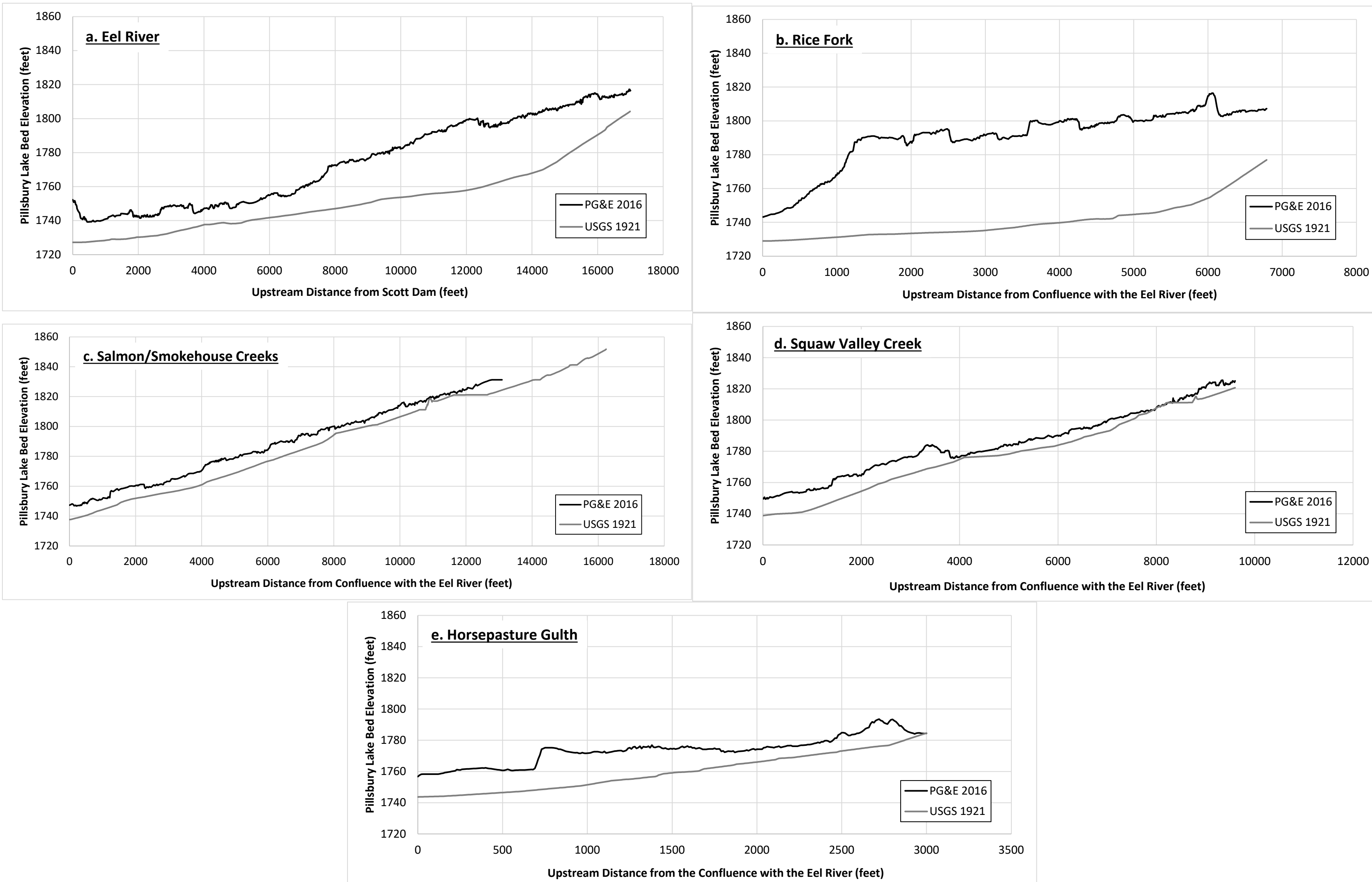

Figure 8. Lake Pillsbury profiles along a) Eel River; b) Rice Fork, c) Salmon/Smokehouse Creeks; d) Squaw Valley Creek; and e) Horsepasture Gulch.

4 METHOD OF ANALYSIS

Following the removal of a dam, the sediment deposit in the impoundment will be eroded and transported downstream as a sediment pulse (i.e., sediment wave) similar to that after the occurrence of a large-scale landslide. There have been extensive studies of sediment pulse evolution in rivers over the past 20^+ years (e.g., Benda and Dunne 1997; Lisle et al. 1997 & 2001; Sutherland et al. 2002; Cui et al. 2003a,b; Cui and Parker 2005) providing the scientific basis for predicting how the river would behave following the removal of a dam. In concert with the studies of evolution of sediment pulses in rivers, dam removal projects have provided not only valuable detailed field observations of sediment pulse movement but also have instigated the development and testing of numerical simulations of sediment transport following dam removal, further enhancing the knowledge base. Examples of past dam removal simulations include the removal of two dams on the Elwha River, Washington (BOR 1996, 2004, 2011), Marmot Dam on the Sandy River, Oregon (Stillwater Sciences 2000; Cui and Wilcox 2008; Cui et al. 2014), the Savage Rapids Dam on the Rogue River, Oregon (Bountry and Randle 2001; Bountry et al. 2013), the San Clemente Dam on the Carmel River, California (MEI 2003), four dams on the Klamath River, California and Oregon (proposed, Stillwater Sciences 2004, 2008; BOR 2011), the Englebright and Daguerre Point Dams on the Yuba River, CA (proposed, Stillwater Sciences 2013), the Simkins and Bloede Dams on the Patapsco River, MD (Cui et al. 2019), and the Matilija Dam on Matilija Creek, CA (proposed, BOR 2004; Stillwater Sciences 2019).

In this document, we fully utilize the knowledge obtained over the past two decades to paint a picture of the potential sediment transport dynamics following the removal of Scott Dam. We first evaluate conditions governing impoundment erosion and subsequent deposition downstream of the dam. Starting with a basic geomorphic understanding is vital to targeting the most important issues pertaining to dam removal, guiding how sediment modeling should be conducted, and evaluating the accuracy of model results. Agreement with professional evaluations would indicate high reliability of modeling results. Disagreement in certain aspects would suggest that either professional evaluation had missed certain factors or mistakes in modeling need to be corrected.

Modeling results, after cross checking with professional evaluations, will be used to estimate the general magnitude and duration of the impact from the release of impoundment sediment following dam removal.

5 SCOTT DAM REMOVAL ALTERNATIVES

There have been several preliminary dam removal alternatives developed to assess potential approaches to removing Scott Dam (e.g., McMillen Jacobs Associates 2018; McBain Associates and Princeton Hydro 2019; Stillwater Sciences 2021a) that vary in their approach to managing lake sediment deposits (e.g., mechanically removed, stabilized, or allowed to erode). This assessment focuses on two dam removal alternatives that would release sediment through natural erosion: 1) a staged sediment release dam removal alternative, in which sediment would be released during multiple seasons (McBain Associates and Princeton Hydro, 2019); and 2) a rapid sediment release dam removal alternative, in which sediment would be released during a single targeted high-flow event either through a vertical notch or through a tunnel (or tunnels) near the base of the dam (Stillwater Sciences 2021a).

For the rapid sediment release dam removal alternative, sediment transport dynamics would be similar for notching and tunneling with a minor difference if a high flow event exceeded the capacity of the tunnel(s). If that occurred, the tunnel would become pressurized, flattening the discharge capacity curve (i.e., the rate of increase in water discharge decreases with the increase in pool level) [3]. This would cause the pool level to rise quickly with the increase in discharge, which in turn, would reduce the rate of sediment erosion in the reservoir area. The differences in sand transport between vertical notching and tunneling are discussed in Section 6 and examined with numerical modeling in Section 7. It is assumed that the dam would ultimately be removed to the original configuration and allows the flow to pass the dam site unhindered as it did before dam construction in both the staged sediment release dam removal and rapid sediment release dam removal alternatives.

6 PROFESSIONAL EVALUATION OF SEDIMENT EROSION AND DEPOSITION FOLLOWING SCOTT DAM REMOVAL

A sediment pulse such as a reservoir deposit released following dam removal evolves primarily according to the grain size of the deposit. Silt and clay are transported downstream with minimal deposition once they become suspended. Sand and gravel pulses evolve through a combination of dispersion (i.e., the deposit becomes progressively thinner and longer) and translation (i.e., the apex of the deposit moves progressively upstream or downstream). Dispersion always dominates; translation only occurs if pulse sediment is significantly finer than the ambient bed material (e.g., Benda and Dunne 1997; Lisle et al. 1997, 2001; Cui et al. 2003a, 2003b, 2005; Cui and Parker 2005; Downs et al. 2009; Sklar et al. 2009). The anticipated evolution of Lake Pillsbury sediment deposits following Scott Dam removal is discussed below for silt and clay, sand, and gravel particles.

6.1 Silt and Clay Deposit

Stillwater Sciences (2021a) provides detailed analysis regarding the potential magnitude of fine suspended sediment concentrations (i.e., silt and clay) and the duration of high concentrations following Scott Dam removal under the staged and rapid sediment release alternatives. Their primary conclusions are briefly summarized below.

For the four-stage removal alternative, maximum suspended sediment concentrations can potentially reach 200,000 milligrams per liter (mg/L) for more than 100 days over at least a three-year period. For the rapid sediment release alternative using vertical notching or tunneling, suspended sediment concentrations can potentially reach between 458,000 and 900,000 mg/L assuming dam removal occurs prior to a high flow event with daily average discharge between 1,000 and 5,000 cfs. The duration of high suspended sediment concentrations would depend on the discharge following dam removal, ranging from less than a day at 5,000 cfs to close to eight days at 1,000 cfs. Most likely, the impact from high suspended sediment concentrations for vertical notching or tunneling would not last past a flood event, assuming an appropriate target flow for dam removal is selected and properly implemented.

Silt and clay will have minimal potential for deposition once eroded from the reservoir deposit and will be transported directly to the Eel River estuary.

[3] Discharge is proportional to hydraulic head to the 3/2 power in case of open-channel flow. Once pressurized, discharge becomes proportional to square root of hydraulic head, flattening the discharge – pool level curve.

6.2 Gravel Deposit

The Eel River is gravel-bedded, and thus a large gravel pulse can potentially result in long-lasting deposition (i.e., years). Past dam removal projects and the study of sediment pulse evolution, however, suggest that a gravel deposit would evolve primarily by dispersion with a limited range of impact (e.g., Lisle et al. 2001; Cui et al. 2003a, 2003b, 2005; Cui and Parker 2005; Cui and Wilcox 2008; Downs et al. 2009; Cui et al. 2014). Figure 9 illustrates how a gravel deposit that completely fills a reservoir would evolve following dam removal, showing that the deposit gradually spreads and "melts away" over time, resulting in minimal impact a certain distance away from the dam.

Perhaps the best case to illustrate how far downstream gravel can be deposited following dam removal is the Marmot Dam removal project on the Sandy River, Oregon. Marmot Dam impounded approximately 1 million CY of sediment within its reservoir area, among which about two thirds (roughly 860,000 ton, assuming a porosity of 0.4) was gravel and pebble sized sediment (Stillwater Sciences 2000; Cui and Wilcox 2008). Following the removal of Marmot Dam, primary gravel deposition occurred in a reach within approximately one river mile downstream of the dam, with minimal observable gravel deposition farther downstream (Major et al. 2012; Cui et al. 2014) (Figure 10).

There is inadequate information to reasonably evaluate the volume and grain size distribution of the gravel deposits in Lake Pillsbury because none of the USGS (1964) and Geosyntec (2020) samples were collected from the topset gravel deposits. Given that gravel deposits are likely concentrated more than one and two river miles upstream of Scott Dam in Rice Fork and Eel River[4] respectively, and the hydrology and geomorphology of Eel River and Sandy River are similar (Table 2), gravel deposition would most likely occur only in the river reach within the current Lake Pillsbury reservoir, and certainly not beyond the two-mile reach downstream of Scott Dam where the channel gradient is relatively low (Figure 11). Because of that, minimal gravel deposition is expected to occur within Van Arsdale Reservoir more than 10 river miles downstream of Scott Dam as a direct result of the erosion of the reservoir gravel deposits[5].

This expectation will be reevaluated once new coring data becomes available, but our expectation is unlikely to change based on our general understanding of sediment production in the basin. Gravel is usually only 5 to 10% of total sediment production, which is predominantly sand, silt, and clay, indicating that the gravel deposit in Lake Pillsbury is no more than approximately 2 million CY (or approximately 800,000–1,600,000 ton using the USGS [1964] average bulk density of 1,590 lb/CY). In comparison, this is at most less than twice the amount of gravel deposit in Marmot Dam impoundment (860,000 ton) prior to dam removal.

Minimal difference is expected in the evolution of gravel pulses between the staged and rapid removal alternatives because gravel transport is a long-term process not significantly affected by short-term actions.

[4] The exact locations of the gravel fronts within Lake Pillsbury are unknown at this point, but it is expected that all of them are located upstream of the profiles shown in Figure 8.

[5] In addition to the potential impact from the erosion of reservoir deposits, there is also potential impact from the re-establishment of sediment transport continuity at the Scott Dam site following dam removal. This aspect is discussed later in this section.

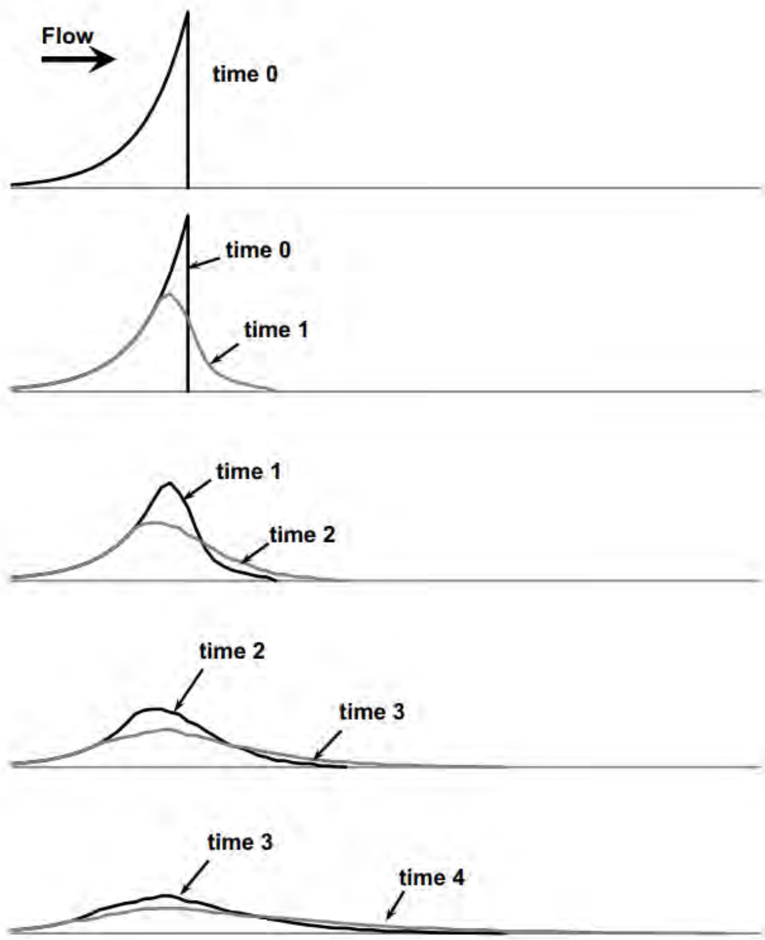

Figure 9. Idealized evolution of a reservoir sediment deposit following dam removal under conditions of constant slope and channel width, and where the deposit has a similar grain size to the downstream channel bed (Downs et al. 2009).

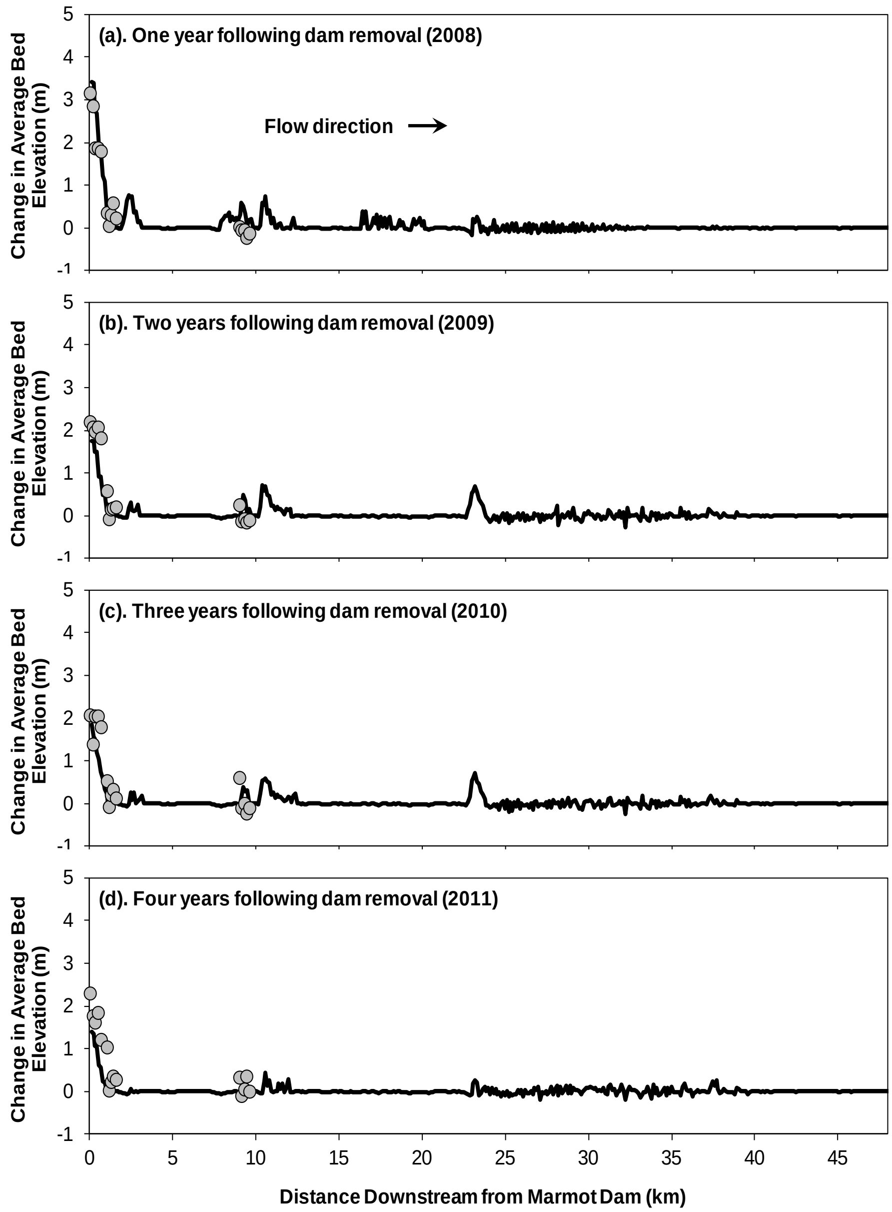

Figure 10. Sediment deposition in the Sandy River downstream of Marmot Dam following dam removal. Symbols are survey data, solid lines are the results of numerical simulation. No survey was conducted in the reaches outside the area with symbols, but casual observations did not reveal any visible sediment deposition. Figure adapted from Cui et al. (2014).

Table 2. Comparison of geomorphic and hydrologic factors affecting gravel deposition following dam removal: Scott Dam vs. Marmot Dam

Geomorphic and Hydrologic Factors	Marmot Dam, Sandy River, OR[1]	Scott Dam, Eel River, CA	Note
Channel gradient (S) and active channel width (B) d/s of dam	S = 0.008; B = 148 ft	S = 0.0033 immediately downstream of the dam, transitioning to 0.008; B = 150 – 180 ft	The slightly gentle slope and wider channel of the Eel River d/s Scott Dam encourages more gravel deposition immediately downstream of the dam, which in turn, reduces the amount of gravel deposition farther downstream.
Downstream bed material	Gravel/pebble	Gravel/pebble	Downstream ambient sediment is (or is expected to be) similar to gravel deposits upstream of the dams in both cases.
Location of sediment deposit	Gravel was filled to the top of the dam	Gravel deposits are more than 1 and 2 RM upstream of the dam for Rice Fork and Eel River, respectively	The extra distance between gravel deposits and the dam for Scott Dam removal provides additional attenuation for the gravel deposit, further reducing the amount of gravel deposition downstream of the dam.
Estimated 2- and 10-year peaks	15,000/28,000 cfs	≥ 10,600/34,300 cfs[b]	Both Sandy and Eel Rivers have large flow events on an annual basis to transport gravel downstream once the dams are removed.
Amount of gravel deposit, all is assumed to be available for transport following dam removal	~ 860,000 ton	Minimal to no more than 1,600,000 ton of gravel deposit.	The amount of gravel deposit for Scott Dam is minimal to no more than twice of that for Marmot Dam. However, most of the gravel deposition would likely occur upstream of Scott Dam because main sediment sources are in Rice Fork and Eel River deltas more than 1 and 2 river miles upstream of the dam, respectively.
Observations (Marmot Dam) or anticipations (Scott Dam)	Gravel deposit occurred within 1 mile downstream of Marmot Dam; minimal gravel deposit was observed farther downstream	Most of gravel deposition would occur upstream of Scott Dam (i.e., in the reach where it is currently occupied by fine sediment); minimal gravel deposition is expected downstream of Scott Dam.	Overall, minimal gravel deposition is expected to occur in the Eel River downstream from Scott Dam following Scott Dam removal.

1. Based on information provided in Stillwater Sciences (2000).
2. The impaired 2- and 10-year peaks are 10,600 cfs and 34,000 cfs at Scott Dam site. Unimpaired peaks are expected to be somewhat higher.

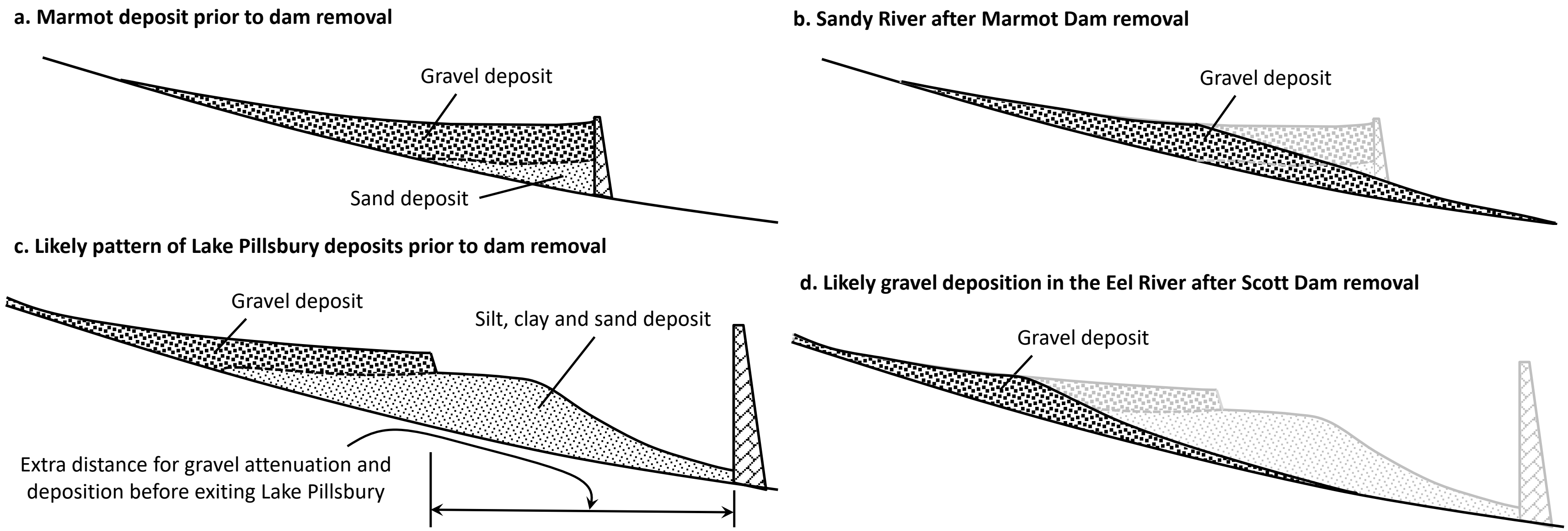

Figure 11. Comparison of sediment deposition patterns between Marmot Dam and Scott Dam. (a) Marmot deposit prior to dam removal, showing gravel deposit filled to the top of the dam; (b) Sandy River after Marmot Dam removal, showing the dispersion of gravel deposit that extends to downstream of the dam; (c) Lake Pillsbury deposit in any one of the forks prior to dam removal, showing gravel deposit is a distance upstream from the dam; and (d) likely gravel deposition in the Eel River and Rice Fork after Scott Dam removal, showing the dispersion of the gravel deposit that may or may not extend all the way to downstream of the dam. Sketches are for illustration purposes and are not to scale.

Apart from the impact of the release of the Lake Pillsbury gravel deposit, there will be long-term effects from re-establishment of sediment transport continuity at the Scott Dam site following dam removal. Out of the 345 mi^2 of catchment upstream of Cape Horn Dam, currently only 56 mi^2 is contributing gravel supply to Van Arsdale Reservoir while gravel production from the other 289 mi^2 catchment is trapped in Lake Pillsbury. The removal of Scott Dam means that the catchment area for gravel supply to Van Arsdale Reservoir will be increased to more than six times the current contributing area, most likely increasing gravel supply by about the same order of magnitude. Considering that there are already sediment management issues at Van Arsdale Reservoir and the water diversion facility and Cape Horn Dam fish ladder, there will certainly be more sediment management challenges ahead once Scott Dam is removed. Potential engineering solutions to the current and future sedimentation problems facing water diversion and fish ladder operation are being evaluated as part of the Feasibility Study Phase 2 (e.g., McMillen Jacobs Associates 2021a and 2021b), in addition to assessing changes in sediment supply (Stillwater Sciences 2021c). Additional modeling and engineering studies focusing on Van Arsdale Reservoir and diversion infrastructure as well as Cape Horn Dam will likely be required to develop solutions for addressing current and future sedimentation issues. Project relicensing study elements that would inform developing solutions for sedimentation issues include characterizing reservoir sediments, and 2-D morphodynamic modeling to estimate potential effects of sedimentation at Van Arsdale Diversion, potential effects on water supply reliability, and to inform improved upstream and downstream fish passage alternatives at Cape Horn Dam (Study AQ 12).

The impact of increased gravel supply after dam removal is expected to be minimal to the reaches outside of Van Arsdale Reservoir area: the steep channel gradient upstream of Van Arsdale Reservoir area (~0.8%) makes additional gravel deposition extremely unlikely, and the reach downstream of Van Arsdale Reservoir is likely outside of the reach of influence of Scott Dam and would be minimally affected by increased gravel supply following removal.

6.3 Sand Deposit

A sand pulse from a reservoir in a gravel-bedded river following dam removal behaves differently from a gravel pulse, as it may translate downstream as a somewhat coherent wave, although dispersion still always dominates (e.g., Lisle et al. 2001; Cui et al. 2003a, 2003b; Cui and Parker 2005). Figure 12 shows the evolution of a sand pulse over a gravel-bedded channel in a flume experiment, illustrating pulse dispersion and translation. Due to the translational behavior, a sand pulse can create a deeper deposit farther downstream following dam removal than a gravel pulse, which is more likely to spread without translation.

Evolution of a sediment pulse depends in part by how it is released, in this case, whether it is released rapidly (e.g., through vertical notching or tunneling) or in stages (e.g., four-stage dam removal). Differences in how these alternatives affect sand pulses from the reservoir can be anticipated using principles of sediment transport and fluvial geomorphology before resulting to numerical modeling. We expect that staged removal would result in prolonged sand deposition on a gravel-bedded channel surface and in the interstices of gravel downstream of Scott Dam compared to vertical notching. While this may seem counterintuitive, it is not difficult to explain:

First of all, we expect that staged removal would release more sediment downstream than rapid removal. In staged removal, the base level that controls lake level is lowered gradually, providing the river with more time (a minimum of 4 years) to meander or braid through the reservoir reach, laterally eroding more sediment as the river swings left and right. Rapid removal, on the other hand, would instantly drop the base level control to a level very close to the historical river bed, resulting in rapid down cutting of the reservoir deposits, and thus less opportunity and time for the river to meander/braid through the deposit. Because the project is located in a confined valley, this would allow the river to quickly settle back into its historical channel and become confined by the historical river banks, virtually terminating further channel meandering/braiding and leaving more sediment behind in the impoundment area as terrace or flood plain deposits.

Secondly, while the intuition is that a staged removal would release sediment in four batches over four seasons, resulting in only a portion of sediment released during each stage of dam removal, the majority, if not all of the sediment released during the early stages of dam removal would be silt and clay in suspension. Sand and coarser particles would be trapped behind the remainder of the dam until base level dropped below the level of deposits just behind the dam during the last stage of dam removal. As a result, staged removal provides less than expected reduction in the volume of sand released during the last stage of dam removal. That is, the perceived advantage for staged removal to spread out the release of sand and reduce downstream deposition is potentially much smaller than expected.

Thirdly and most importantly, dam removal and sediment release for the staged dam removal alternative would occur during the summer dry season, during which sand transport capacity is limited. As the height of the dam becomes sufficiently small during the last stages of removal, sand would start to be flushed from the reservoir area due to the ever increasing energy gradient within the impoundment area. During the summer months, however, flow would be too low to quickly transport the sand far downstream, causing it to deposit on the surface and in the interstices of the gravel river bed. Once settled, sand, especially sand deposited in the interstices of the gravel would not be flushed from the gravel bed until a high winter flow event. For rapid dam removal, sediment release is timed to target a high flow event, and the high energy during the event would be orders of magnitude more capable of transporting sand downstream than the summer low flow, resulting in a much shorter duration of sand deposition and a cleaner gravel bed afterward.

All three factors discussed above, as summarized in Table 3 below, either favor the rapid dam removal alternative or show minimal difference among the alternatives regarding downstream sand deposition. It is our pre-modeling expectation that the rapid dam removal alternative using vertical notching or tunneling will result in less impact from sand deposition than the staged dam removal alternative. Without modeling, and with the expectation that staged removal is not more cost effective than vertical notching or tunnelling due the requirement of multiple mobilization/demobilization, we are unable to find any factor that would favor the staged dam removal alternative regarding potential sand deposition downstream of Scott Dam following dam removal.

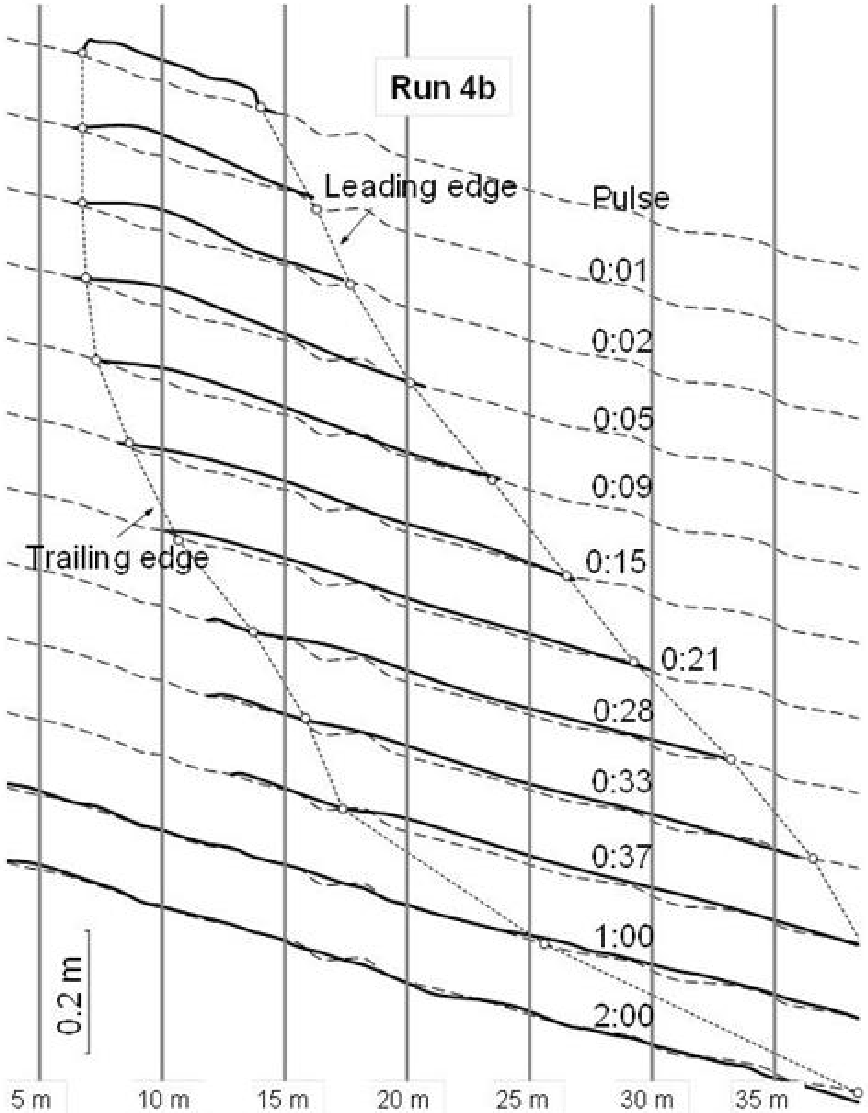

Figure 12. Observed longitudinal profiles of cross-sectionally averaged bed elevation for sand pulse evolution over a gravel-bedded channel. The times are in (hour:min). Figure adapted from Cui et al. (2003b).

Table 3. List of factors affecting downstream sand deposition for the staged and rapid dam removal alternatives

Factors	**Staged Dam Removal Alternative** (four-stage)	**Rapid Dam Removal Alternative** (vertical notching or tunneling)	**Comparison**
Channel meander/braid	More meander is expected, resulting in more sediment release.	Less meander is expected, resulting in less sediment release.	Vertical notching or tunneling preferred
One vs. four releases	Although sediment release will be divided into four batches, most, if not all the sand and coarser particles within the deposit will be released during the last stage of dam removal.	The entire sediment deposit is made available for erosion following dam removal.	Minimal difference
Hydraulics	Sediment release occurs during summer low flow months, a condition that encourages downstream sand deposition.	Sediment release occurs prior to a target large flow event, promoting rapid sand transport with less and shorter-term sand deposition.	Vertical notching or tunneling preferred

In the numerical examinations for sand transport presented below in Section 7, the first factor that favors vertical notching or tunneling discussed above and shown in Table 3 is not included in the modeling because the difference in the amount of sand erosion between alternatives cannot be reasonably quantified. The examination will focus on the difference in timing (i.e., summer flow vs. target high flow event), assuming both alternatives erode the same amount of sand. That is, modeling results for rapid removal using vertical notching or tunneling are likely more conservative (i.e., predict more deposition) than that for the staged removal alternative. Also, sand deposition in the interstices of the gravel river bed cannot be simulated in the numerical model (i.e., a simulated zero sand deposition does not mean there is no sand deposited in the gravel interstices), and we trust our professional evaluation that staged removal would result in more sand deposition in gravel interstices over a longer period of time regardless of modeling results.

There are likely some differences in sand transport and deposition between vertical notching and tunneling if the flood event following opening of the tunnel exceeds the design flow for the tunnel, forcing pressurized flow. Once pressurized, the discharge – pool level curve flattens, and the water surface in Lake Pillsbury would rise quickly with increasing inflow, which would slow down or even end sand erosion from Lake Pillsbury; efficient sand erosion would resume only after the flow receded to the point that open-channel flow in the tunnel resumed. This would present a significant disadvantage compared with vertical notching, in which erosion and transport of sand would occur during the entire flood event, potentially flushing sand from the river downstream by the time the flood receded. In the case of tunneling, little erosion would occur during peak flow, and would increase only after the peak had passed. The gradually decreasing discharge may be inadequate to flush sand from the river bed after the event. There is no doubt that vertical notching would perform better than or as well as tunneling in flushing sand regardless of whether water discharge following notch/tunnel opening exceeded design capacity for open channel flow. The degree to which the alternatives differ is examined with numerical simulation in Section 7 below.

7 SEDIMENT TRANSPORT MODELING

7.1 Selection of Sediment Transport Model

The DREAM-1 sediment transport model is selected to carry out the modeling exercise based on the available information: all of the Lake Pillsbury sediment deposit data are for sand and finer particles; there is no useful information regarding the volume and grain size distribution of gravel deposits. DREAM-1 is one of two Dam Removal Express Assessment Models (DREAM-1 and DREAM-2) (Cui et al. 2006a, 2006b) developed at Stillwater Sciences to simulate sediment transport after dam removal: DREAM-1 is suitable for the case where the reservoir deposit is primarily sand, and DREAM-2 is for simulation of gravel transport. The model has been examined extensively using laboratory experiments (e.g., Cui et al. 2003b; Cui et al. 2008) and found to be accurate with minimal calibration at least under laboratory settings. The model was also applied in several sedimentation projects such as the removal of Simkins and Bloede Dams on the Patapsco River, Maryland (Cui et al. 2019), the proposed removal of Soda Springs Dam on the North Umpqua River, Oregon, the proposed removal of Freeman Dam on Santa Clara River, California, and the proposed removal of Englebright Dam on the Yuba River, California. The results of DREAM-1 modeling for Simkins Dam removal project were found to be especially useful for stakeholders to make decisions in the planning stage of the project (Cui et al. 2019).

Similar to all one-dimensional sediment transport models, DREAM-1 provides modeling results that are accurate only on a reach-averaged basis and lacks the resolution for accurately depicting sediment transport characteristics at a finer scale such as sand deposition and erosion in a pool. As such, modeling results need to be interpreted by experienced professionals to extend to finer scales, if necessary. In addition, although there are many uncertainties affecting modeling accuracy, results become especially reliable when used to compare different alternatives under the same conditions (Cui et al. 2011).

7.2 Model Set Up and Simplification

Differentiating between USGS 1922 and PG&E 2015 digital terrain models, Stillwater Sciences et al. (2021) estimated that there is approximately 21 million CY of sediment in Pillsbury Lake, among which 12 million CY is available for erosion and transport once Scott Dam is removed.

Stillwater Sciences et al. (2021a) further estimated that the amount of sediment erosion from Salmon/Smokehouse Creeks, Squaw Valley Creek and Horsepasture Gulch is approximately 1,820,000 CY, or approximately 15% of the total volume for erosion following dam removal (i.e., 1,820,000/12,080,000 = 15%). Because of the relatively small amount of potential sediment erosion, we decided to simplify the modeling effort by ignoring these tributaries. This is compensated by slightly adjusting the sand fraction in the deposit (discussed below in Section 7.3) so that the total mass of sand available for erosion in the model is unaffected. The simplification should result in minimal differences in modeling results. Sensitivity tests of dam-removal simulations conducted by Cui et al. (2006b) indicate that the volume of reservoir sediment is not a sensitive parameter in modeling. The volume of eroded sediment is unaffected by this simplification, the only difference being where sediment is eroded and making the difference in sediment transport even smaller.

7.3 Input Parameters

Primary input parameters include a) longitudinal profile and active channel width downstream of the dam; b) pre-dam longitudinal profile upstream of the dam; c) thickness of sediment deposit upstream of the dam; d) grain-size distribution of the reservoir deposit; e) long-term average annual sand supply; and f) daily average water discharge during and after dam removal. These parameters are discussed briefly below:

7.3.1 Longitudinal Profile and Active Channel Width Downstream of Scott Dam

Longitudinal profile and channel width (Figure 5 and Figure 6 in Section 2) are smoothed by taking moving average values of channel elevation and width, respectively, and then interpolating into the computational nodes as model input. The reason for smoothing values is that DREAM-1 is a one-dimensional model, which is accurate only on a reach-averaged basis, and the smoothed values better represent reach-averaged properties.

7.3.2 Pre-Dam Longitudinal Profile and Thickness of Sediment Deposit Upstream of Scott Dam

The USGS 1921 profiles for the Eel River and Rice Fork (Figure 8a and b) are extended upstream of the surveyed reaches and interpolated to computational nodes to serve as pre-dam longitudinal profiles. The upstream extension is carried out by eyeballing to maintain the same channel gradient of the surveyed reach, the accuracy of which has a minimal effect on modeling results. The PG&E 2016 profiles are similarly extended upstream until they intersect the extended USGS 1921 profile. Thicknesses of the sediment deposit are then calculated by subtracting the USGS 1921 elevations from the PG&E 2016 elevations.

7.3.3 Grain Size Distribution of the Reservoir Deposit

DREAM-1 recognizes that the reservoir sediment deposit is usually stratified, with variations in grain size distributions both longitudinally and vertically. Given that such variations are not available in detail, we assumed that the grain-size distribution is uniform throughout the deposit and is represented by the average of the USGS (1964) samples (Figure 7). The format of the grain size input is a grain-size distribution of the sand-sized particles (normally defined as 0.0625 – 2 mm, but expanded here to up to 4 mm), plus the fraction of sand in the deposit.

Figure 13 below shows the average-grain size distribution of the USGS (1964) samples to be used as DREAM-1 input. The geometric mean grain size is 0.34 mm and the geometric standard deviation is 1.31. While the average grain-size distribution indicates that there is 34% sand in the deposit (Figure 7), this fraction cannot be used directly as model input because a large amount of organic matter that cannot be directly simulated in the model comprises much of the volume of the reservoir deposit. USGS (1964) data indicate that the average bulk density of the reservoir deposit is 1,590 lb/CY (dry weight over bulk volume), meaning that erosion of 1 CY of bulk sediment deposit would result in 541 lb (= 1590×0.34) of sand. In DREAM-1 model, however, sediment particles are given a solid density of 4,467 lb/CY (2,650 kg/m^3; dry weight over solid volume), which translates to a bulk density of 2,680 lb/CY by assuming a porosity of 0.4 for the deposit [i.e., 4467× (1-0.4) = 2680]. As a result, directly using 34% as the fraction of sand in the deposit would result in an over-prediction of sand mass erosion. Therefore, the fraction of sand in the deposit must be corrected to 20.2% (i.e., 1590/2680×34% = 20.2%). The sand fraction value is further adjusted to account for the 15% sediment deposits in Salmon/Smokehouse Creeks, Squaw Valley Creek and Horsepasture Gulch that are not accounted for in the model, resulting in a final value of sand fraction of 23.7% [i.e., 20.2%/(1-15%) = 23.7%] for DREAM-1 input.

7.3.4 Long-term Average Annual Sand Supply

There was an estimated 21 million CY of sediment deposited in Lake Pillsbury in 2015 (Stillwater Sciences et al. 2021) over the 93-year (WY1923 through 2015) dam operation. Using an average bulk density of 1,590 lb/CY and a sand fraction of 34% (USGS, 1964), the total sand deposit is estimated to be 5.7 million tons, which translates to a 61,000 ton/year long-term average sand production in the Eel River above Scott Dam. Assuming all upstream sand production is from the Eel River and Rice Fork sub-catchments, the value is distributed according to their respective catchment areas, resulting in 37,500 ton/year from the Eel River and 23,500 ton/year from the Rice Fork.

It is worthwhile to note that the long-term average annual sand supply is a relatively insensitive parameter in most DREAM-1 applications, mainly because the amount of upstream sand supply is negligible compared to the amount of sand in the reservoir deposit. As an input parameter to DREAM-1, the long-term average annual sand supply is important only if long-term sand deposition is expected (e.g., there are sand-bedded sub-reaches within the study reach, or reaches subject to seasonal sand deposition).

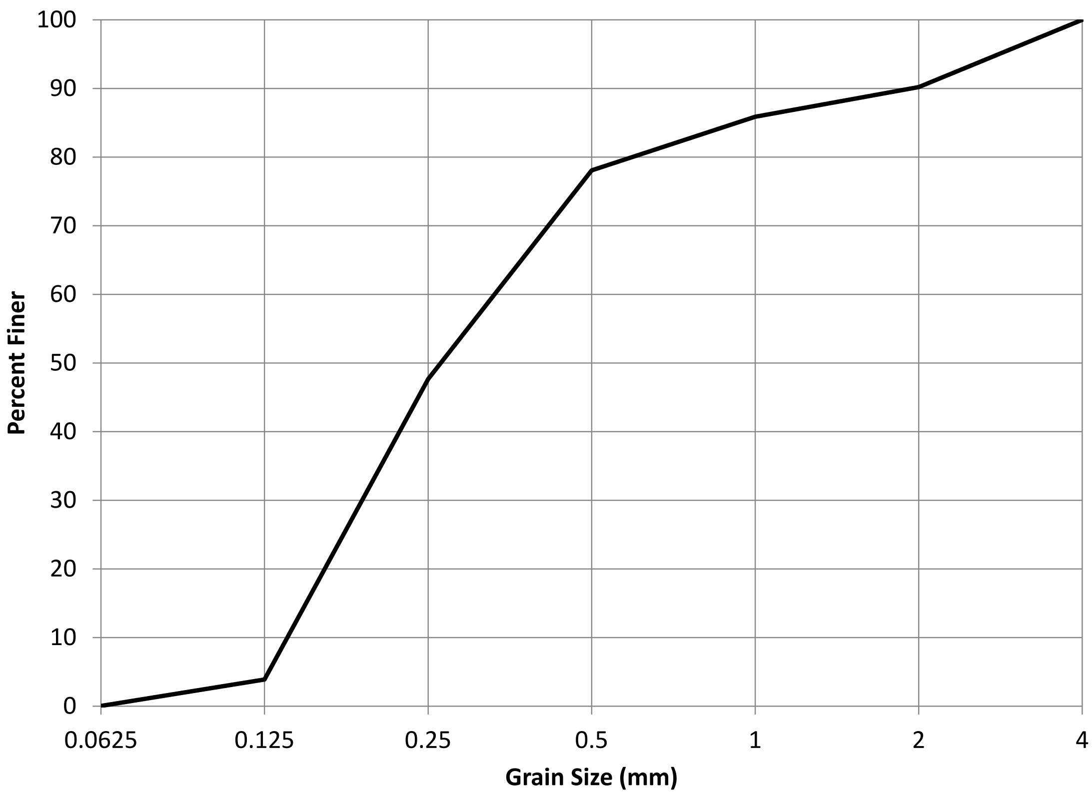

Figure 13. Average grain size distribution of USGS (1964) samples for particles coarser than 0.0625 millimeters (mm).

7.3.5 Daily Average Discharge During and After Dam Removal

The simulated unimpaired daily average water discharge flowing into Lake Pillsbury for WY 1911 through 2017 (Addley et al., 2019) is used to serve as model input for dam removal simulation because water discharge in the study reach will be unimpaired following Scott Dam removal. Post-Scott Dam (impaired) discharge recorded at USGS 11470500 (Eel River downstream of Scott Dam) is used for simulation of current conditions with Scott Dam in place.

For modeling purposes, three representative dates are selected to start dam removal for the rapid sediment release dam removal alternative using vertical notching or tunneling: January 3, 1995 with unimpaired daily average discharge of 329 cfs, followed with a 24,046 cfs flow a few days later in a wet year (approximately 10% exceedance probability); December 8, 2015 with unimpaired discharge of 487 cfs, followed with a 1,336 cfs flow five days later, a 3,957 cfs flow 15 days later, and a 10,204 cfs flow three months later in a median year (50% exceedance probability); and February 9, 1992 with unimpaired discharge of 162 cfs, followed with a 4,579 cfs discharge 10 days later in a dry year (approximately 90% exceedance probability). Each model run would last for at least six years starting from the date of dam removal. The plotting positions of these three annual maximum daily average flows are shown in Figure 14.

The stepped removal occurs over a 4-year span, thus it is not possible to select a starting date based on one peak discharge. As a result, we randomly selected 2009 to start the first stage of dam removal. The modeling for staged removal, however, starts on June 1, 2010 by assuming that the second stage starts on that day, and there is minimal sand released during the first stage.

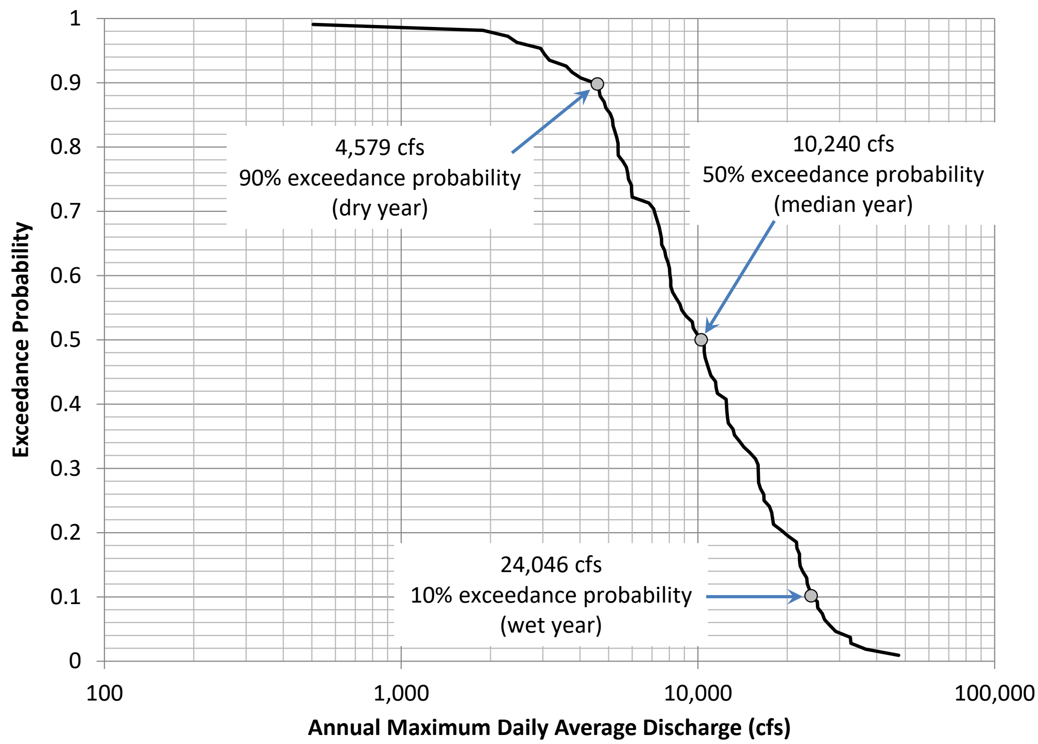

Figure 14. Plotting positions of unimpaired annual maximum daily average flow series into Lake Pillsbury.

The simulation for current and future condition would also start on June 1, 2010, using impaired and unimpaired discharge as model input, respectively.

7.4 Boundary Conditions and Assumptions

The study reach that includes Lake Pillsbury and the Eel River downstream to the Middle Fork Eel River confluence is simulated piece-wise. We first simulate the reach that includes Lake Pillsbury and Eel River down to Cape Horn Dam. We then simulate the Eel River between Cape Horn Dam and Middle Fork Eel River confluence using the output of the first set of modeling results as its upstream boundary condition. The reason for conducting the modeling in two pieces is that Cape Horn Dam provides a physical separation that allows for such division, and the two reaches need different assumptions for effective simulation.

7.4.1 Upstream of Cape Horn Dam

The upstream boundary is set at the Eel River 3.8 river miles upstream of Scott Dam and Rice Fork 2.1 river miles upstream of Scott Dam. The long-term average sand supply discussed in Section 7.3 and unimpaired daily average water discharge serve as the upstream boundary conditions. Water discharges in the Eel River and Rice Fork are assumed to be proportional to their respective catchment areas and summed to be the total inflow to Lake Pillsbury (i.e., flow from other minor tributaries are lump-summed to these two major tributaries). Flow and sediment contributions from tributaries between Scott Dam and Cape Horn Dam for dam removal runs are neglected for simplicity, because of their minor catchment areas.

The crest at Cape Horn Dam is the downstream boundary where bed elevation is fixed; water depth is set at slightly deeper-than-critical as depth is always transitioning through critical at this location.

An inner boundary condition is required at Scott Dam, because the remainder of which serves as a physical barrier between upstream and downstream reaches before the dam is completely removed. Water-surface elevation just upstream of the dam is obtained through reservoir flow routing using a combination of (1) inflow to Lake Pillsbury; (2) the Lake Pillsbury storage capacity curve; and (3) the discharge capacity curve of the outlet structures for the remainder of the dam. The Lake Pillsbury storage capacity curve was constructed using bathymetric data obtained by PG&E during their 2016 bathymetric survey (PG&E, 2017b), and discharge capacity curves for different dam removal alternatives are developed using assumed design parameters (Appendix A).

7.4.2 Cape Horn Dam to Middle Fork Eel River Confluence

The simulated daily sand transport rate at Cape Horn Dam serves as the upstream boundary condition for the modeling the reach between Cape Horn Dam and Middle Fork Eel River. The downstream boundary is assumed to have a constant bed elevation and normal water depth. A constant bed elevation at Middle Fork Eel River confluence implies that channel aggradation induced by dam removal would not reach this point, which is reasonable because a) Middle Fork Eel River confluence is 49.1 river miles downstream of Scott Dam, well beyond the primary influence of dam construction or removal, and b) Middle Fork Eel River is a large tributary with a catchment area of 754 mi^2, which is slightly larger than the Eel River catchment area at the confluence (709 mi^2).

Flow and sediment contributions from tributaries between Cape Horn Dam and Middle Fork Eel River assuming flow and sediment production are proportional to catchment area are included in the modeling (Appendix B).

7.5 Model Results

Rapid sediment release using vertical notching or tunneling was simulated under three hydrological conditions: sediment release during a wet year, during a median year, and during a dry year, as discussed in Section 7.3. A 20-ft wide notch is assumed for the vertical notching alternative, and three tunnel diameters are examined for the tunneling alternative: 10 ft, 12 ft, and 15 ft.

Staged dam removal and sediment release has a different schedule and cannot be compared with the rapid dam removal alternative using vertical notching and tunneling under the same hydrological conditions. Because of that, the water year to start dam removal for staged removal was selected randomly as discussed in Section 7.3. Only one run was conducted for the staged dam removal alternative, because sediment release would start to occur during the summer when water discharge does not vary significantly from year to year.

A total of 15 runs were conducted (Table 4). The runs are named using a combination of alternative name and the hydrological condition in the year dam removal started, making them easier to identify without the need to reference their definitions. For example, Run C and Run F are simulations of current (with Scott Dam in place) and future (with Scott Dam removed) conditions, Run S is the simulation of staged removal, Run N20(M) is the simulation of notching with 20-ft wide notch that starts during a median year, and Run T15(D) is the simulation of tunneling with a 15-ft tunnel diameter that starts during a dry year. Only selected model runs are presented below, as they are adequate to paint a full picture of patterns of sediment deposition downstream of Scott Dam. The full set of modeling results are provided in Appendix C for interested readers to examine and/or reference.

Table 4. List of model runs

Simulation (Dam Removal) Starts in		Wet Year	Median Year	Dry Year	Hand Picked[1]
Current condition		n/a	n/a	n/a	Run C
Staged dam removal	Four-stage	n/a	n/a	n/a	Run S
Rapid dam removal	20-ft notch	Run N20(W)	Run N20(M)	Run N20(D)	n/a
	10-ft tunnel	Run T10(W)	Run T10(M)	Run T10(D)	n/a
	12-ft tunnel	Run T12(W)	Run T12(M)	Run T12(D)	n/a
	15-ft tunnel	Run T15(W)	Run T15(M)	Run T15(D)	n/a
Future Condition		n/a	n/a	n/a	Run F

1 Runs C, S and F simulation starts on the same day, which was Jun 1 of a randomly selected year (2010).

7.5.1 Current Condition (Run C)

With Scott Dam in place under current conditions, sand contribution to the study reach comes from the tributaries downstream of Scott Dam. For simulation purposes and simplicity, the rate of sand supply is assumed to be proportional to catchment area as determined for the Eel River and Rice Fork catchments upstream of Scott Dam, resulting in a total average sand supply of 11,830 ton/year entering Van Arsdale Reservoir. Daily average water discharge for the four-year period starting June 1, 2010 at USGS #11470500 (Eel River below Scott Dam, i.e., the impaired discharge) is used as input to simulate current conditions, rather than the unimpaired discharge series that is used for all other runs (dam removed and future condition).

Run C continued for 10 years. Results for Run C (Figure 15) show minimal sand deposition throughout the study reach (Scott Dam to Middle Fork Eel River confluence) except in Van Arsdale Reservoir just upstream of RM 156.8. Under current conditions, sand is transported to Van Arsdale Reservoir and temporarily stored there during low-to-moderate flow, and is flushed during peak discharges. Reach-averaged sand deposition in Van Arsdale Reservoir is predicted to reach up to 6 inches (0.5 ft)[6] from time to time, and the amount of sand deposition is generally kept under 20,000 tons[7] almost all the time. Results for Run C are used as the base run to evaluate dam removal alternatives and future impacts.

6 Modeling results represent reach-averaged depth of sand deposition. A 6-inch reach-averaged sand deposition does not preclude several feet of deposition in local scour holes. The reach-averaged nature applies to all model results.

7 The periodic mechanical removal of sediment from Van Arsdale Reservoir is not included in the modeling exercise. In general, sand deposition following sediment removal should be greater than the modeled values because sediment removal creates deeper water where sand particles can settle more easily.

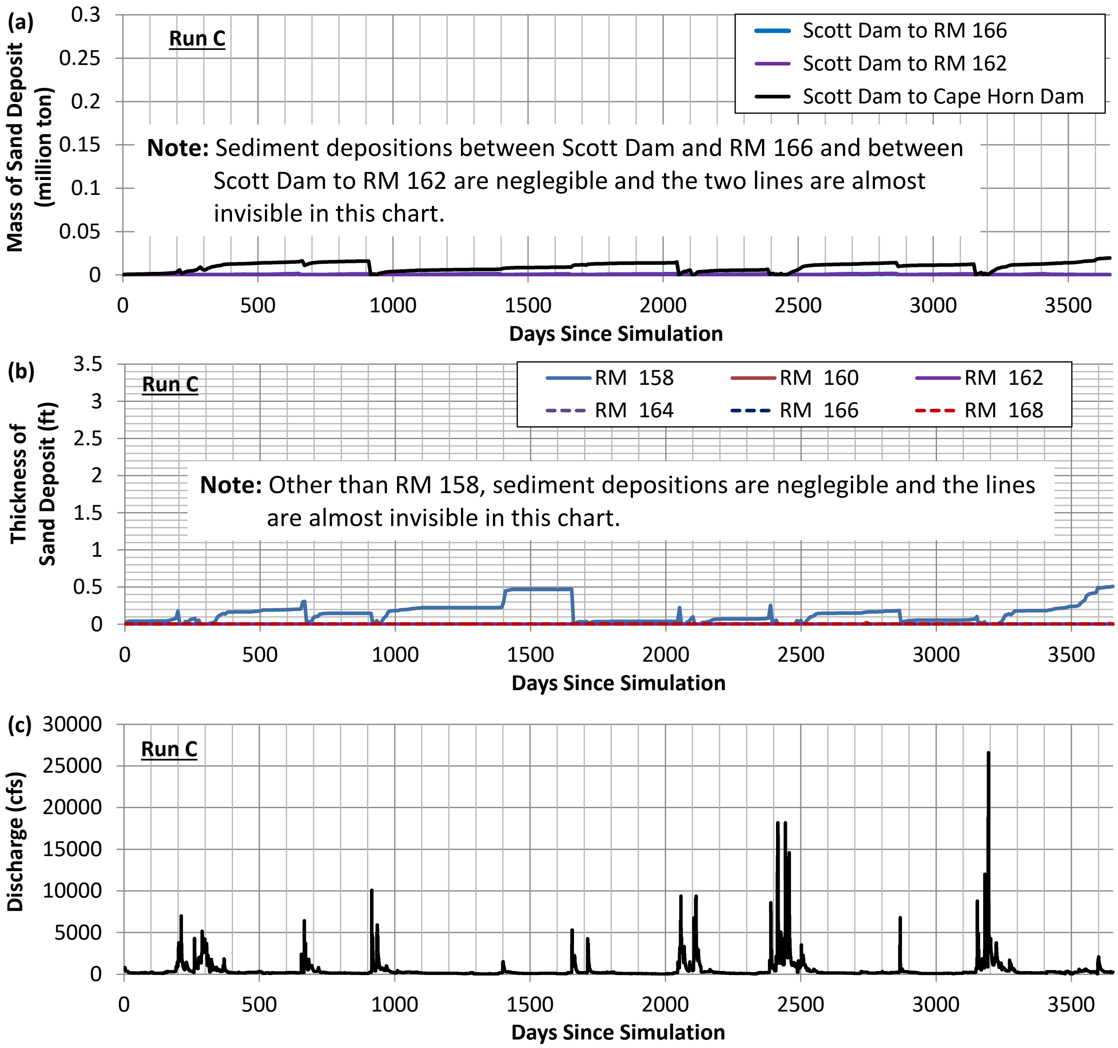

Figure 15. Simulated mass of sand deposition at selected reaches (a) and thickness of sand deposition at selected locations (b) under current conditions (i.e., with Scott Dam in place), and water discharge at Scott Dam site (c). Simulated sand deposition downstream of Cape Horn Dam is negligible and not presented.

7.5.2 Rapid Sediment Release Dam Removal Alternative

For both vertical notching and tunneling, it is assumed that the top section of the dam is removed to an elevation of 1781.22 ft prior to opening the notch or tunnel, and no erosion occurs during this process. Once the top of the dam is removed, explosives are detonated during a relatively low discharge just before a forecasted target high-flow event. The dam is assumed to be completely removed one full year after the opening of the notch or tunnel.

Below we simulate this procedure done in a median year as an example. Following the opening of the notch/tunnel at an inflow discharge of 487 cfs, Lake Pillsbury pool level drops quickly for all the alternative openings (Figure 16). Once the inflow increases during the storm events, however, pool level rises for all alternatives, with the notch causing the least rise, and the smallest tunnel (10-ft diameter) rising the most, as expected.

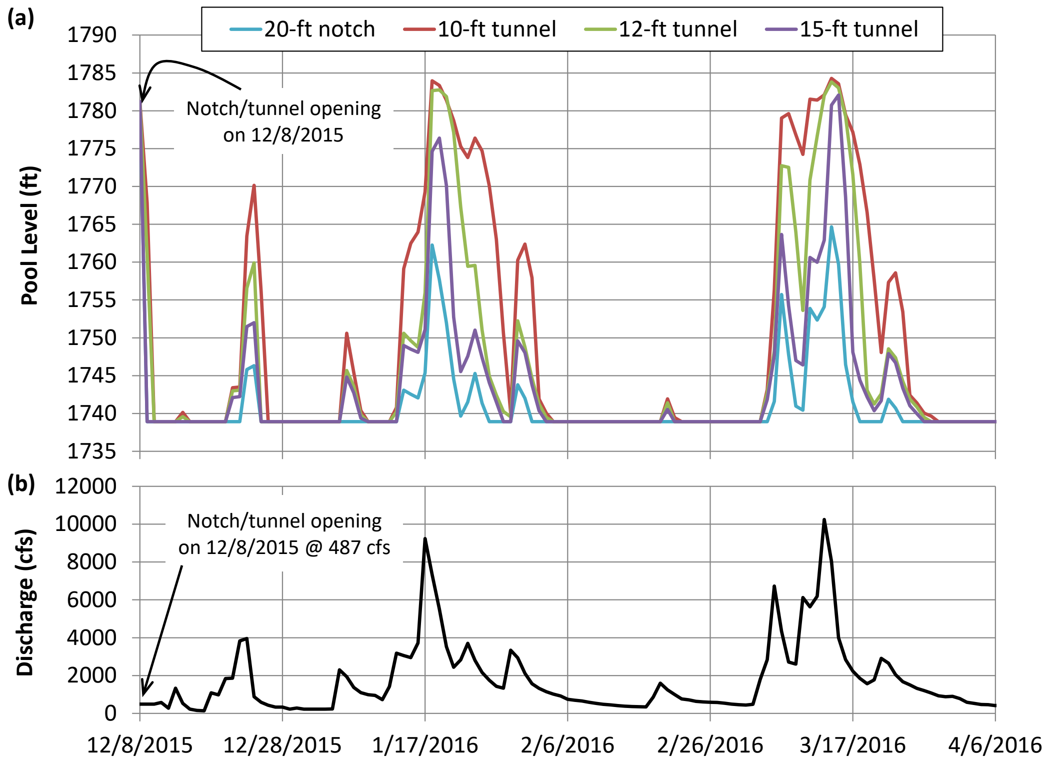

Figure 16. Simulated Lake Pillsbury pool level for rapid sediment release dam removal in a median year for notching and tunneling (a), and the water discharge (inflow to Lake Pillsbury) for the first five months after the opening of the notch/tunnel (b).

The consequence of different Lake Pillsbury pool levels is reflected in the rate of sediment erosion, as shown in the cumulative sand transport at Scott Dam (Figure 17). The 20-ft notch would cause the largest cumulative sand transport for wet, median, and dry years, while the 10-ft tunneling alternative would cause the least sand transport during the early days following dam removal, as expected in the pre-modeling analysis presented above in Section 6.

Note that there is some difference among the alternatives at the end of simulation for dam removal in median and dry years (Figure 17). Other than possible differences in the amount of sand left in Lake Pillsbury at the end of the simulation, cumulative errors in the simulation may have contributed to the differences, which is not a concern as it constitutes less than 10% of the total mass eroded, well within the generally acknowledge possible range of errors in such simulations.[8]

[8] The generally acknowledged accuracy of simulated sediment transport rate (mass per unit time) is within factors of 2 (i.e., one being 50% to 200% of the other) to 3 (i.e., one being 33% to 300% of the other). Channel aggradation and degradation, however, is not proportional to sediment transport rate but rather to the derivative of sediment transport rate over distance, making the simulated channel aggradation/degradation much more accurate than sediment transport rate.

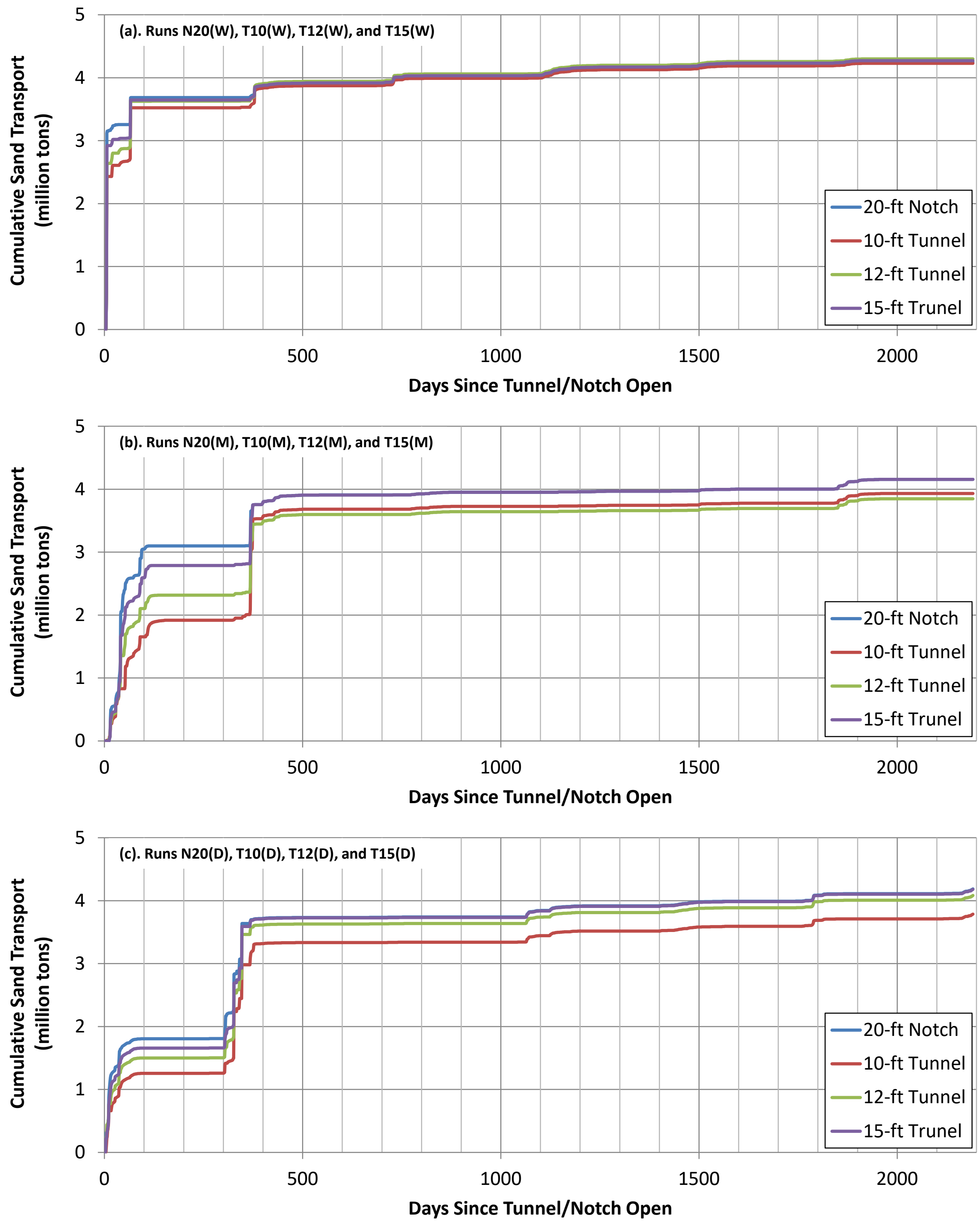

Figure 17. Simulated cumulative sand transport at Scott Dam for rapid sediment release dam removal alternative using vertical notching or tunneling starting in (a) wet year, (b) median year, and (c) dry year.

With the lowering of Lake Pillsbury pool level following the opening of the notch or tunnel, the lake deposit is eroded, and sand is deposited downstream of Scott Dam (Figure 18 and Appendix C). Note in Appendix C that some bed profiles upstream of Scott Dam show oscillation, which results from numerical instability due to the inclusion of two arms of the Eel River (i.e., the Eel

River and Rice Fork) that we were unable to completely eliminate. The oscillation is only for a short period of time in the simulation and does not introduce errors in mass conservation because no numerical viscous terms were introduced to dampen the oscillation, as is often done to deal with numerical instabilities.

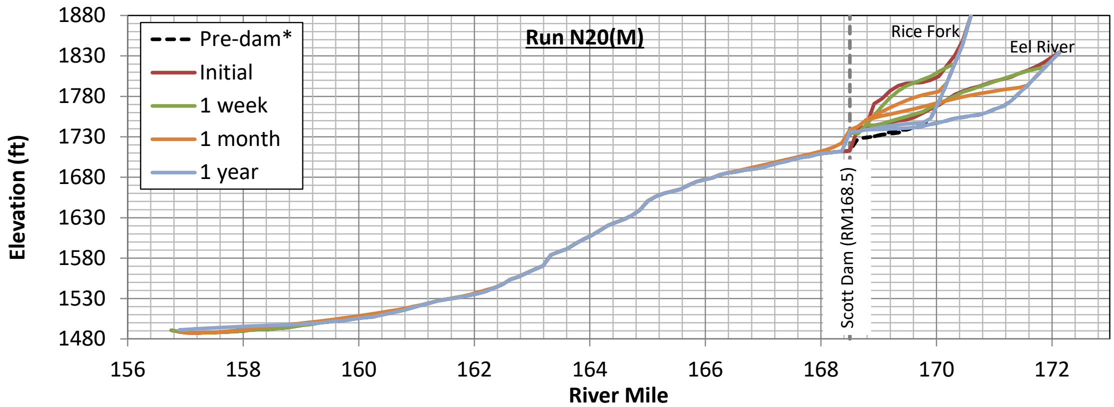

Figure 18. Simulated bed profiles at various times following Scott Dam removal. Temporal variations that are not apparent at this scale are shown in other diagrams below.

Sand deposition downstream of Scott Dam is seen primarily within Van Arsdale Reservoir (RM 162 to Cape Horn Dam, Figure 19). In the reach immediately downstream of Scott Dam, up to 5 ft of sand would be deposited only during the early days following dam removal and would vanish quickly. Otherwise, minimal deposition would occur upstream of Van Arsdale Reservoir (i.e., Scott Dam to RM 162).

Simulated sand deposition between Scott and Cape Horn Dams for rapid dam removal using vertical notching and tunneling (Figure 20) varies among model runs in response to variations in discharge in the Eel River. Most sand deposition would occur within Van Arsdale Reservoir between RM 162 and Cape Horn Dam, and only a small amount would settle upstream of RM 162. Considering the stochastic nature of hydrology, it is interesting to note that results in Figure 20 do not show a clear advantage for one alternative over the others in terms of the total amount of deposition. For example, the notching alternative, which would cause the lowest Lake Pillsbury pool level and fastest erosion of reservoir sediment following dam removal, would produce high sand deposition during the early days in the first year in median and dry years but low deposition during a wet year or during the second year in median and dry years. In either case, sand would nearly vanish after roughly a 20,000-cfs event (daily average flow), which occurs approximately every 5 years (exceedance probability = 0.2) (Figure 14). Additional sand deposition would still occur after a 20,000 cfs event as continuity in sand transport coming from upstream of the former reservoir is re-established (discussed below in Section 7.5.4).

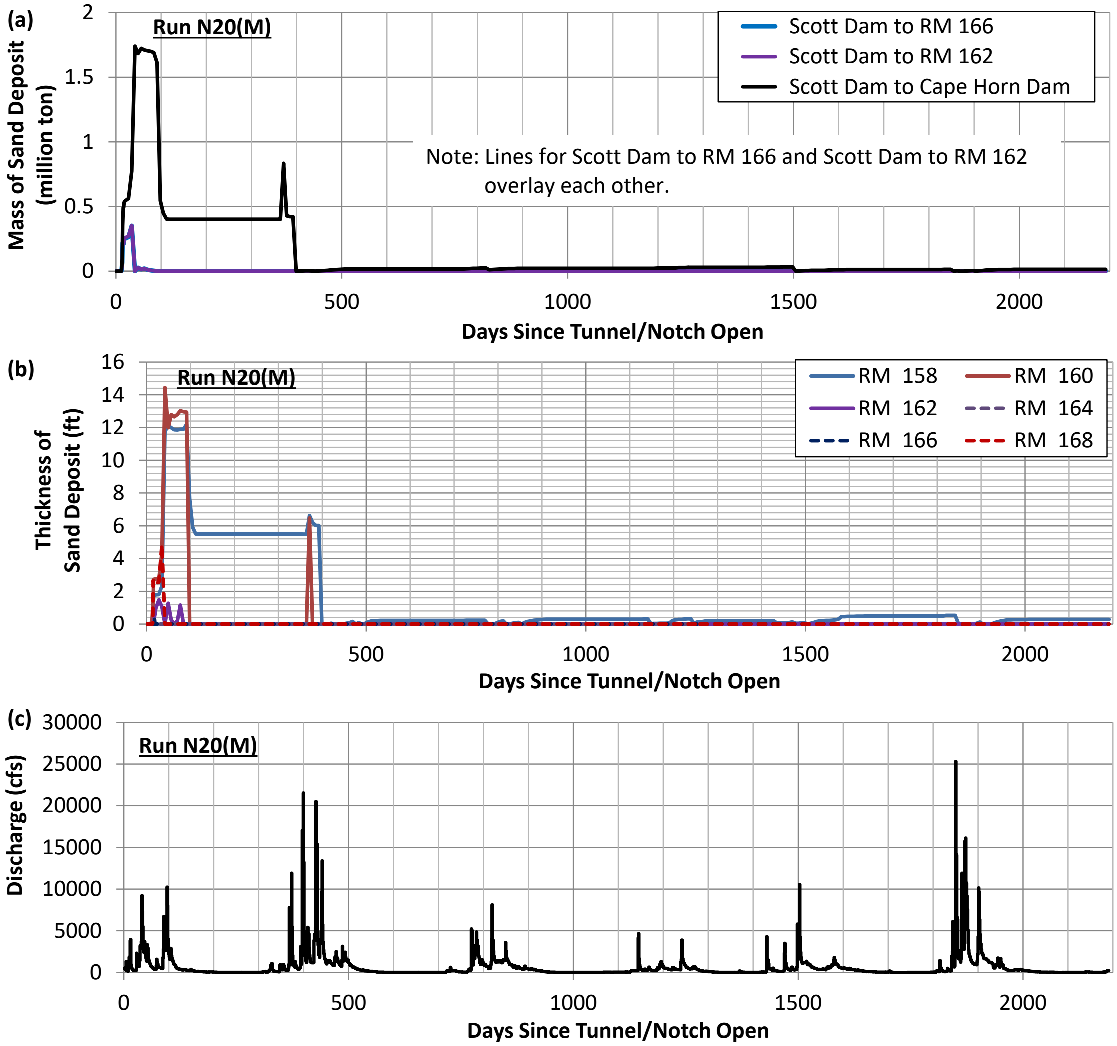

Figure 19. Simulated mass of sand deposition in selected reaches upstream of Cape Horn Dam (a) and thickness of sand deposition in selected locations upstream of Cape Horn Dam (b), along with water discharge at Scott Dam for reference (c), Run N20(M).

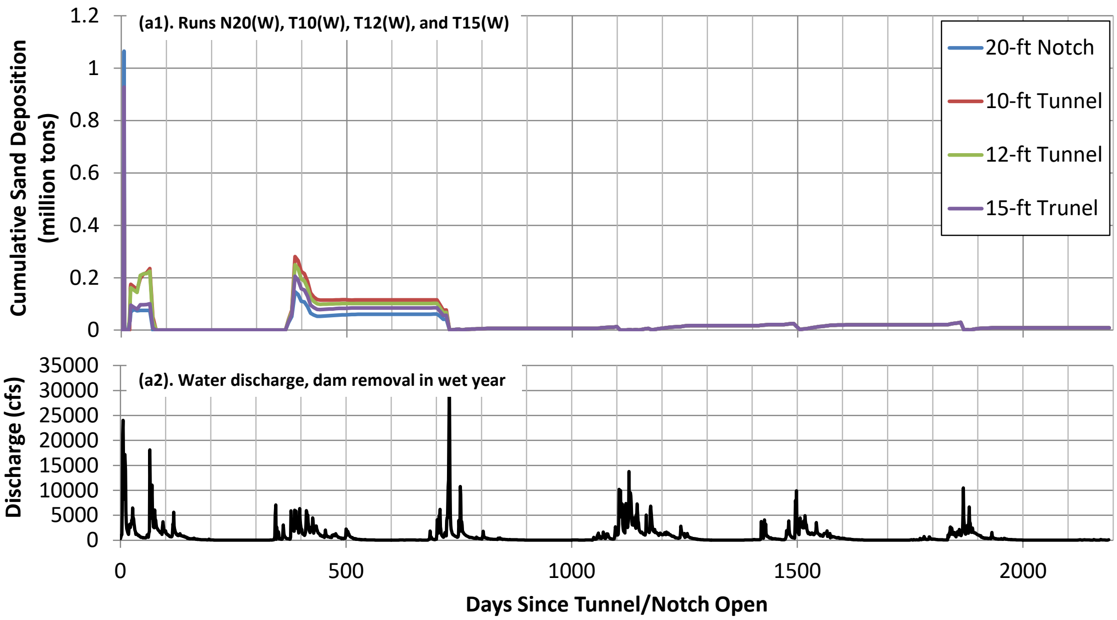

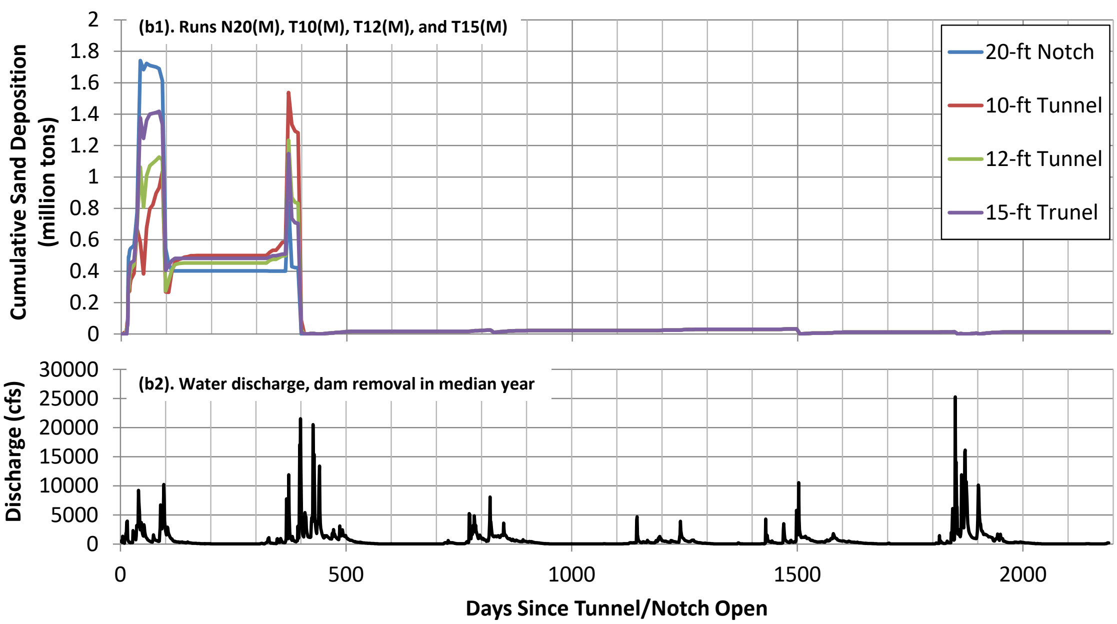

Figure 20 continues on the next page

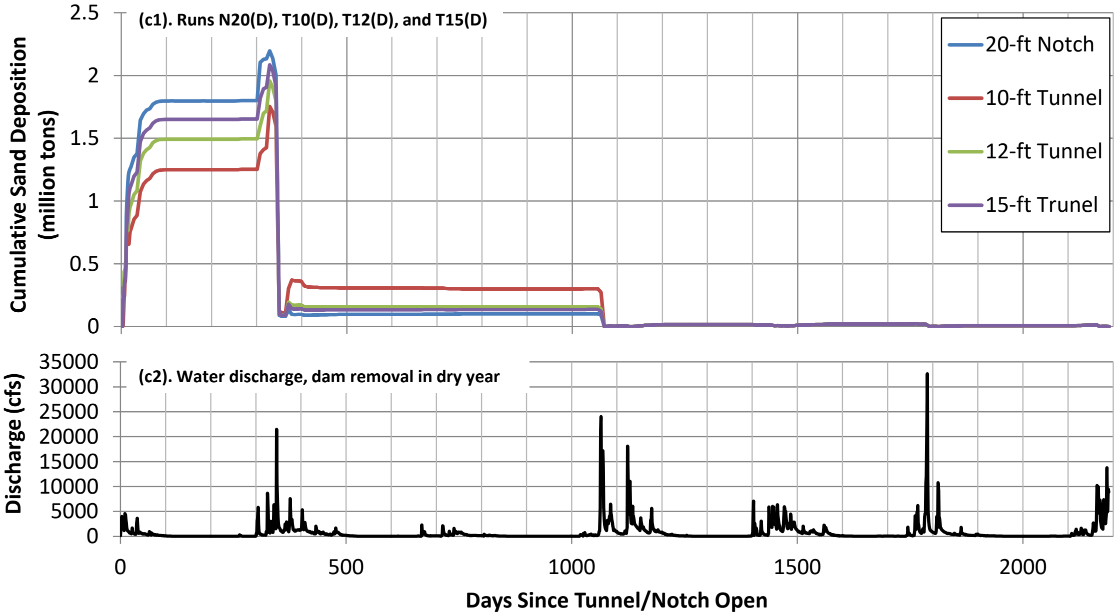

Figure 20. Simulated cumulative sand deposition between Scott and Cape Horn Dams for rapid dam removal alternative using vertical notching or tunneling starting in (a1) a wet year, (b1) a median year, and (c1) a dry year. Water discharges used for simulation are provided in (a2), (b2) and (c2) for reference.

If the small amount of sand deposition in the reach between Scott Dam and RM 162 (i.e., upstream of Van Arsdale Reservoir) is of concern for spawning and rearing habitat, vertical notching or a larger tunnel diameter appear to be more advantageous in reducing the amount and duration of sand deposition as demonstrated for the cases of dam removal in a median year (Figure 21).

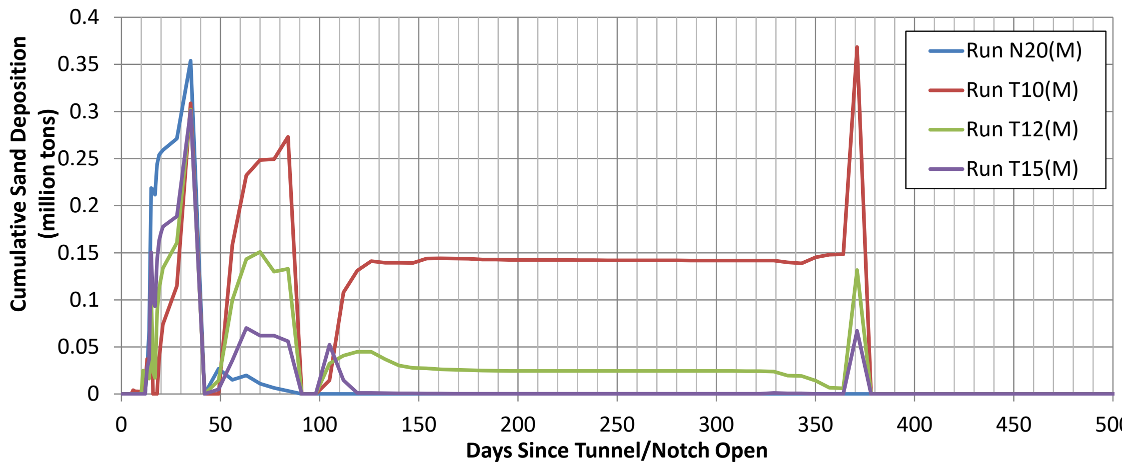

Figure 21. Simulated cumulative sand deposition between Scott Dam and RM 162 (i.e., upstream of Van Arsdale Reservoir) for rapid dam removal alternative using vertical notching or tunneling, Runs N20(M), T10(M), T12(M), and T15(M).

A small amount of transitory sand deposition is predicted in the 37-mile reach between Cape Horn Dam and the Middle Fork Eel River confluence, with a maximum value of 1 million tons that occurred for the 20-ft notch alternative in a dry year during a 21,486 cfs discharge (daily average discharge at Scott Dam site) on day 247 following dam removal (Table 5). Simulated maximum thickness of sand deposition is approximately 4 ft (Figure 22), but this occurs only once and rises and recedes quickly with the prominent deposition lasting only a single day (Table 5). Moreover, deposition is nonuniform with many reaches showing insignificant deposition.

Table 5. Simulated maximum sand deposition in the 37-river-mile reach between Cape Horn Dam and Middle Eel River confluence, in million tons. The values within the parentheses are the amount of sand deposition on the day that follows the occurrence of maximum sand deposition.

	Wet	Median	Dry
20-ft Notch	0.89 (0.08)	0.24 (0.18)	1.00 (0.64)
10-ft Tunnel	0.62 (0.03)	0.27 (0.19)	0.54 (0.22)
12-ft Tunnel	0.70 (0.03)	0.16 (0.13)	0.92 (0.56)
15-ft Tunnel	0.81 (0.06)	0.15 (0.12)	0.99 (0.63)
Discharge when maximum deposition occurred[1]	21,244 cfs	10,242 cfs [2]	21,486 cfs

1. Daily average discharge at Scott Dam site
2. For Run T12(M), deposition during the day of 11,918 cfs is slightly higher than during the day of 10,242 cfs.

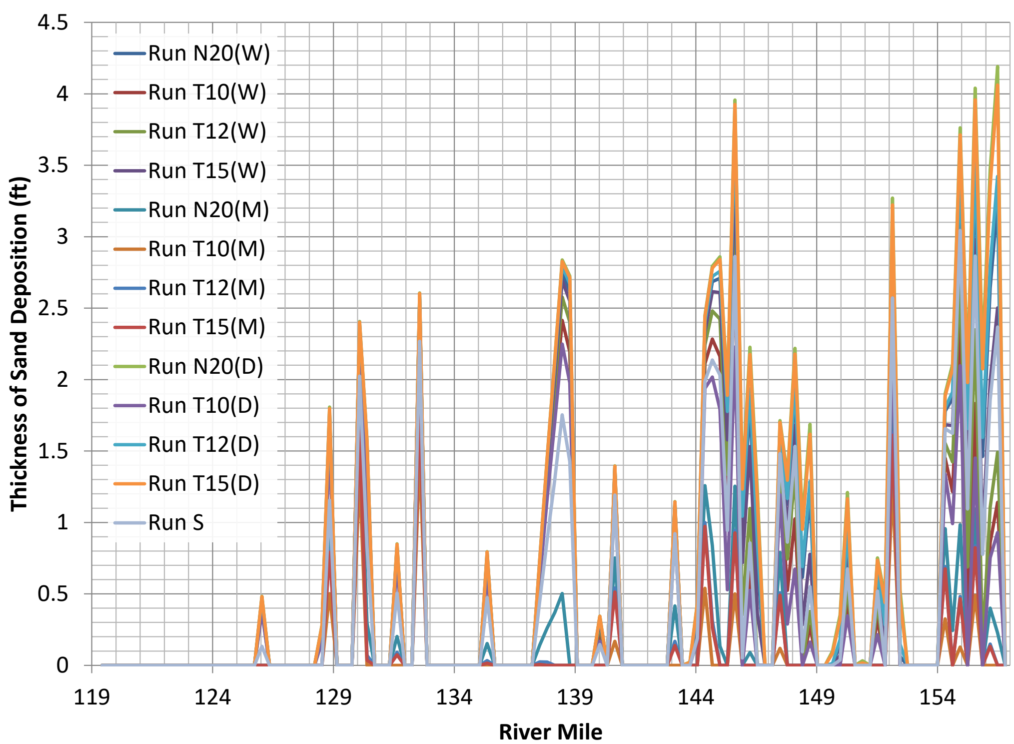

Figure 22. Simulated maximum thickness of sand deposit between Cape Horn Dam (RM 156.8) and Middle Fork Eel River confluence (RM 119.4) for all model runs. The purpose of the diagram is to illustrate the general area and magnitude of sand deposition instead of presenting results for individual runs.

7.5.3 Staged Dam Removal Alternative (Run S)

The first stage of a staged removal is to remove the top of the dam to an elevation of 1771.22 ft. Minimal sediment release is assumed to occur during this stage because Lake Pillsbury pool level was only approximately 10 ft below the pool level during the draught in summer of 2014. The second and third stages of dam removal each would remove another 20 ft of the dam to elevations of 1751.22 ft and 1731.22 ft, respectively. Each step of removal is assumed to take 5 months (June through October) to complete. The fourth and last stage would remove the dam to the base at an elevation of approximately 1708.92 ft, at which point no more obstacle would remain to obstruct the flow. For simplicity, it is assumed that the dam's crest would be lowered at a constant rate during the 5-month construction season.

Staged removal would result in a smaller peak sand deposition between Scott and Cape Horn Dams (Figure 23) compared with rapid (i.e., single-season) removal (Figure 19 to Figure 20), but the duration of deposition would be longer (Figure 24).

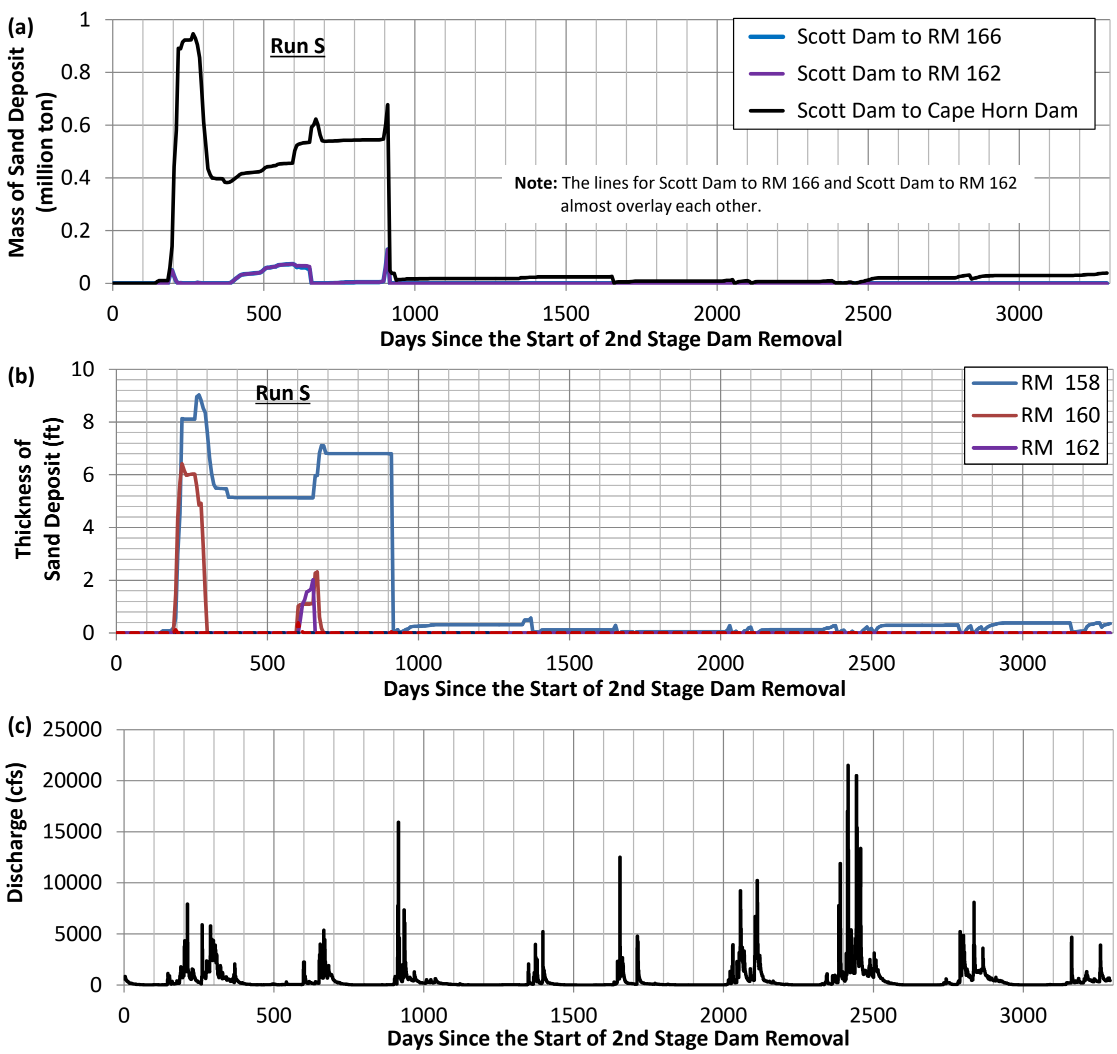

Figure 23. Simulated mass of sand deposition at selected reaches (a), thickness of sand deposition at selected locations (b), and water discharge at Scott Dam site (c). Time 0 is the day the 2nd stage of dam removal started.

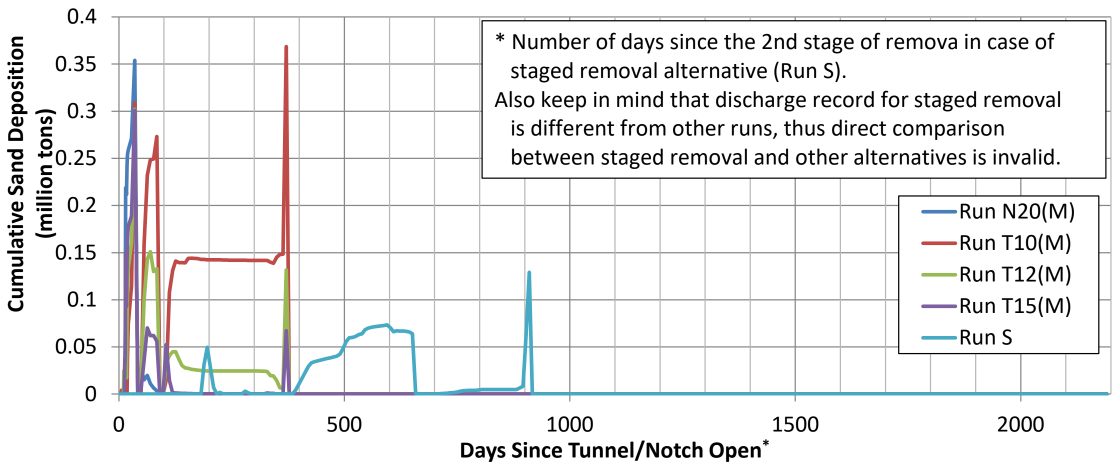

Figure 24. A side-by-side plot of sand deposition between Scott Dam and Cape Horn Dam during and following Scott Dam removal for Runs N20(M), T10(M), T12(M), T15(M), and S.

It is also important to reiterate that sand depositing in the interstices of the gravel bed is expected during at least three of the four summers when staged dam removal was ongoing, even when modeling results suggest minimal sand deposition, because the model is not capable of simulating such details.

Maximum sediment deposition between Cape Horn Dam and Middle Fork Eel River for staged removal (0.63 million tons) is within the range of that from other alternatives (0.16 to 1.0 million tons) (Table 5).

7.5.4 Long-term Impact (Run F)

There is only 56 mi^2 of watershed between Scott and Cape Horn Dams contributing sand to Van Arsdale Reservoir. The contributing catchment area will be increased to 345 mi^2 following the removal of Scott Dam, increasing sand supply accordingly.

Run F is a 10-year simulation that examines future post-dam removal conditions resulting from the increased sand supply (from 11,830 ton/year to 72,860 ton/year entering Van Arsdale Reservoir). Results indicate that the maximum reach-averaged thickness of sand deposits at RM158 in Van Arsdale Reservoir would increase from the current 6 inches (Figure 15) to approximately 3 ft (Figure 25), and the maximum mass of sand deposition between Scott Dam and Cape Horn Dam would increase from the current under 20,000 tons (Figure 15) to slightly more than 200,000 tons (Figure 25), a 5-fold increase in maximum thickness and 10-fold increase in mass. Such high values would culminate from periods of low-to-moderate flow between large flushing events. Minimal sand deposition is predicted in the reach between Scott Dam and RM 162 (i.e., upstream of Van Arsdale Reservoir area).

Minimal sand deposition is predicted for the reach between Cape Horn Dam and Middle Fork Eel River confluence, with identifiable deposition occurring only three times during the 10-year simulation at three locations (RM 152.1, RM 132.6, and RM 130.1). The predicted maximum sand deposition is roughly 4 inches, which is well below the potential errors for such modeling exercise and should be interpreted as no significant additional sand deposition in this reach.

Note that gravel supply would also increase downstream of Scott Dam following dam removal. If a gravel transport model were developed to simulate future gravel deposition, the predicted total sediment deposition due to increases in both sand and gravel supply would not be a simple sum of the predicted deposition of each (i.e., the overall sediment deposition ≠ simulated sand deposition + simulated gravel deposition). In the absence of modeling to simultaneously simulate both gravel and sand transport, combined gravel and sand deposition is expected to be only slightly higher than predicted sand deposition, as gravel deposition would mostly displace rather than add to sand deposition. Because of that, we recommend that the predicted sand deposition be used to approximate overall future sediment deposition (gravel + sand) for planning purposes until additional information is available.

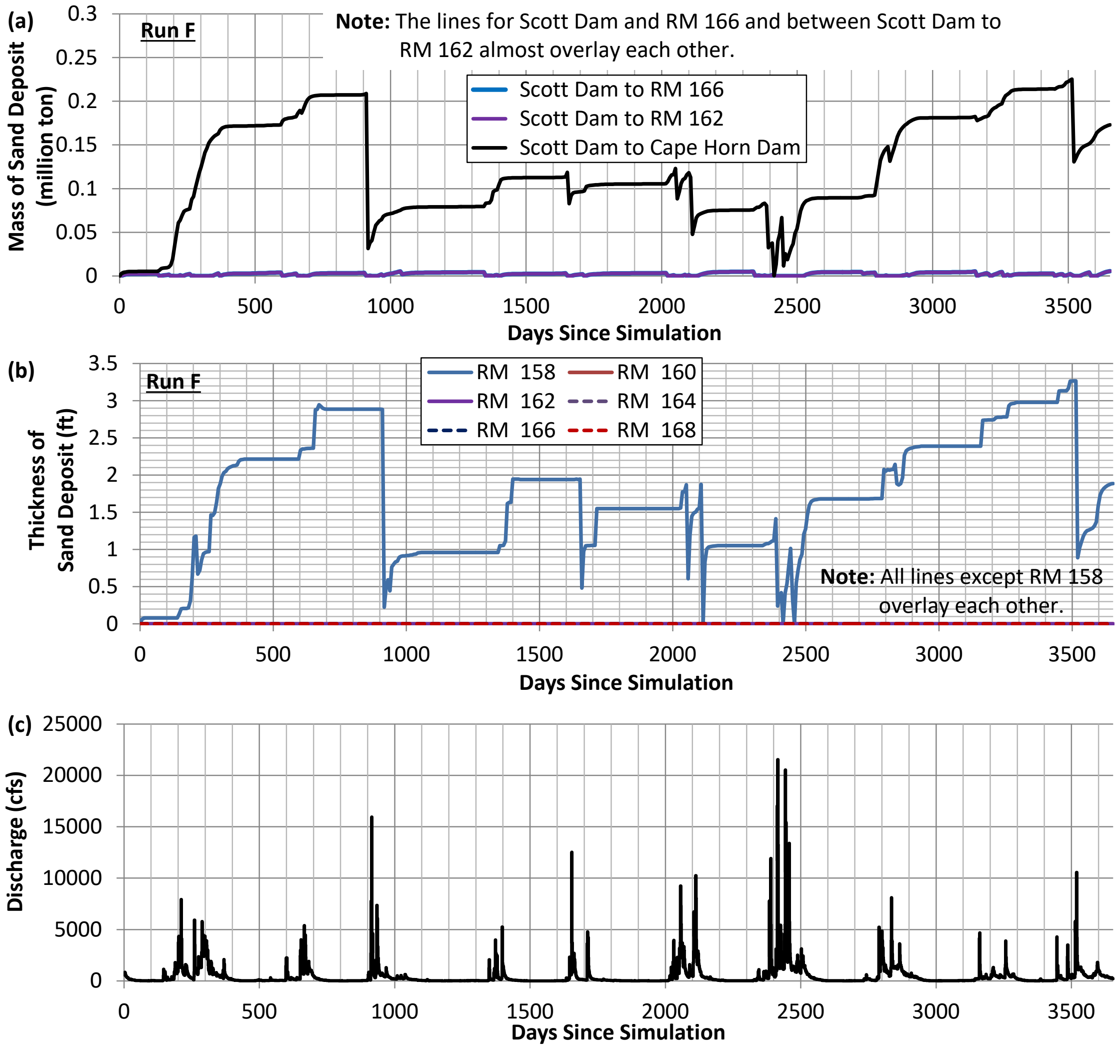

Figure 25. Simulated mass of sand deposition at selected reaches (a), thickness of sand deposition at selected locations (b) for Run F, along with water discharge at Scott Dam site (c).

7.5.5 Cross Check with Pre-modeling Analysis

Modeling results presented above are in general agreement with the pre-modeling analysis presented in Section 6.3 with perhaps one exception. The analysis predicts that sand deposition is greatest for the staged removal alternative for the following reasons

a. Staged removal would erode more Lake Pillsbury deposit to the downstream reach than rapid removal using vertical notching or tunneling. This factor was not examined in modeling because the difference in sediment erosion volume cannot be reliably estimated.
b. Erosion of Lake Pillsbury deposit would occur primarily during the last stage of dam removal for staged removal, providing less than expected advantage in distributing sediment erosion over a longer period of time.
c. Sediment erosion for staged removal would occur during the summer low-flow season, promoting more deposition downstream than the other alternatives, which erode sediment during the high-flow season.

Modeling results are in agreement with the above expectation if sediment deposition between Scott Dam and RM 162 is considered, but the predicted sand deposition for staged removal alternative is generally less than that for other alternatives if the examination extends to include Van Arsdale Reservoir area (Table 6). The discrepancy is largely due to the fact that modeled sediment release for staged removal would occur as early as the winter high flow event after the completion of the second stage of dam removal, effectively spreading sediment release into multiple years as opposed to a concentrated sediment release during the last stage of dam removal as expected in bullet (b) above. The early sand release after the second stage of removal is reasonable as more than two thirds of the dam would have been removed at that time. The pre-modeling expectation of sand release only during the last stage of dam removal was not met. More importantly, while all the model runs predicted minimal sand deposition in the summer in the reach between Scott Dam and upstream of the Van Arsdale Reservoir affected area (i.e., Scott Dam to RM 162), they do not tell whether sand would be deposited in the interstices of the gravel bed. We contend that the staged removal alternative would most likely cause sand to deposit in gravel interstices during at least three of the four summers during dam removal.

Table 6. Predicted peak sand deposition between Scott and Cape Horn Dams following Scott Dam removal, in million tons.

	Wet Year Runs	Median Year Runs	Dry Year Runs	Run S
20-ft Notch	1.06	1.74	2.20	n/a
10-ft Tunnel	0.65	1.53	1.75	n/a
12-ft Tunnel	0.77	1.23	1.95	n/a
15 ft Tunnel	0.93	1.42	2.08	n/a
Staged Removal	n/a	n/a	n/a	0.95

Modeling results are either in agreement with pre-modeling expectations or with a discrepancy that can be explained. We deem modeling results reliable with the caveat that some of the input parameters are still preliminary and will need to be re-examined to decide whether the model needs to be updated once new information regarding Lake Pillsbury sediment deposit characteristics become available.

8 SUMMARY AND DISCUSSIONS

It was estimated that 12 million CY of sediment would be eroded and transported downstream following the proposed removal of Scott Dam (Stillwater Sciences et al. 2021), resulting in high suspended sediment concentrations and sediment deposition downstream. Stillwater Sciences (2021a) provided an order-of-magnitude analysis for the potential suspended sediment concentration under the rapid sediment release dam removal alternative (i.e., either vertical notching or tunneling) and a staged sediment release dam removal alternative (i.e., four-stage removal), concluding that the vertical notching or tunnel alternative would result in extremely high suspended sediment concentrations (in the mid- to high hundred thousand milligrams per liter) that would last for a short period of time (days) if dam removal were timed to target a high flow event. Staged removal would result in lower suspended sediment concentrations (in the low hundred thousand milligrams per liter) that would last longer (exceeding 100 days). Following dam removal, fine sediment (i.e., silt and clay) is expected to be transported directly to the Eel River estuary with minimal intervening re-deposition.

Gravel and sand have the potential to be deposited in downstream reaches after dam removal. No model was developed to simulate gravel transport dynamics because there is inadequate data to do so. Instead, potential gravel transport dynamics is examined based on sediment pulse evolution research in rivers and observations of dam removal projects. Analysis of sand transport dynamics is based on sediment pulse theory and past experiences, and a DREAM-1 sediment transport model is developed to simulate sand transport dynamics under the current condition (with Scott Dam in place), following dam removal, and when sediment transport continuity is re-established past the Scott Dam site.

Based on sediment pulse theory, the gravel in Lake Pillsbury would spread only a short distance from its main deposits more than one river mile upstream of Scott Dam in Rice Fork and more than two river miles upstream of Scott Dam in the Eel River. Observations in the Sandy River, Oregon, following the removal of Marmot Dam, where gravel deposited only within one mile from the main body of the reservoir gravel deposit, indicate that minimal gravel deposition will occur downstream of Scott Dam following its removal. Dam removal, however, would re-establish gravel transport continuity, allowing gravel produced in the Eel River watershed upstream of Scott Dam to spread downstream and deposit in Van Arsdale Reservoir.

The large sand pulse released from Lake Pillsbury following Scott Dam removal would evolve by a combination of dispersion and translation, making sand more likely to deposit in the downstream reach. This prospect was further examined with the DREAM-1 model.

Five dam removal alternatives are examined with DREAM-1 simulations: four rapid-removal alternatives and one staged-removal alternative. Rapid-removal alternatives include a 20-ft wide vertical notch opened down to the base of the dam and tunnels with diameters of 10, 12, and 15 ft opened near the base of the dam. All would occur prior to a targeted high flow event. Modeling results show that rapid removal would result in up to 2.1 million tons of sand deposited between Scott and Cape Horn Dams and concentrated in Van Arsdale Reservoir, and up to 1.0 million tons of sand deposition between Cape Horn Dam and Middle Fork Eel River. Sand deposition is predicted to vanish after an approximately five-year flow event in the reach upstream of Cape Horn Dam. Prominent sand deposition downstream of Cape Horn Dam would be short-lived, lasting once for only one day. Staged removal would produce a smaller amount of peak sand deposition (approximately 1 million tons between Scott and Cape Horn Dams, and up to 0.6 million tons between Cape Horn Dam and Middle Fork Eel River confluence for the run conducted), but the temporary sand deposition upstream of Cape Horn Dam would last longer. Given that short-term sand deposition would vanish at roughly the same magnitude of high flow event regardless of alternative, it can be expected that sand deposits would persist approximately two years longer with staged removal, because sediment deposition is expected to start after the second stage of removal, and would not vanish until a high flow event occurred after the last (fourth) stage of removal two and a half years later.

There is no clear advantage among the four rapid dam removal alternatives with regard to sand deposition in Van Arsdale Reservoir: smaller-diameter tunneling would likely produce smaller peak deposition compared to larger diameter tunneling and notching, but sand deposition during subsequent high flow events would be greater and the duration of a significant sand deposition would be longer. If sand deposition upstream of Van Arsdale Reservoir area is a concern for spawning and rearing habitats, then vertical notching or large-diameter tunneling would be more advantageous as they present the least amount and the shortest duration of sand deposition in this reach. Staged removal would be the least advantageous as prolonged sand deposition in gravel interstices would be expected during at least three of the four years after the start of dam removal. Sand deposition outside of Van Arsdale Reservoir would be small (up to 5 ft immediately downstream of Scott Dam and up to 4 ft in isolated locations downstream of Cape Horn Dam) and would vanish quickly.

Scott Dam removal would result in long-term impact in sediment deposition in Van Arsdale Reservoir as sediment continuity is re-established at the Scott Dam site. Modeling results indicate that, without considering increased gravel deposition, maximum sand deposition in Van Arsdale Reservoir would increase from the current 20,000 tons to a maximum of 200,000 tons. Long-term gravel deposition is not modeled, but it is expected that gravel would mostly displace the predicted sand deposition, so together would be only slightly greater than or equal to the predicted sand deposition. Minimal long-term sand deposition is predicted in the study reach outside of Van Arsdale Reservoir area.

The current study used a DREAM-1 model to simulate sand transport dynamics following Scott Dam removal, and no gravel model was developed due to limitations of available information with regard to particle size characteristics of Lake Pillsbury gravel deposits and upstream gravel supply. Although a reach-wide gravel model (Dream-2) could be developed once additional particle size data becomes available, the outcome of such a model is largely known with minimal uncertainty. It is our recommendation that future studies focus on addressing short-term and long-term sediment impacts at Van Arsdale Reservoir, Van Arsdale Diversion, and Cape Horn Dam fish passage facilities.

Analyses and modeling results presented in this document clearly show that any alternative that attempts to manage the sediment deposit (such as mechanical removal) in Lake Pillsbury prior to dam removal should not be advanced. Instead of directly treating any of the several million tons of sediment, a much smaller amount can be managed at Van Arsdale Reservoir, if necessary. Dam removal alternatives that allow the river to naturally transport the sediment deposit downstream present a huge cost saving and significantly reduce technical difficulty.

9 REFERENCES

Benda L. and Dunne T. 1997. Stochastic forcing of sediment routing and storage in channel networks. Water Resources Research 33: 2865–2880.

Bountry, J., and T. Randle. 2001. Hydraulic and sediment transport analysis and modeling, appendix B in Savage Rapids Dam Sediment Evaluation Study. Department of the Interior, Bureau of Reclamation, Pacific Northwest Region, Portland, Oregon.

Bountry, J. A., Y. G. Lai, and T. J. Randle. 2013. Sediment impacts from the Savage Rapids Dam removal, Rogue River, Oregon. Reviews in Engineering Geology 21: 93–104. doi:10.1130/2013.4121(08).

BOR (U.S. Bureau of Reclamation). 1996. Sediment analysis and modeling of the river erosion alternative. Elwha Technical Series PN-95-9. Elwha River Ecosystem and Fisheries Restoration Project, Washington.

BOR. 2004. Hydrology, hydraulics and sediment studies of alternatives for the Matilija Dam Ecosystem Restoration Project, Ventura, CA. Final Report.

BOR. 2011. Hydrology, hydraulics and sediment transport studies for the Secretary’s determination on Klamath Dam removal and basin restoration. Technical Report No. SRH-2011-02. Prepared for Bureau of Reclamation, Mid-Pacific region, Denver, Colorado.

Chow, W.T. 1959. Open Channel Hydraulics. McGraw-Hill Book Company, New York – Toronto – London, ISBN 07-0100776-9.

Cui, Y., G. Parker, and C. Paola. 1996. Numerical simulation of aggradation and downstream fining. Journal of Hydraulic Research, 34(2), 185-204.

Cui, Y., Parker, G., Lisle, T.E., Gott, J., Hansler-Ball, M.E., Pizzuto, J.E., Allmendinger, N.E., and Reed, J.M. 2003a. Sediment pulses in mountain rivers: 1. Experiments. Water Resources Research, 39(9), 1239, doi: 10.1029/2002WR001803.

Cui, Y., Parker, G., Pizzuto, J.E., and Lisle, T.E. 2003b. Sediment pulses in mountain rivers: 2. Comparison between experiments and numerical predictions. Water Resources Research, 39(9), 1240, doi: 10.1029/2002WR001805.

Cui, Y., and Parker, G. 2005. Numerical model of sediment pulses and sediment-supply disturbances in mountain rivers. Journal of Hydraulic Engineering, 131(8), 646-656, doi: 10.1061/(ASCE)0733-9429(2005)131:8(646).

Cui, Y., Parker, G., Lisle, T.E., Pizzuto, J.E., and Dodd, A.M. 2005. More on the evolution of bed material waves in alluvial rivers. Earth Surface Processes and Landforms, 30(1), 107-114, doi: 10.1002/esp.1156.

Cui, Y., G. Parker, C. Braudrick, W. E. Dietrich, and B. Cluer. 2006a. Dam Removal Express Assessment Models (DREAM). Part 1: Model development and validation. Journal of Hydraulic Research 44: 291–307.

Cui, Y., C. Braudrick, W. E. Dietrich, B. Cluer, and G. Parker. 2006b. Dam Removal Express Assessment Models (DREAM). Part 2: Sample runs/sensitivity tests. Journal of Hydraulic Research 44: 308-323.

Cui, Y., and A. Wilcox. 2008. Development and Application of Numerical Models of Sediment Transport Associated with Dam Removal. Pages 995–1,020 *in* M. H. Garcia, editor. Sedimentation engineering: processes, measurements, modeling, and practice, ASCE Manual 110. ASCE, Reston, Virginia.

Cui, Y., Wooster, J.K., Venditti, J.G., Dusterhoff, S.R., Dietrich, W.E., and Sklar, L.S. 2008. Simulating sediment transport in a flume with forced pool-riffle morphology: examinations of two one-dimensional numerical models, Journal of Hydraulic Engineering, 134(7), 892-904, doi: 10.1061/(ASCE)0733-9429(2008)134:7(892).

Cui, Y., Dusterhoff, S.R., Wooster, J.K., and Downs, P.W. 2011. Practical considerations for modeling sediment transport dynamics in rivers. Stream Restoration in Dynamic Fluvial Systems: Scientific Approaches, Analyses, and Tools, Simon, A., Bennett, S.J., and Castro, J. eds., 503-527, American Geophysical Union, ISBN 978-0-87590-483-2.

Cui, Y., J. K. Wooster, C. A. Braudrick, and B. K. Orr. 2014. Marmot Dam removal project, Sandy River, Oregon: lessons learned from sediment transport model predictions and long-term post-removal monitoring. Journal of Hydraulic Engineering 140: doi:10.1061/(ASCE)HY.1943-7900.0000894.

Cui, Y. D. B. Booth, J. Monschke, S. Gentzler, J. Roadifer, B. Greimann, and B. Cluer. 2017. Analyses of the erosion of fine sediment deposit for a large dam-removal project: an empirical approach. The International Journal of River Basin Management 15: 103–114. doi:10.1080/15715124.2016.1247362.

Cui, Y., Mathias J. Collins, Mary Andrews, Graham C. Boardman, John K. Wooster, Marty Melchior & Serena McClain. 2019. Comparing 1-D sediment transport modeling with field observations: Simkins Dam removal case study, International Journal of River Basin Management, 17:2, 185-197, DOI: 10.1080/15715124.2018.1508024

Downs, P.W., Cui, Y., Wooster, J.K., Dusterhoff, S.R., Booth, D.B., Dietrich, W.E., and Sklar, L. 2009. Managing reservoir sediment release in dam removal projects: an approach informed by physical and numerical modeling of non-cohesive sediment. The International Journal of River Basin Management, 7(4), 433-452.

Geosyntec 2020. Lake Pillsbury and Van Arsdale Reservoir sediment characterization. Memorandum to Michael Bowen, California State Coastal Conservancy.

Lisle TE, Pizzuto JE, Ikeda H, Iseya F, Kodama Y. 1997. Evolution of a sediment wave in an experimental channel. Water Resources Research 33: 1971–1981.

Lisle, T.E., Cui, Y., Parker, G., Pizzuto, J.E., and Dodd, A.M. 2001. The dominance of dispersion in the evolution of bed material waves in gravel - bed rivers. Earth Surface Processes and Landforms,26, 1409-420, doi: 10.1002/esp.300.

Major, J. J., et al. 2012. Geomorphic response of the Sandy River, Oregon, to removal of Marmot Dam. Professional Paper 1792, U.S. Geological Survey, Washington, DC.

McBain Associates and Princeton Hydro. 2019. Conceptual approach for Scott Dam decommissioning and Lake Pillsbury sediment management, slide presentation, March 25.

MEI (Mussetter Engineering, Inc.) 2003. San Clemente Reservoir and Carmel River sediment transport modeling to evaluate potential impacts of dam retrofit options. Prepared for American Water Works Service Company, Voohees, New Jersey, MEI Project No. 01-18.2, April.

McMillen Jacobs Associates. 2018. Potter Valley Project Capital Modifications Feasibility Study Report, Potter Valley Project, FERC No. 77-110. Final Report.

McMillen Jacobs Associates. 2021a. Scott Dam and Cape Horn Dam Removal. Prepared for Two-Basin Solution Partners. Draft Technical Memorandum, July.

McMillen Jacobs Associates. 2021b. Cape Horn Dam Fish Passage Improvements. Prepared for Two-Basin Solution Partners. Draft Technical Memorandum, July.

PG&E (Pacific Gas and Electric Company). 2017a. Relicensing Pre-Application Document (PAD), Volume 1: Public Information, Sections 1-7. Potter Valley Hydroelectric Project, FERC Project No. 77.

PG&E. 2017b. Lake Pillsbury bathymetric survey 2016, Report No. 026.11-16,3, prepared by PG&E Applied Technology Services, prepared for PG&E Electric Supply Aquatic and Natural Resources.

Sklar, L.S., Fadde, J., Venditti, J.G., Nelson, P., Wydzga, M.A., Cui, Y., and Dietrich, W.E. 2009. Translation and dispersion of sediment pulses in flume experiments simulating gravel augmentation below dams. Water Resources Research, W08439, doi: 10.1029/2008WR007346.

Stillwater Sciences. 2000. Numerical modeling of sediment transport in the Sandy River, OR following removal of Marmot Dam. Technical Report. Prepared for Portland General Electric Company, Portland, Oregon.

Stillwater Sciences. 2004. A preliminary evaluation of the potential downstream sediment deposition following the removal of Iron Gate, Copco, and J.C. Boyle Dams, Klamath River, CA. Final Report, prepared for American Rivers, May.

Stillwater Sciences. 2008. Klamath River dam removal study: sediment transport DREAM-1 simulation. Technical Report. Prepared for California Coastal Conservancy, Oakland, California.

Stillwater Sciences. 2013. Modeling sediment transport dynamics and evaluating flooding risks in the Yuba and Feather Rivers, California, following modifications to Englebright and Daguerre Point Dams. Prepared for National Marine Fisheries Service, Southwest Region, Habitat Conservation Division, June.

Stillwater Sciences. 2019. Matilija Dam removal 65% design subtask 2.2: detailed sediment transport modeling from dam to ocean. Technical Report, prepared for AECOM Technical Service Inc., February.

Stillwater Sciences. 2021a. Analyses of fine sediment erosion following the proposed Scott Dam removal, Eel River, California. Draft Technical Memorandum, prepared for Two-Basin Solution Partners, July.

Stillwater Sciences. 2021b. Hydraulic Model Development and Potential Flood Implications Following the Proposed Scott Dam Removal, Eel River, California. Prepared for Two-Basin Solution Partners. Potter Valley Project Feasibility Study Phase 2, Draft Technical Memorandum. August.

Stillwater Sciences. 2021c. Sediment Supply to the Upper Eel River. Prepared by Stillwater Sciences for Two-Bain Solution Partners. July.

Stillwater Sciences, McBain Associates, McMillen Jacobs Associates, M.Cubed, Princeton Hydro, and Geosyntec Consultants. 2021. Potter Valley Project Feasibility Study: Capital Improvements. Prepared by Stillwater Sciences and McBain Associates, Arcata, California; McMillen Jacobs Associates, Boise, Idaho; M.Cubed, Davis, California; Princeton Hydro, South Glastonbury, Connecticut; and Geosyntec Consultants, Oakland, California for the Potter Valley Project Planning Agreement Parties.

Sutherland, D. G., Hansler-Ball, M., Hilton, S. J., and Lisle, T. E. 2002. Evolution of a landslide-induced sediment wave in the Navarro River, California." GSA Bull., 114(8), 1036–1048.

USGS. 1964. Sedimentation of Lake Pillsbury, Lake County, California. Geological Survey Water-Supply Paper 1619-EE, US Government Printing Office, D.C. 20402.

APPENDIX A

DISCHARGE CAPACITY CURVES FOR DIFFERENT DAM REMOVAL ALTERNATIVES

APPENDIX A
DISCHARGE CAPACITY CURVES FOR DIFFERENT DAM REMOVAL ALTERNATIVES

A.1 Staged Removal

For staged removal, the remainder of the dam is assumed to be a broad-crested weir, and the following equation is used to generate a discharge capacity curve (Chow 1959):

$$Q_w = 5.1BH^{1.5} \quad \text{(A1)}$$

in which Q_w denotes water discharge in cfs; B denotes the width of the broad-crested weir in ft; and H denotes the elevation difference between the surface of the lake and the crest of the remainder of the dam. The weir is assumed to be 250 ft wide.

A.2 Vertical Notching

Water depth within the notch is calculated with Manning's equation:

$$Q_w = \frac{1.49}{\mathrm{n}} bHR^{2/3}S^{1/2} \quad \text{(A2)}$$

in which n denotes Manning's n, b denotes notch width in ft, H denotes water depth inside the notch in ft; R denotes hydraulic radius in ft, and S denotes slope of the notch. Hydraulic radius is expressed as

$$R = \frac{Hb}{\mathrm{b+2H}} \quad \text{(A3)}$$

Water surface elevation is then approximated as

$$h = h_0 + H + \frac{\left({}^{Q_w}/_{(bH)}\right)^2}{2g} \quad \text{(A4)}$$

in which η denotes lake water surface elevation; η_0 denotes invert elevation of the notch; and g denotes acceleration of gravity.

In the case the lake surface overtops the overflow section (Figure A-1), the overflow is treated as a broad crested weir and equation (A3) applies to the overflow section.

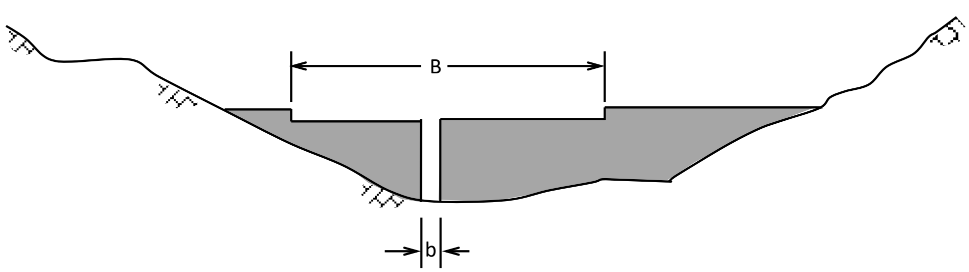

Figure A-1. Sketch showing the flow path after opening of the notch for vertical notching dam removal alternative.

The combined water discharge – water depth relation is then expressed as

$$Q_w = \frac{1.49}{\text{n}} bHR^{2/3}S^{1/2} + 5.1(B-b)(h-h_1)^{1.5} \qquad \text{(A5)}$$

in which η_1 denotes the crest elevation of the overflow section.

A combination of above equations was used to develop a flow capacity curve (Figure A-2) using the following parameters (Table A-1):

Table A-1. Parameters used to develop discharge capacity curve for vertical notching alternative.

Parameter	Assumed value
Manning's n	0.022
Slope in the notch (S)	0.05
Notch invert elevation (η_0)	1800 ft
Notch width (b)	20 ft
Overflow weir crest elevation (η_1)	1781.22 ft
Overflow weir width (B)	250 ft

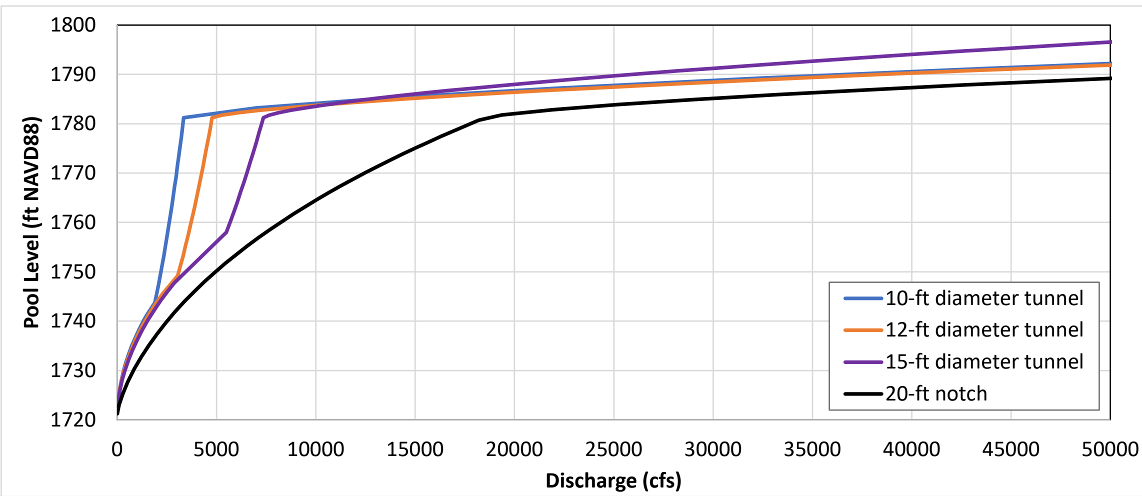

Figure A-2. Discharge capacity curves developed for vertical notching and tunneling alternatives.

A.3 Tunneling

A schematic sketch of the flow path for tunneling is provided in Figure A-3, showing the tunnel and the overflow section. Similar to the notching alternative, Manning's equation is applied to calculate the flow depth within the tunnel in case the flow within the tunnel is open-channel flow.

$$Q_w = \frac{1.49}{\text{n}} AR^{2/3}S^{1/2} \qquad \text{(A6)}$$

In which A denotes the area of the tunnel occupied by the flow; and the similar to vertical notching alternative, R denotes hydraulic radius.

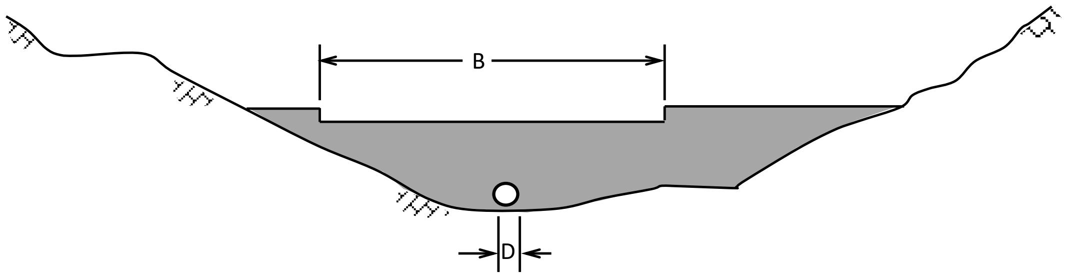

Figure A-3. Sketch showing the flow path after opening of the tunnel for tunneling removal alternative.

Flow area A and hydraulic radius R are calculated with the following equations in reference to the sketch shown in Figure A-4:

$$\theta = 2ArcCos\left(\frac{abs(H-D/2)}{D/2}\right) \quad \text{(A7)}$$

$$P = \begin{cases} \frac{\theta D}{2}, H \le \frac{D}{2} \\ \pi D - \frac{\theta D}{2}, H > \frac{D}{2} \end{cases} \quad \text{(A8)}$$

$$A = \begin{cases} \frac{D^2[\theta - Sin(\theta)]}{8}, H \le \frac{D}{2} \\ \frac{\pi D^2}{4} - \frac{D^2[\theta - Sin(\theta)]}{8}, H > \frac{D}{2} \end{cases} \quad \text{(A9)}$$

and

$$R = A/P \quad \text{(A10)}$$

in which P denotes the wetted perimeter within the tunnel. The lake surface elevation is then estimated to be

$$h = h_0 + H + \frac{\left(Q_w/_A\right)^2}{2g} \quad \text{(A11)}$$

in which η_0 denotes the invert elevation of the tunnel.

The flow in the tunnel will transition to pressured flow if lake level is high enough. Once that occurs, water discharge in the tunnel is calculated as

$$Q_w = 0.63\frac{\pi D^2}{4}\sqrt{2g(\eta - D/2)} \quad \text{(A12)}$$

The transition between open channel flow and pressured flow is realized when lake surface elevation obtained by solving equation (A12) matches that obtained by solving equations (A6) through (A11).

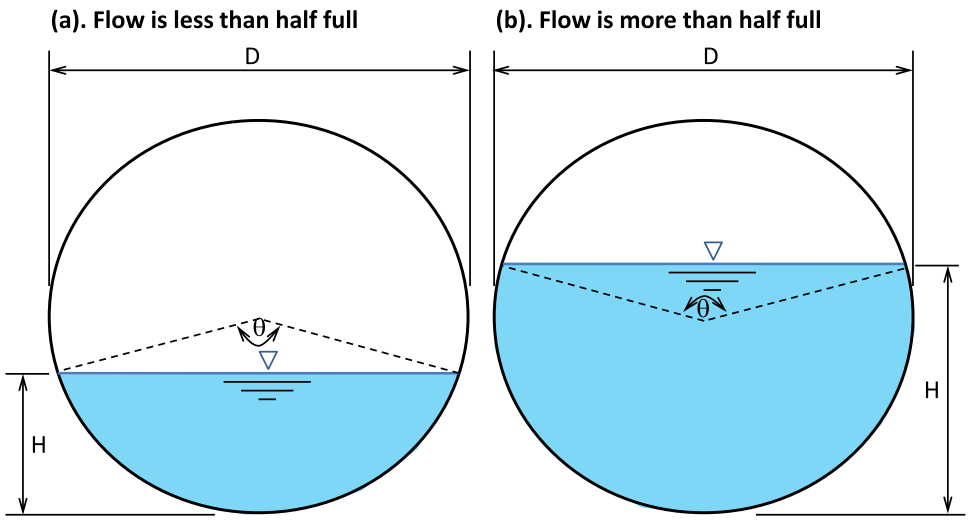

Figure A-4. Sketch showing open channel flow inside a circular tunnel.

Similar to notching alternative, the weir is treated as a broad-crested weir once overflow occurs, with water discharge over the weir calculated with equation (A1).

A combination of equations (A1) and (A6) through (A12) was used to develop flow capacity curves (Figure A-2) using the following parameters (A-2):

Table A-2. Parameters used to develop discharge capacity curve for vertical notching alternative.

Parameter	Assumed value
Manning's n	0.022
Slope in the notch (S)	0.05
Tunnel invert elevation (η_0)	1800 ft
Tunnel diameter (D)	10, 12, and 15 ft
Overflow weir crest elevation (η_1)	1781.22 ft
Overflow weir width (B)	250 ft

APPENDIX B

ASSUMPTIONS REGARDING TRIBUTARY CONTRIBUTIONS BETWEEN CAPE HORN DAM AND MIDDLE FORK EEL RIVER CONFLUENCE

APPENDIX B

ASSUMPTIONS REGARDING TRIBUTARY CONTRIBUTIONS BETWEEN CAPE HORN DAM AND MIDDLE FORK EEL RIVER CONFLUENCE

B.1 Water Discharge

Discharge at any computational node is assumed to be proportional to local catchment area:

$$Q_{wi} = \frac{A_i}{A_0} Q_{w0} \qquad \text{(B1)}$$

in which Q_{wi} denotes daily average discharge at the i-th computational node; A_i denotes catchment area at the i-th computational node; A_0 denotes catchment area at the Scott Dam site; and Q_{w0} denotes daily average discharge at the Scott Dam site. The calculated unimpaired discharge at Scott Dam (Addley et al., 2019) is used for simulation, representing hydrological conditions after dam removal.

B.2 Natural Sand Supply

Similarly the rate of natural sand supply (i.e., under unimpaired conditions) is assumed to be proportional to local catchment area:

$$Q_{si} = \frac{A_i}{A_0} Q_{s0} \qquad \text{(B2)}$$

in which Q_{si} denotes the rate of natural sand supply from the area upstream of the i-th computational node; and Q_{s0} denotes the rate of natural sand supply from the area upstream of Scott Dam site, both under unimpaired conditions.

The rate of natural sand supply between node i-1 and node i (ΔQ_{si}) is then expressed as

$$\Delta Q_{si} = \frac{\Delta A_i}{A_0} Q_{s0} \qquad \text{(B3)}$$

in which $\Delta A_i = A_i - A_{i-1}$ denotes catchment area between computational node i-1 and node i. Note that computational node is sequenced from upstream to the downstream direction.

As discussed in Section 7.3, there had been an estimated 5.7 million tons of sand deposited in Lake Pillsbury during the 93-year dam operation between WY1923 and 2015, resulting in a long-term average sand production rate of 61,000 ton/year in the Eel River above Scott Dam. This estimate needs to be partitioned into the rate of sand supply on a daily basis to provide a daily average sand supply – daily average water discharge relation for modeling purposes. This is accomplished by assuming a power relation between water discharge and sediment transport:

$$Q_{s0} = \alpha {Q_{w0}}^{\beta} \qquad \text{(B4)}$$

in which α and β are fitting parameters to be determined.

There is no sand transport data throughout the Eel River basin, but suspended sediment (primarily sand and silt combined) data at Scotia CA (USGS 114777000) is available between WY 1960 and

1980. This would provide us with a rough estimate of parameter β if we assume sand and silt have the same β value in a power relation, resulting in an estimated β value of 2.15 (Figure B-1). We further assume that the β value at Scott Dam site is identical to that estimated at Scotia, CA.

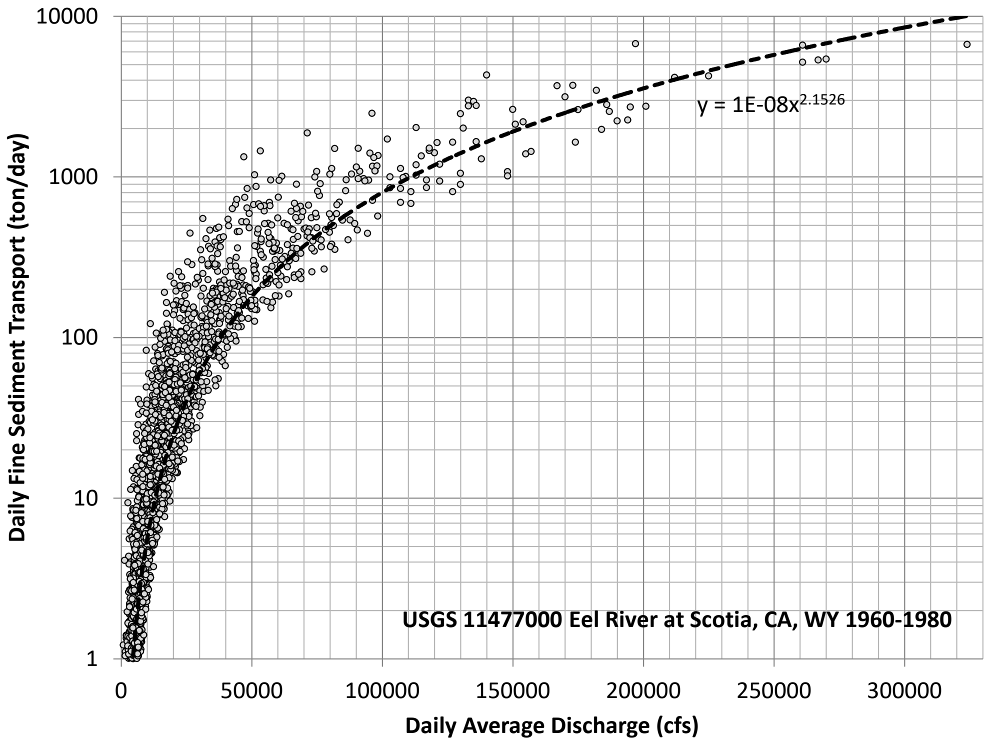

Figure B-1. Daily fine sediment transport – daily average discharge relation in the Eel River at Scotia, CA. Based on daily average discharge and suspended sediment concentration record between WY 1960 and 1980 at USGS 11477000.

Parameter α is then determined so that the sum of sand transport between WY1923 and 2015 is 5.7 million tons:

$$\alpha \int_{WY1923}^{WY2015} {Q_{w0}}^{\beta}\, dt = 5.7\ million\ tons \tag{B5}$$

This would result in $\alpha = 1.755\times10^{-5}$ and

$$Q_{s0} = 1.755 \times 10^{-5} {Q_{w0}}^{2.15} \tag{B6}$$

in which Q_{s0} is in tons/day, and Q_{w0} is in cfs.

A combination of Equations (B3) and (B6) provides tributary sand supply throughout the study reach over the entire duration of simulation.

APPENDIX C

COMPLETE SET OF MODEL RESULTS

APPENDIX C

COMPLETE SET OF MODEL RESULTS

A complete set of model results is provided here for interested readers to examine and reference. Note a few of these figures have already been presented in the main body of this document but are duplicated here to present a complete set.

Naming convention: The first letter represents alternative (*i.e.*, C = current condition, F = future, N = notching alternative, T = tunneling alternative, and S = staged removal alternative); the number following the first letter, if any, represents size of opening (*e.g.*, N20 = notching alternative with 20 ft wide notch, T12 = tunneling alternative with 12 ft diameter tunnel); and the letter within the parentheses, if any, represents the hydrological condition when dam removal starts (*i.e.*, W = wet year, M = median year, and D = dry year). A list of all runs can be found in Section 7.5, Table 4.

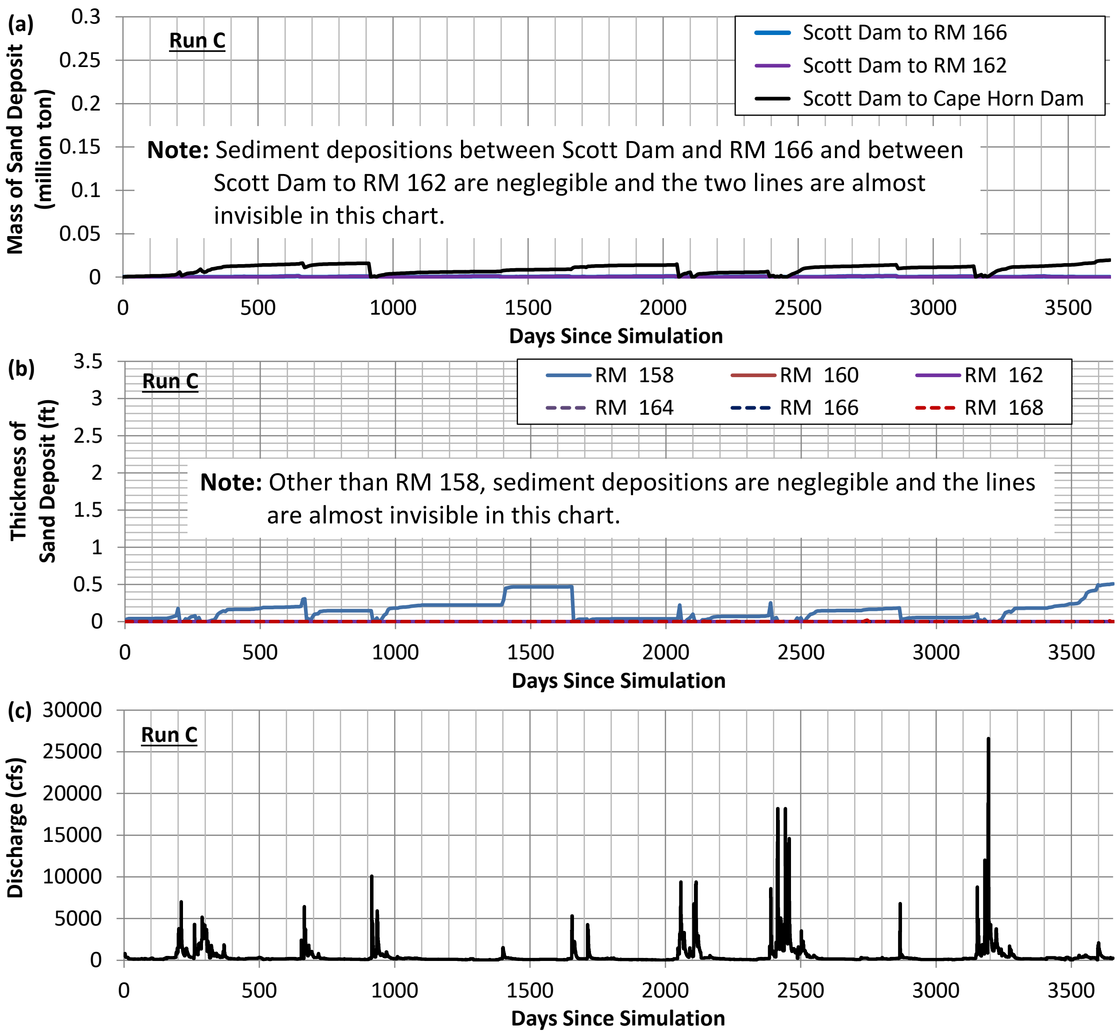

Figure C-1. Simulated mass of sand deposition at selected reaches (a) and thickness of sand deposition at selected locations (b) under current conditions (i.e., with Scott Dam in place), along with water discharge at Scott Dam site (c). Simulated sand deposition downstream of Cape Horn Dam is negligible and not presented.

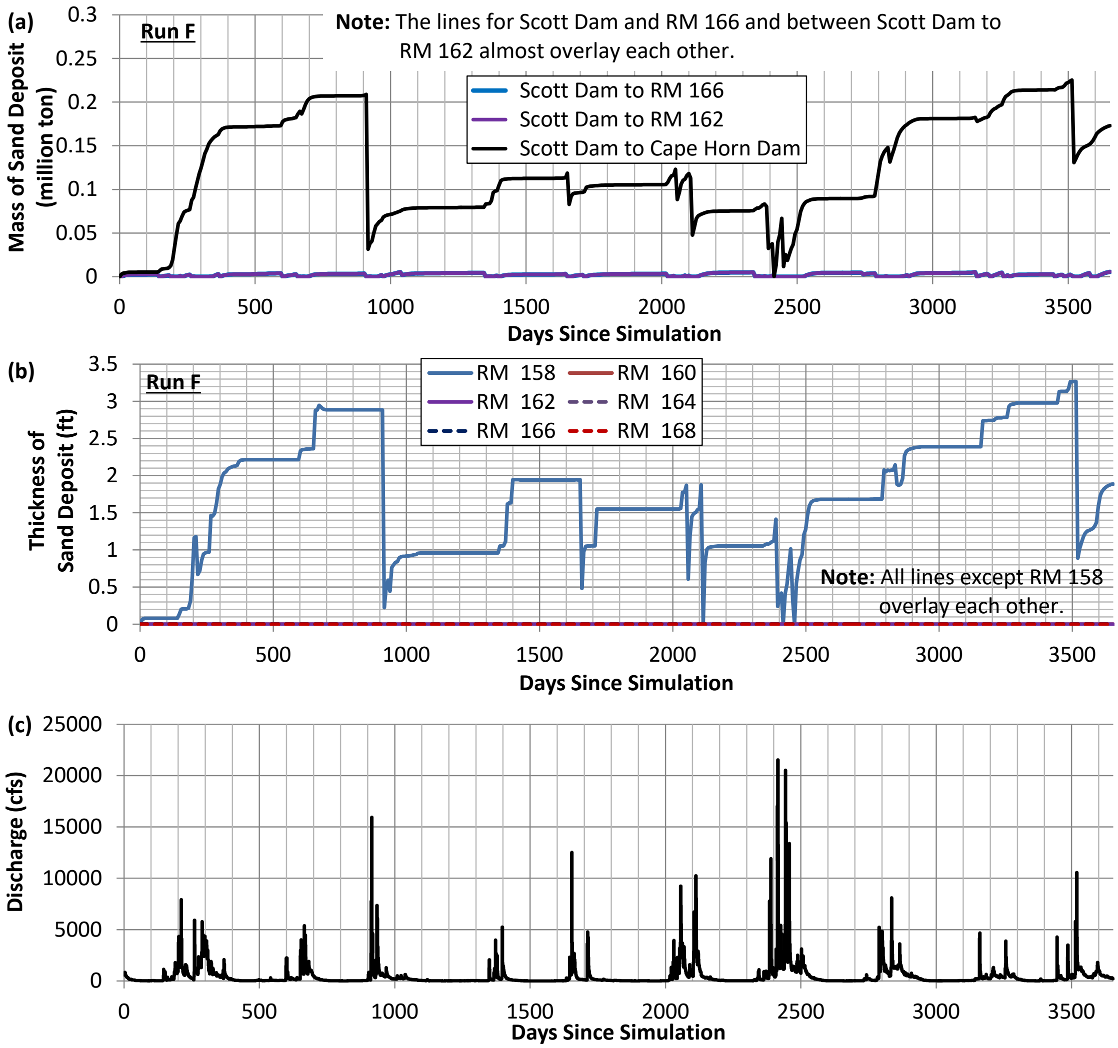

Figure C-2. Simulated mass of sand deposition at selected reaches (a), thickness of sand deposition at selected locations (b) for Run F, along with water discharge at Scott Dam site (c).

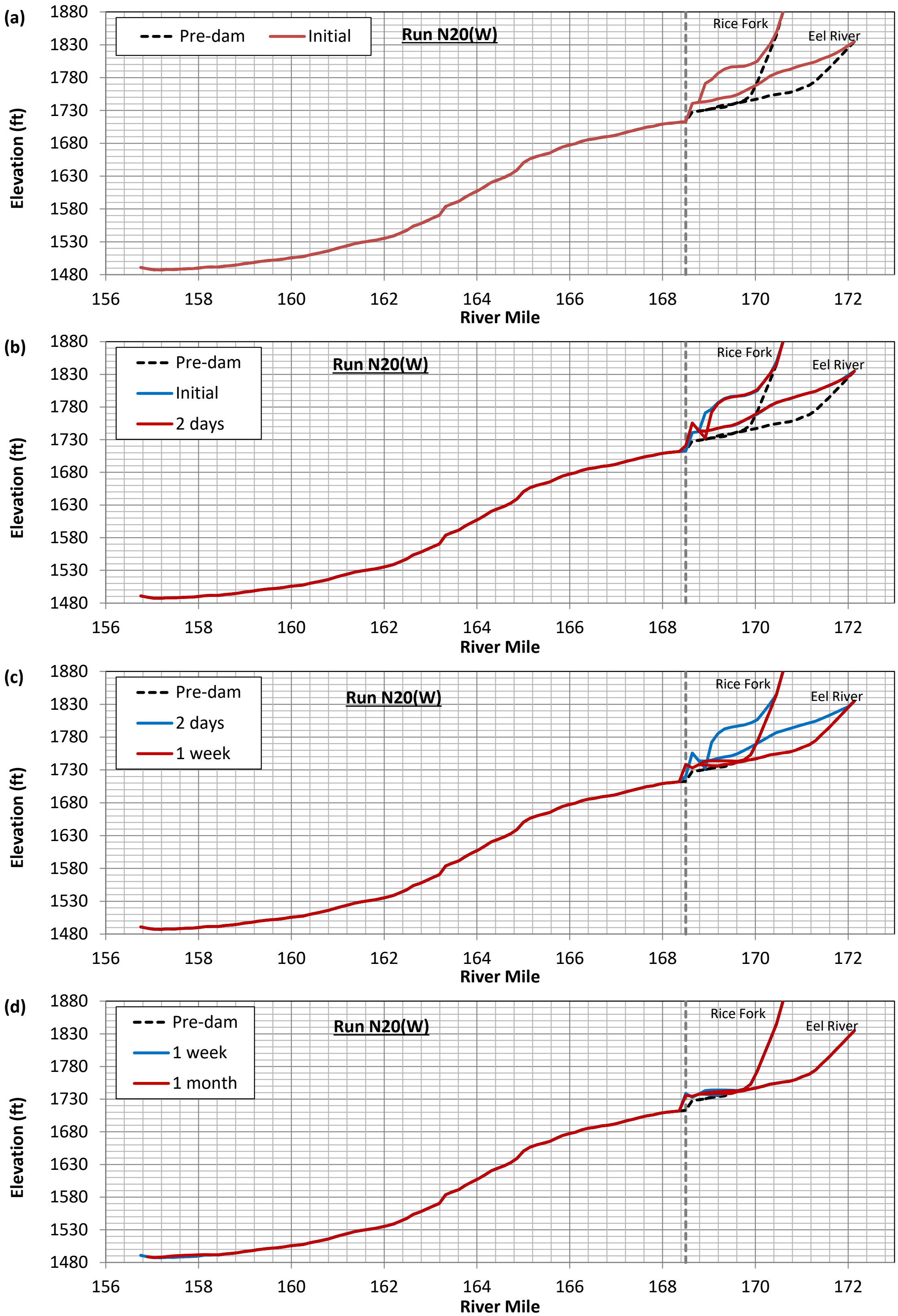

Figure C-3 continues on the next page

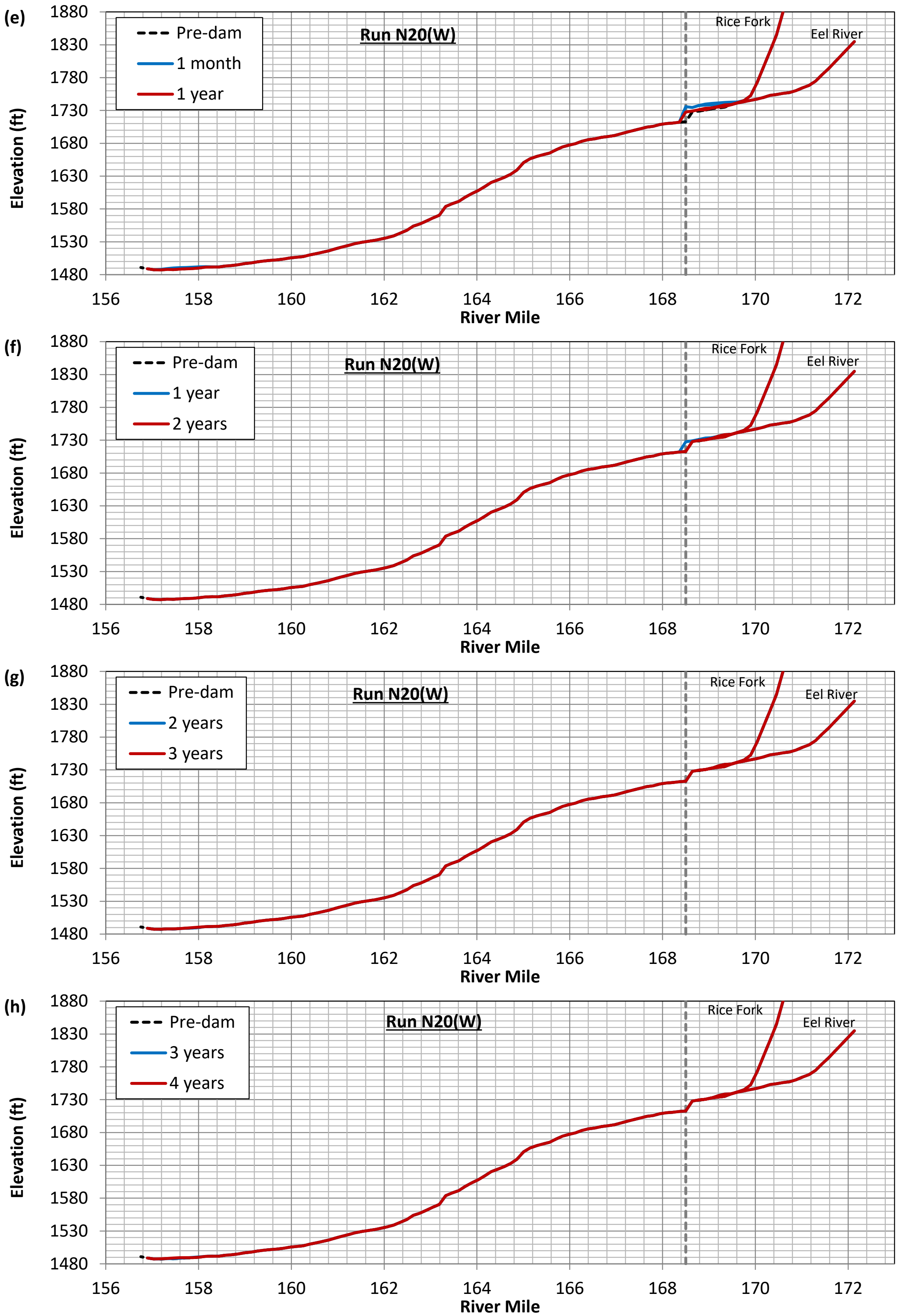

Figure C-3. Bed profile following Scott Dam removal for vertical notching alternative with 20 ft notch width, dam removal starts in a wet year [Run N20(W)].

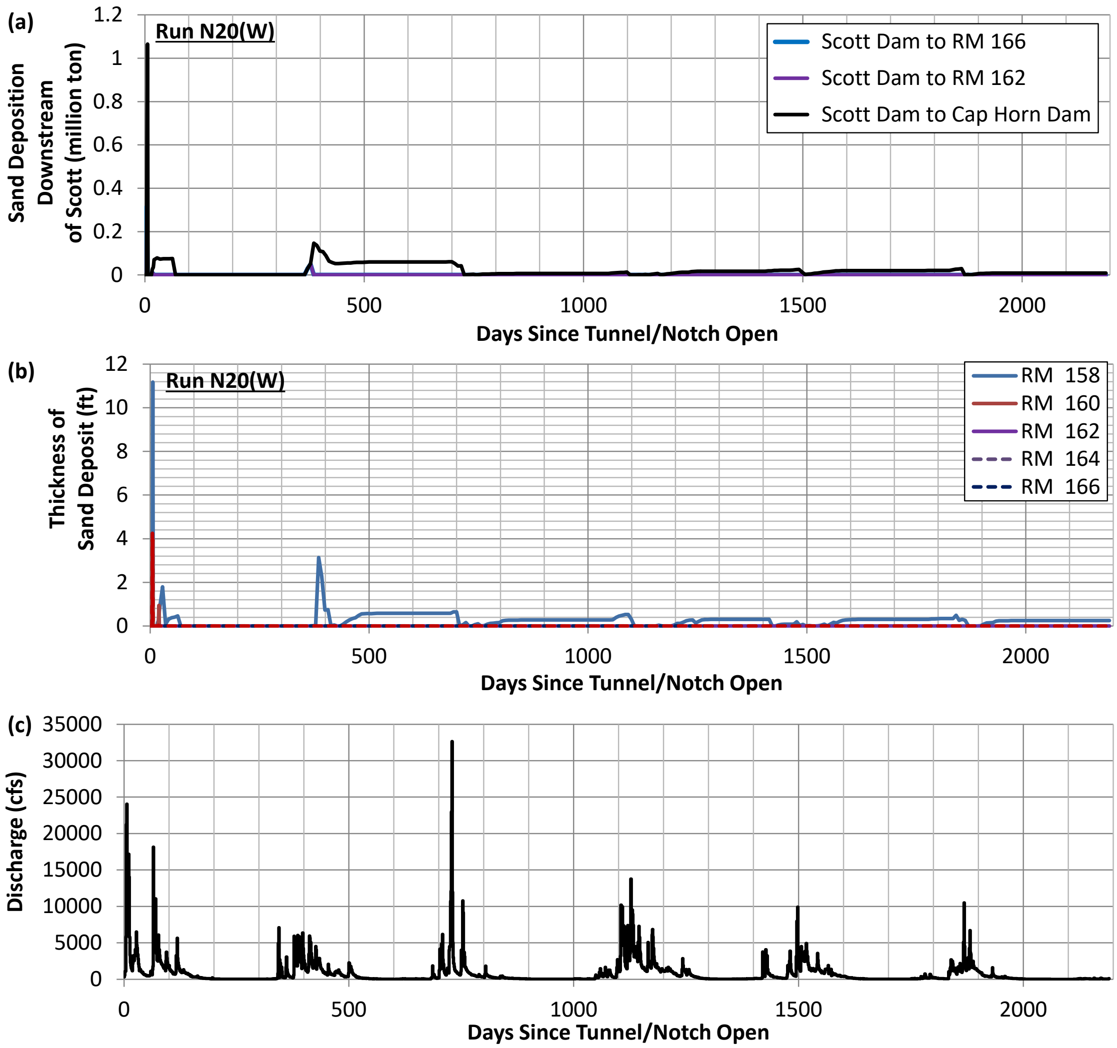

Figure C-4. Simulated mass of sand deposition in selected reaches upstream of Cape Horn Dam (a) and thickness of sand deposition in selected locations upstream of Cape Horn Dam (b), along with water discharge at Scott Dam for reference (c), Run N20(W).

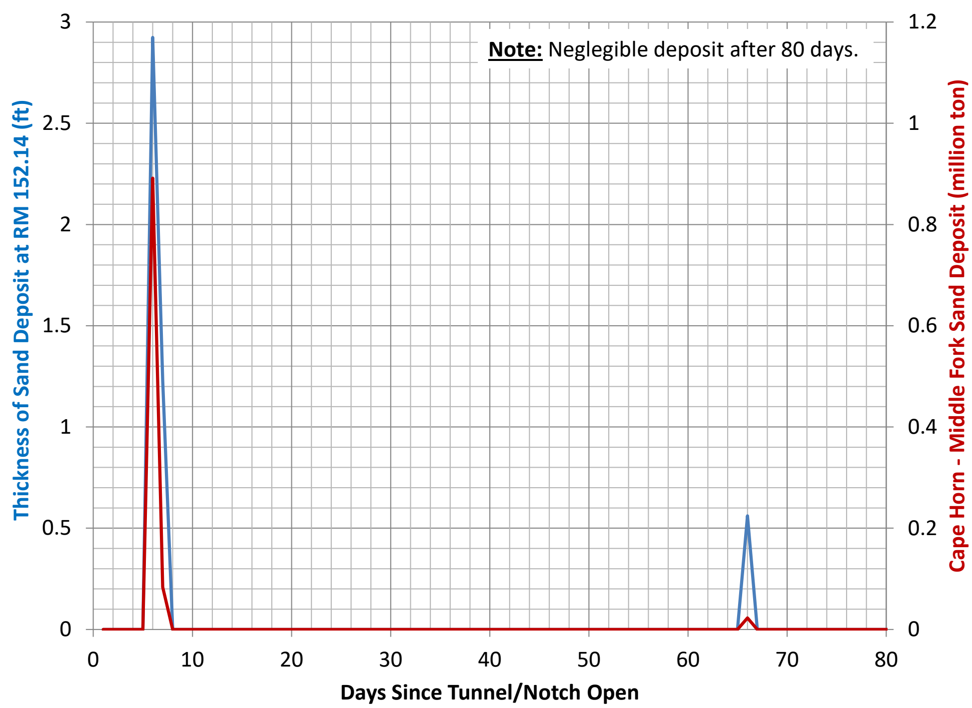

Figure C-5. Simulated thickness of sand deposit at the location where maximum sand deposit occurs downstream of Cape Horn Dam (blue line), and mass of sand deposit between Cape Horn Dam and Middle Fork Eel River confluence (red line), Run N20(W).

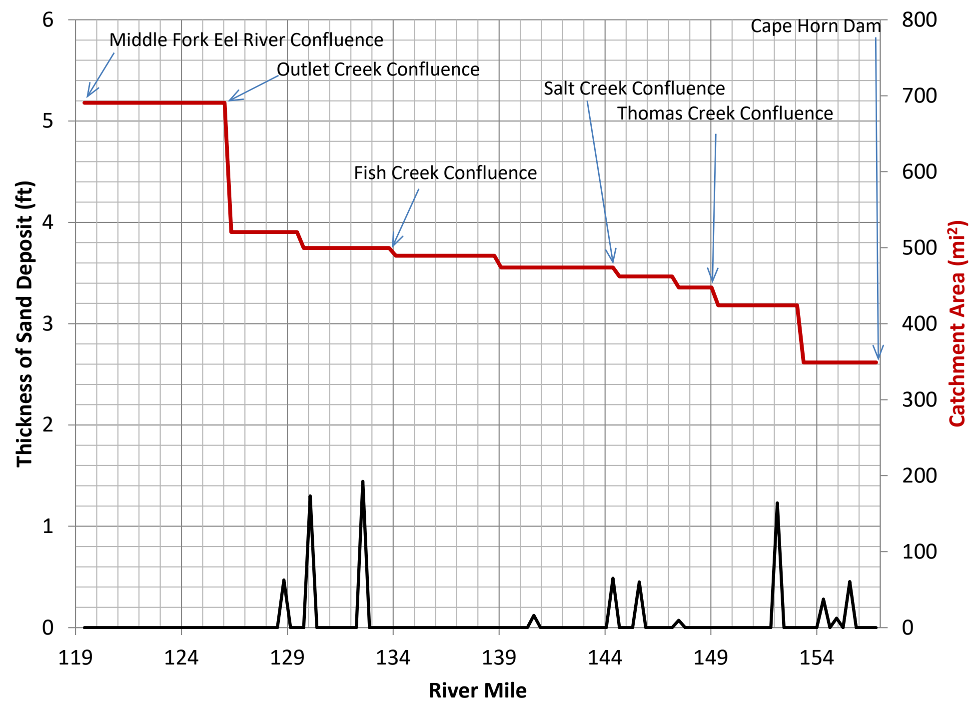

Figure C-6. Simulated thickness of sand deposit between Cape Horn Dam and Middle Fork Eel River confluence on the day maximum sand deposition occurred, Run N20(W). Catchment area and tributary locations are provided for reference.

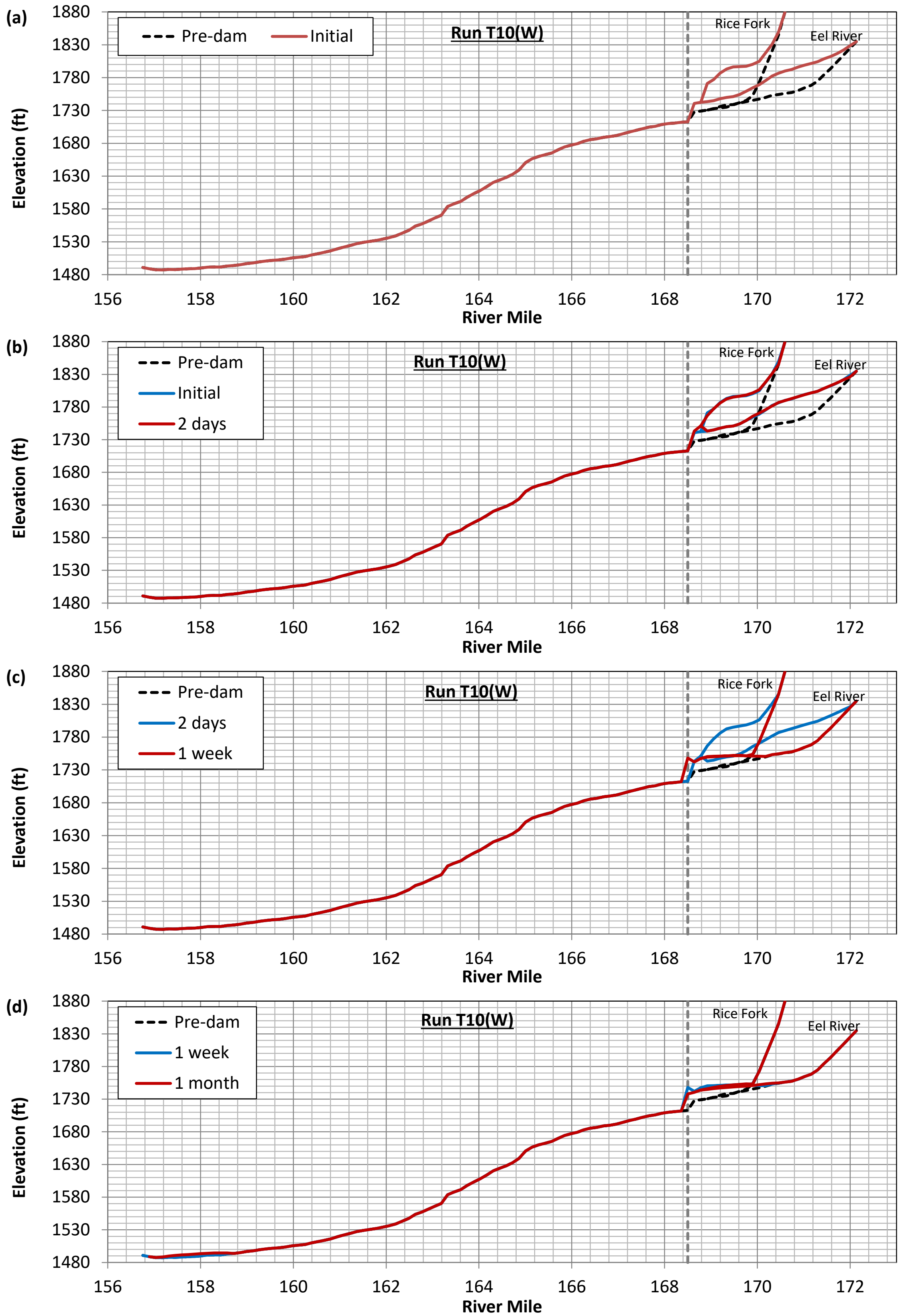

Figure C-7 continues on the next page

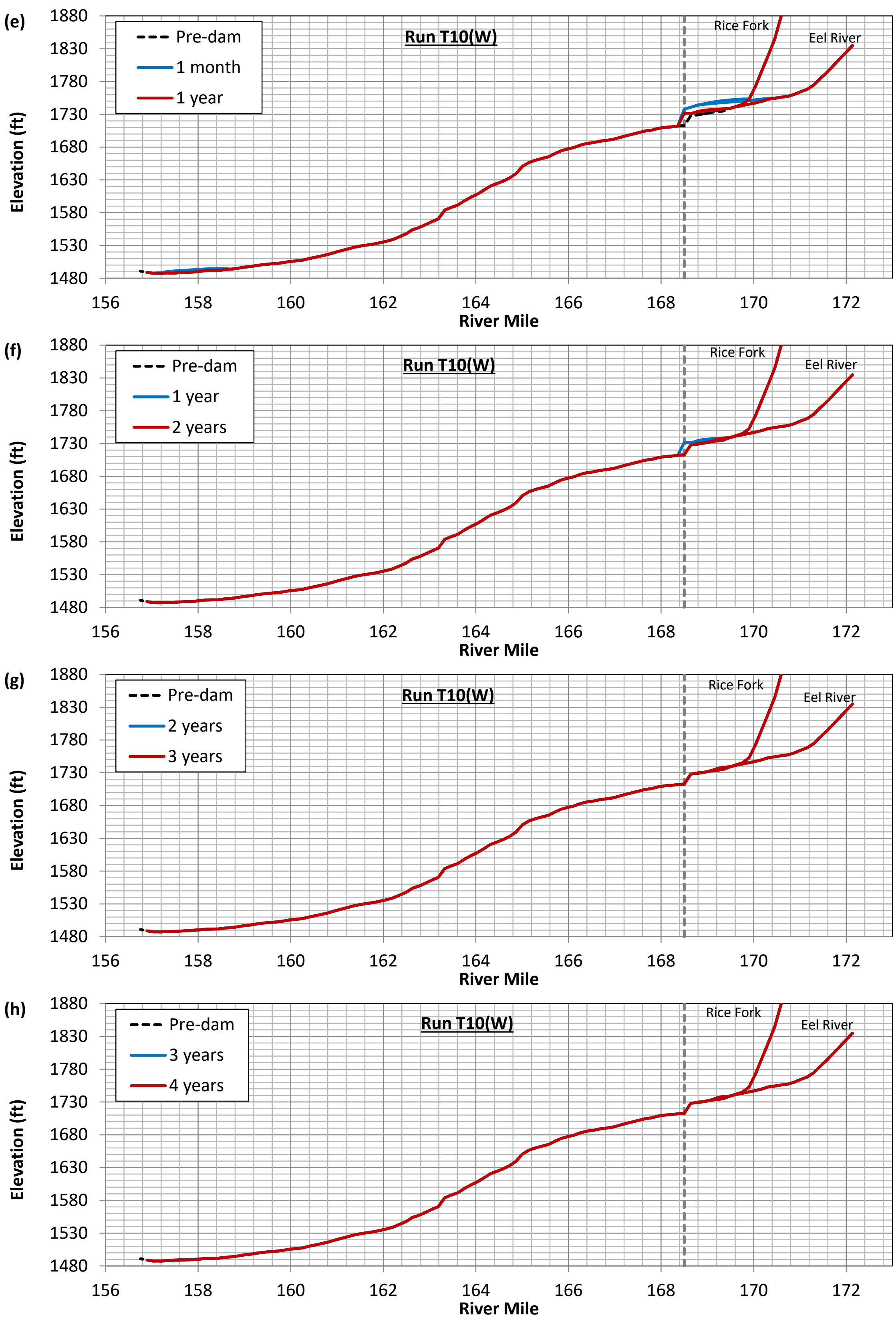

Figure C-7. Bed profile following Scott Dam removal for tunneling alternative with 10 ft tunnel diameter, dam removal starts in a wet year [Run T10(W)].

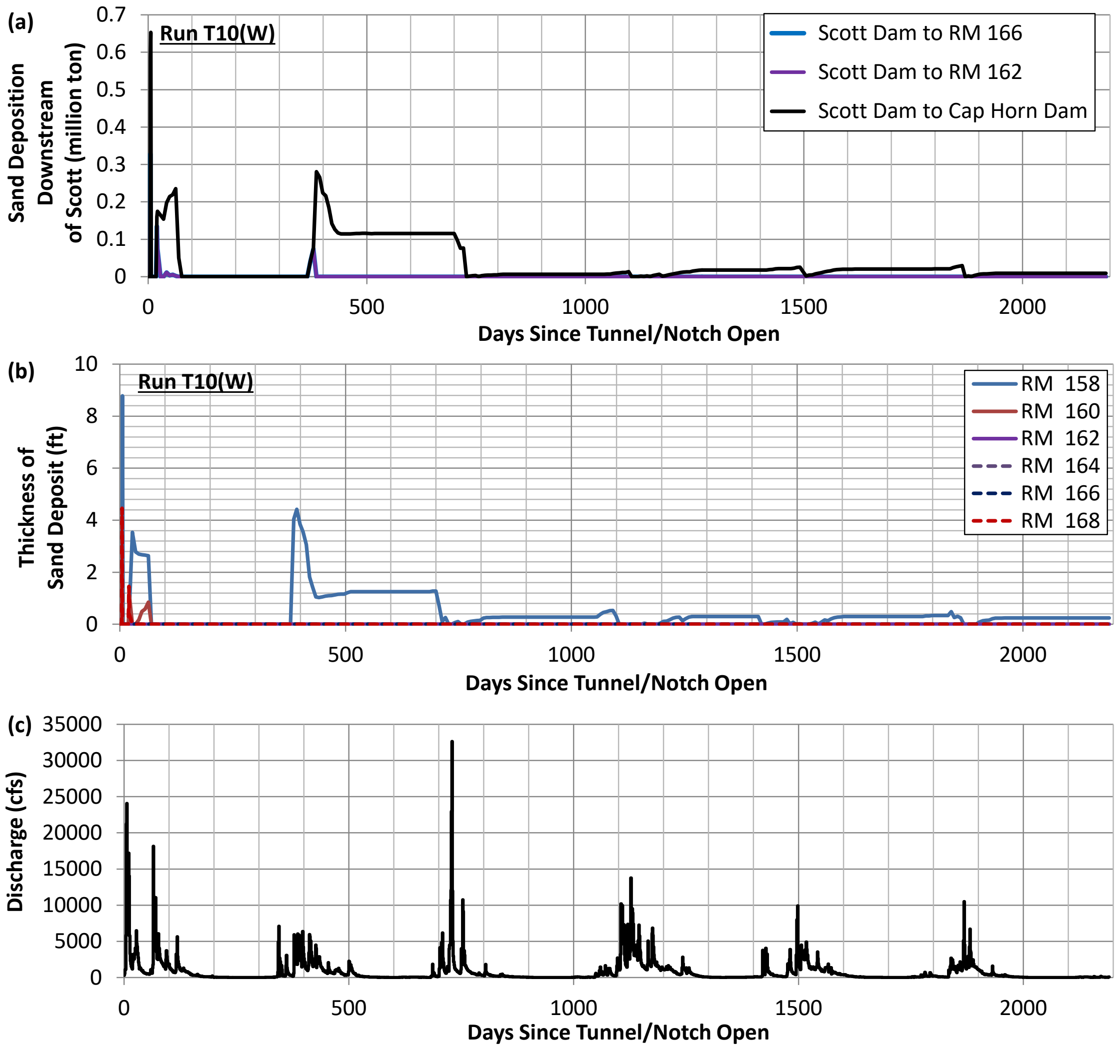

Figure C-8. Simulated mass of sand deposition in selected reaches upstream of Cape Horn Dam (a) and thickness of sand deposition in selected locations upstream of Cape Horn Dam (b), along with water discharge at Scott Dam for reference (c), Run T10(W).

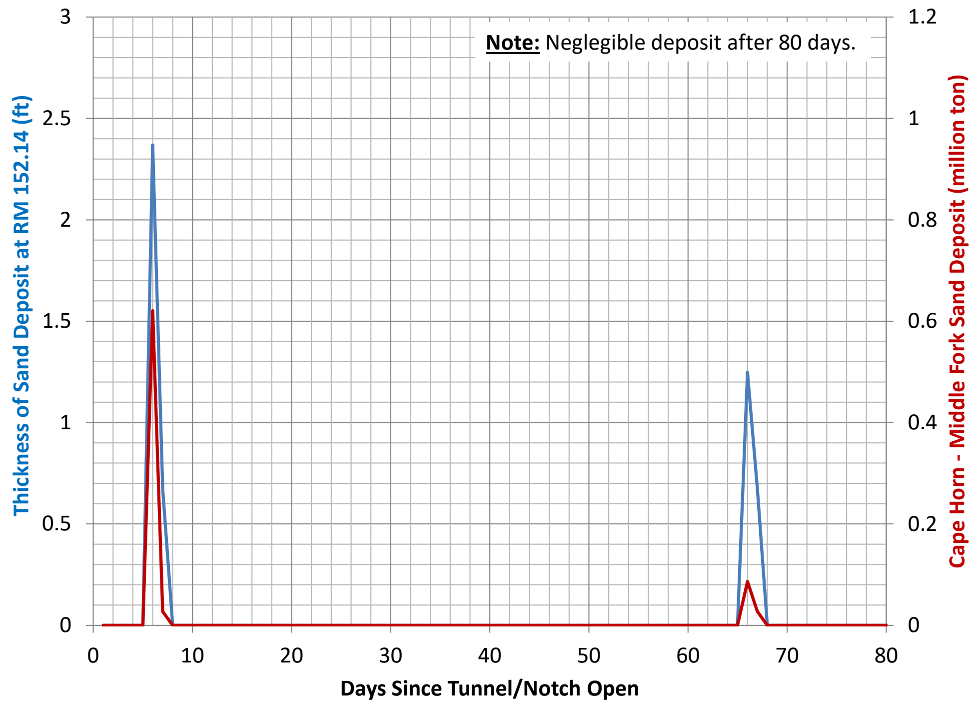

Figure C-9. Simulated thickness of sand deposit at the location where maximum sand deposit occurs downstream of Cape Horn Dam (blue line), and mass of sand deposit between Cape Horn Dam and Middle Fork Eel River confluence (red line), Run T10(W).

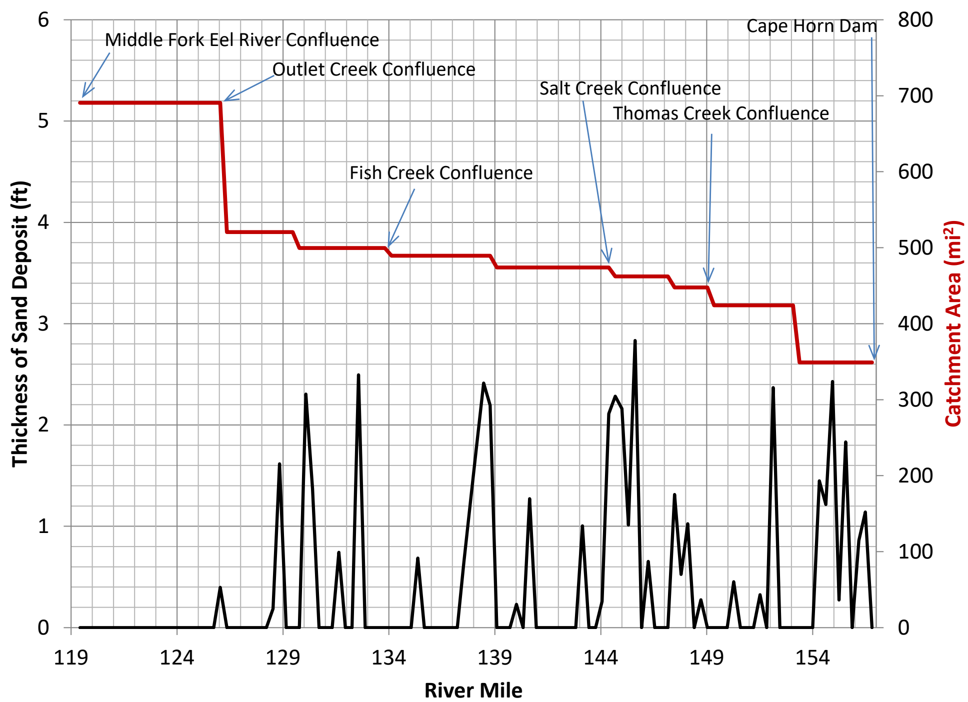

Figure C-10. Simulated thickness of sand deposit between Cape Horn Dam and Middle Fork Eel River confluence on the day maximum sand deposition occurred, Run T10(W). Catchment area and tributary locations are provided for reference.

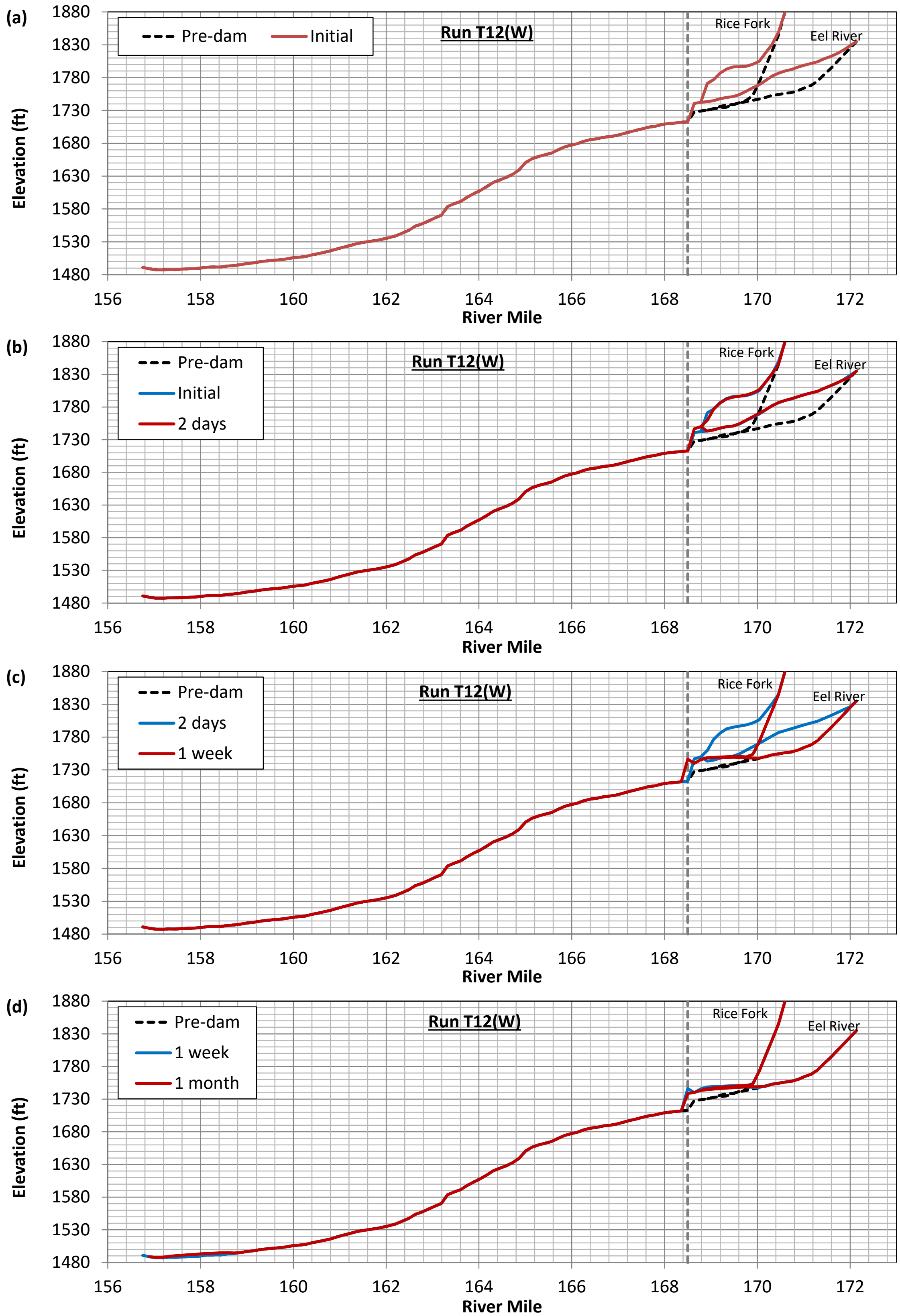

Figure C-11 continues on the next page

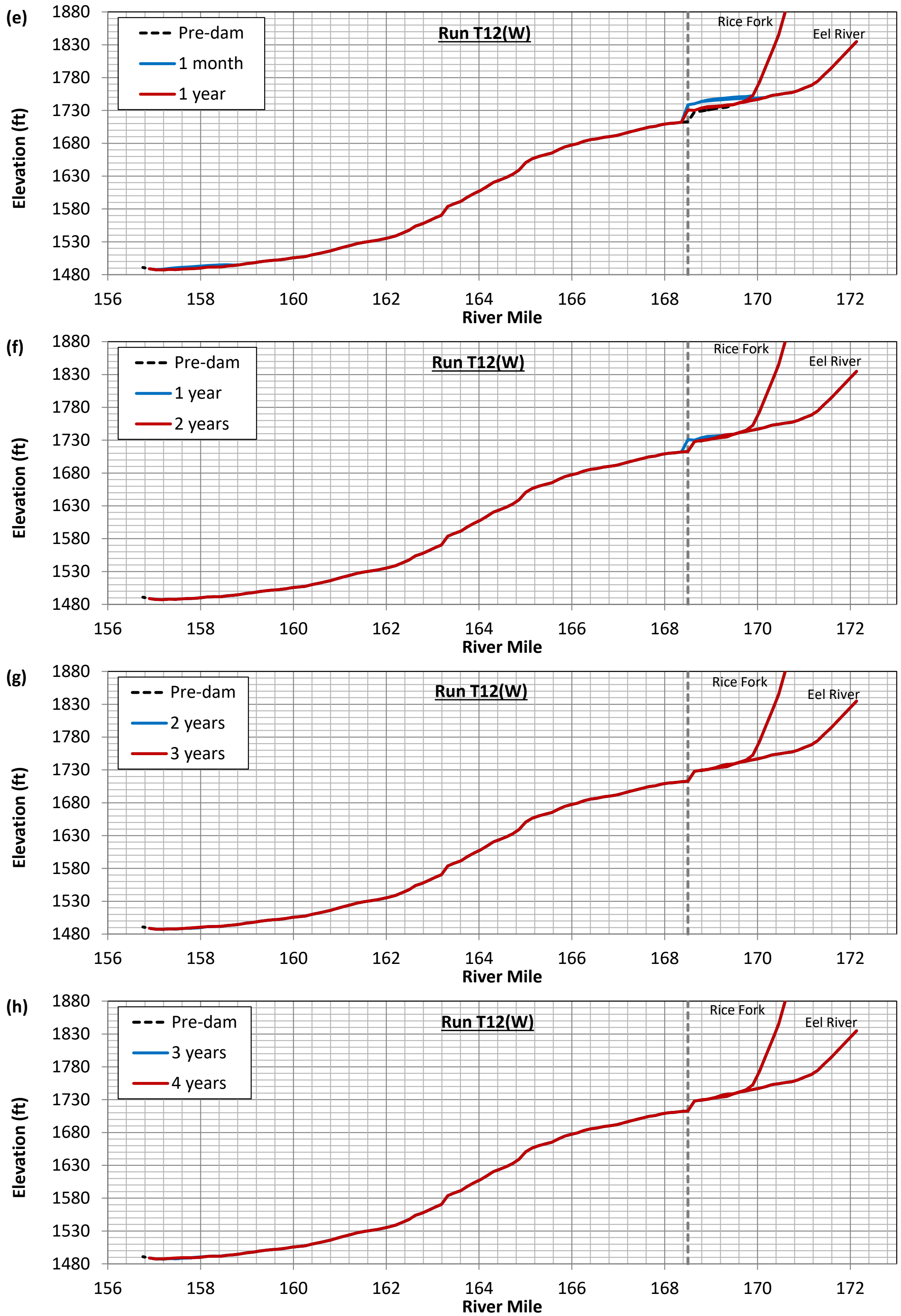

Figure C-11. Bed profile following Scott Dam removal for tunneling alternative with 12 ft tunnel diameter, dam removal starts in a wet year [Run T12(W)].

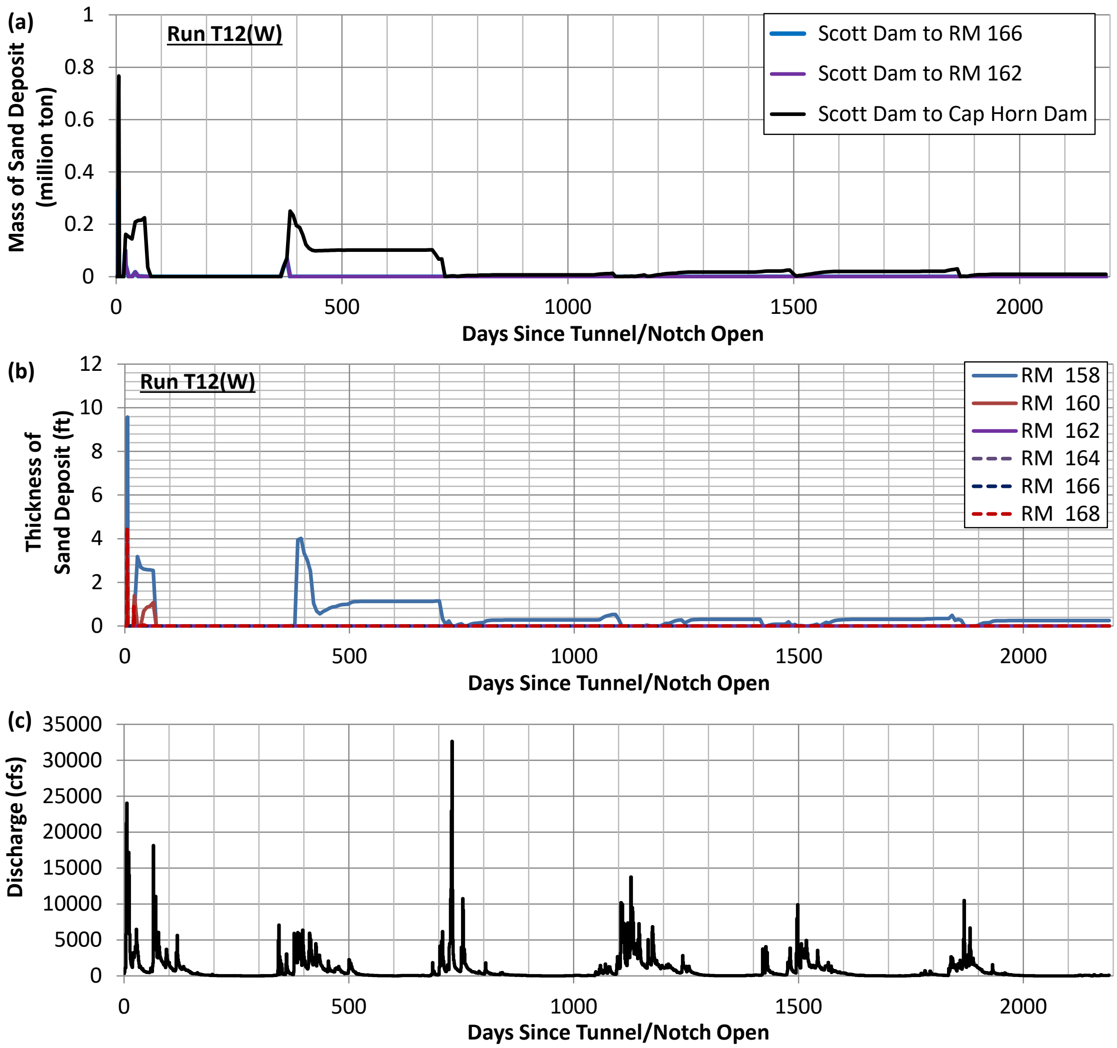

Figure C-12. Simulated mass of sand deposition in selected reaches upstream of Cape Horn Dam (a) and thickness of sand deposition in selected locations upstream of Cape Horn Dam (b), along with water discharge at Scott Dam for reference (c), Run T12(W).

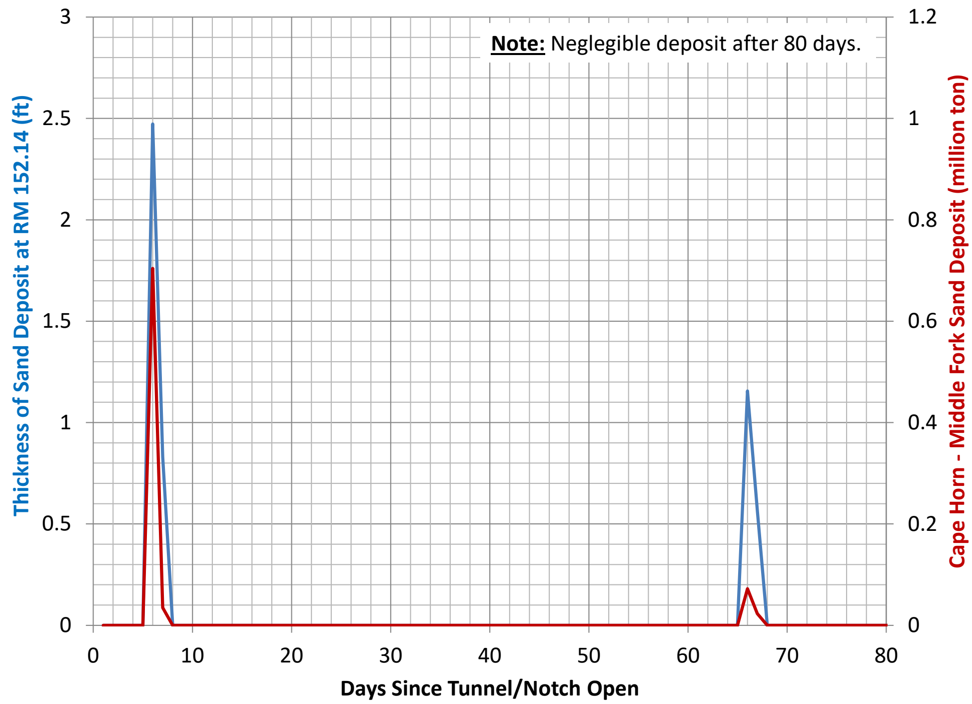

Figure C-13. Simulated thickness of sand deposit at the location where maximum sand deposit occurs downstream of Cape Horn Dam (blue line), and mass of sand deposit between Cape Horn Dam and Middle Fork Eel River confluence (red line), Run T12(W).

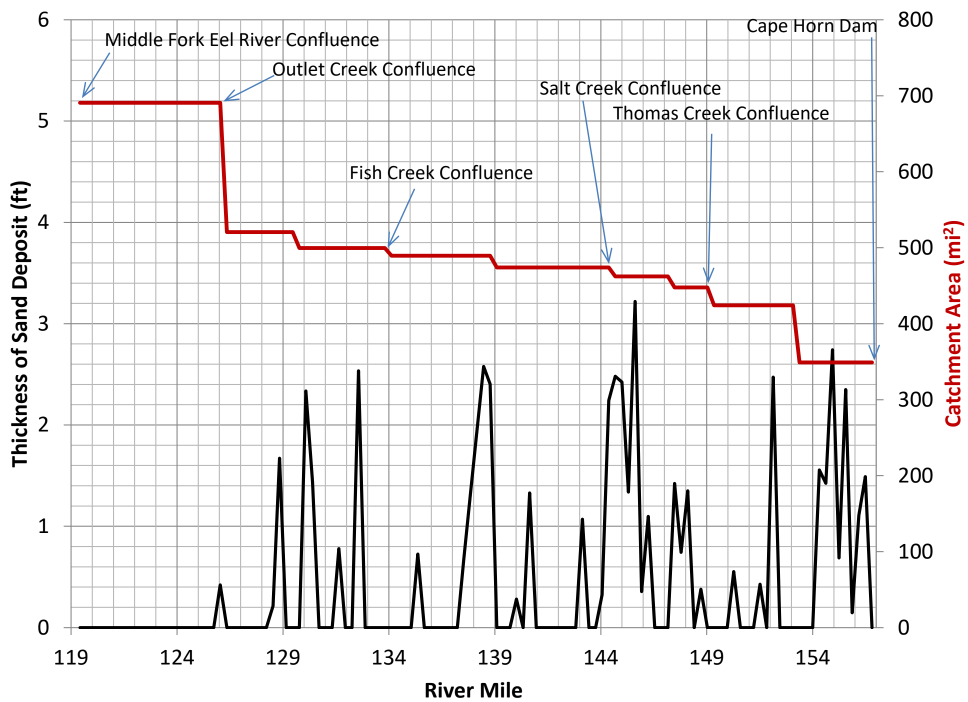

Figure C-14. Simulated thickness of sand deposit between Cape Horn Dam and Middle Fork Eel River confluence on the day maximum sand deposition occurred, Run T12(W). Catchment area and tributary locations are provided for reference.

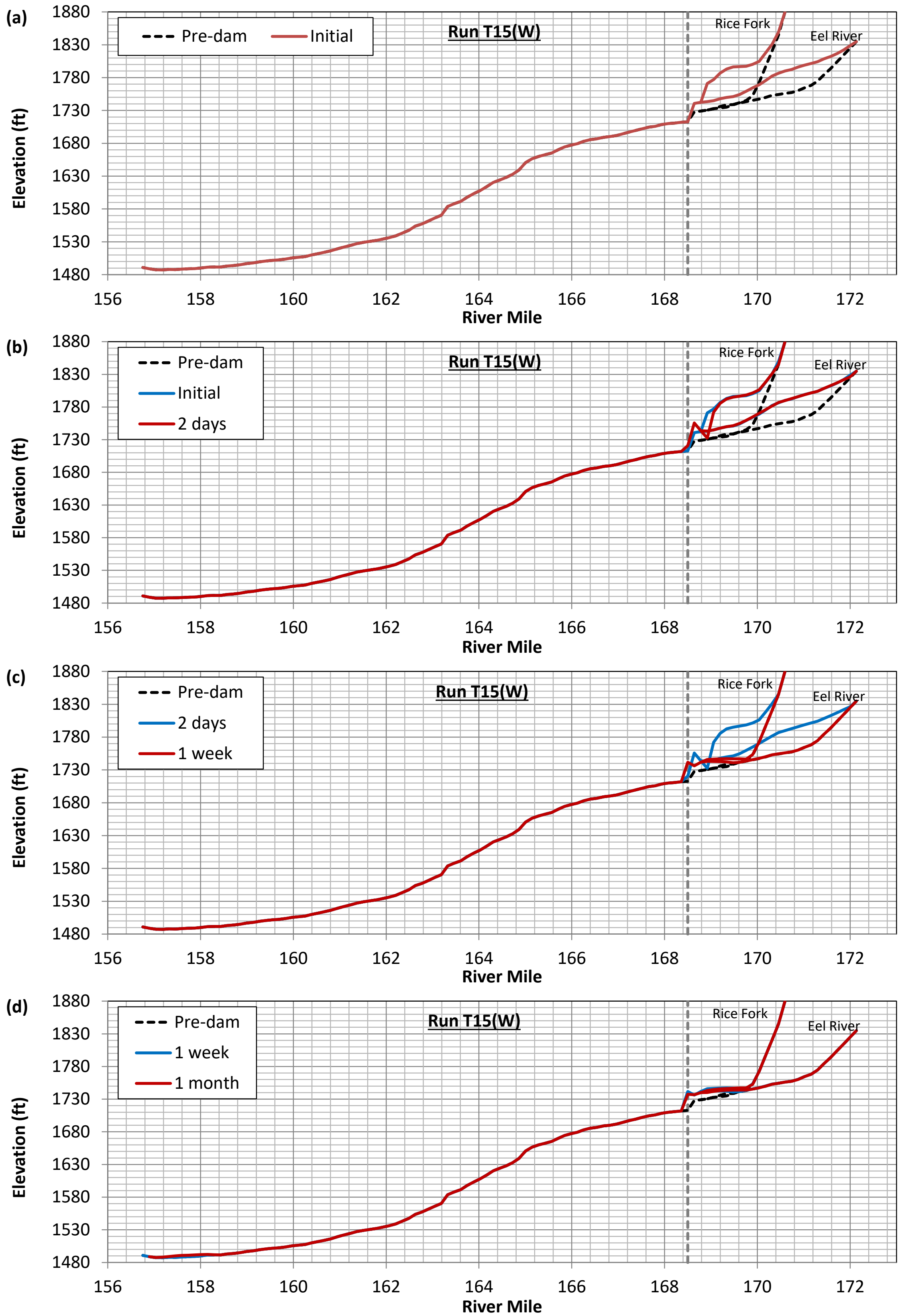

Figure C-15 continues on the next page

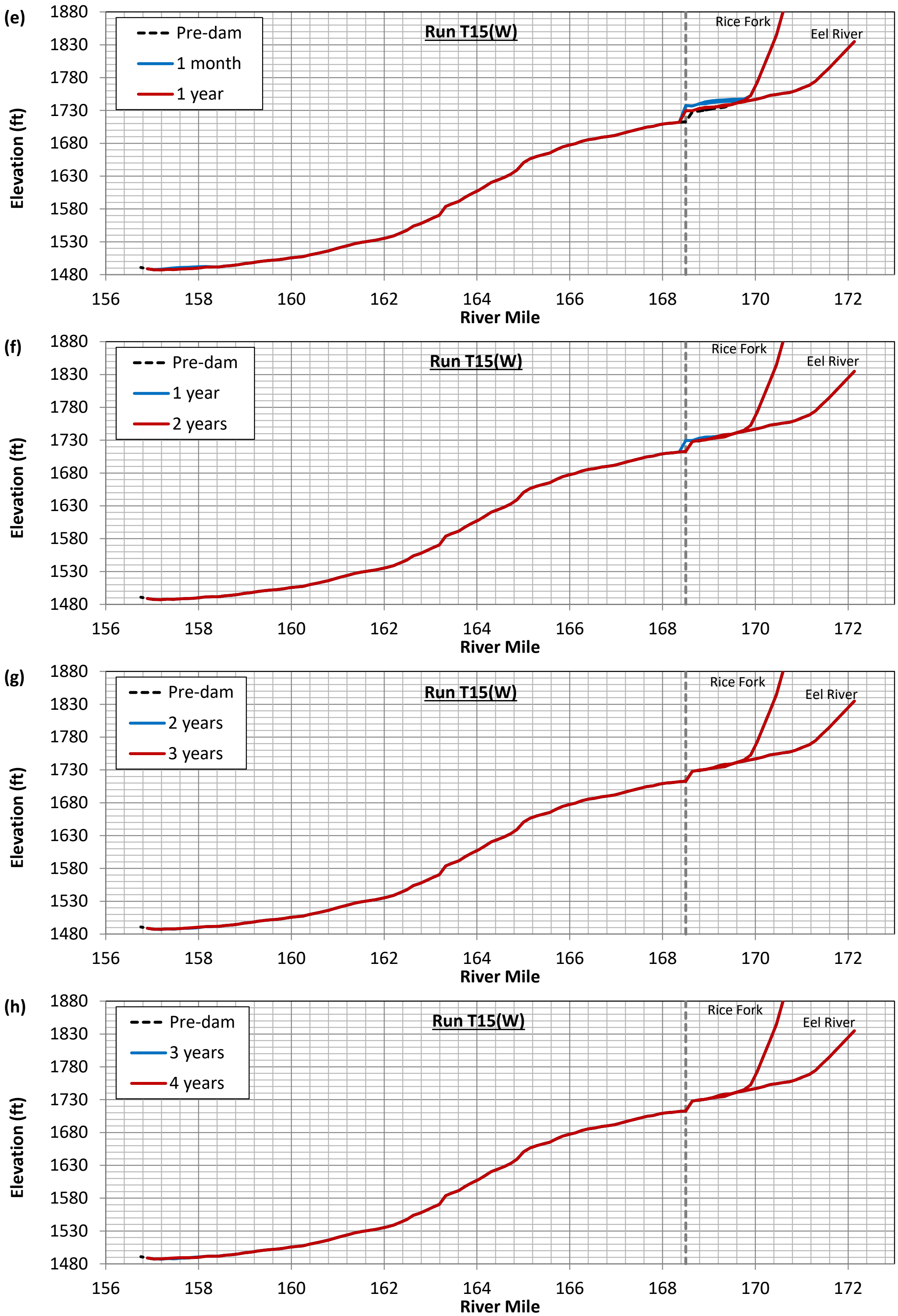

Figure C-15. Bed profile following Scott Dam removal for tunneling alternative with 15 ft tunnel diameter, dam removal starts in a wet year, Run T15(W).

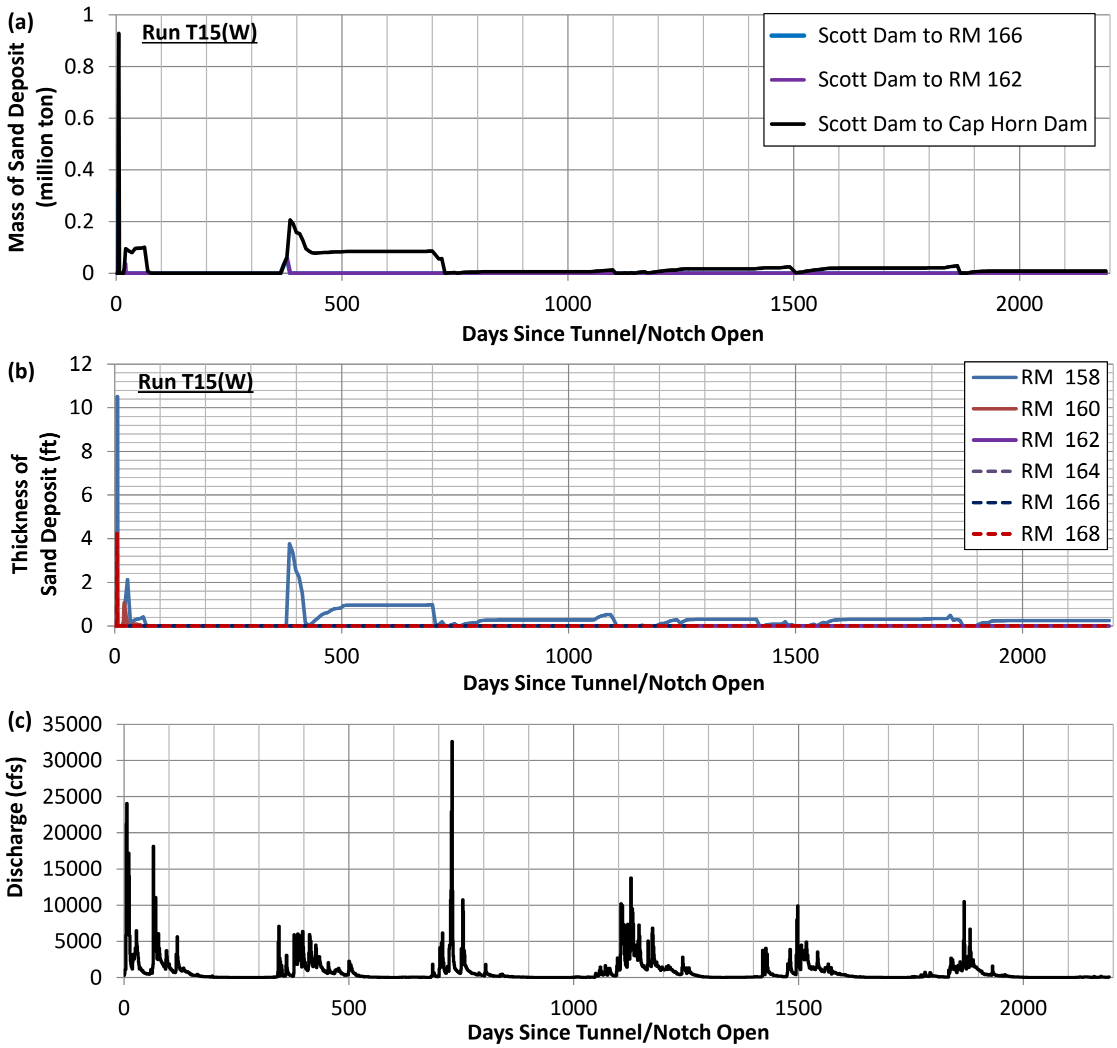

Figure C-16. Simulated mass of sand deposition in selected reaches upstream of Cape Horn Dam (a) and thickness of sand deposition in selected locations upstream of Cape Horn Dam (b), along with water discharge at Scott Dam for reference (c), Run T15(W).

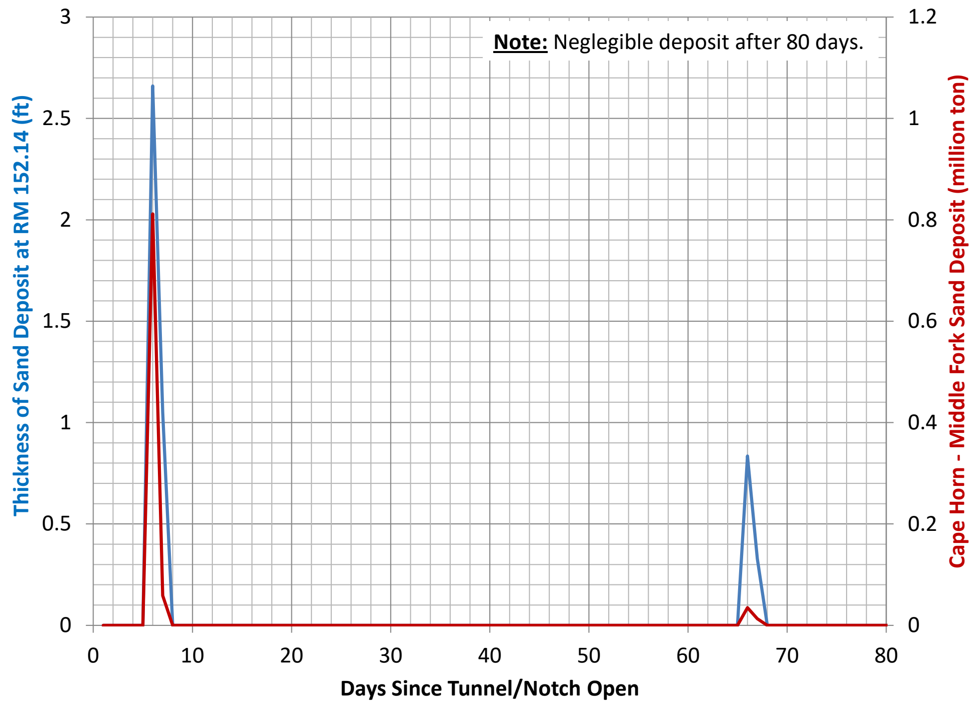

Figure C-17. Simulated thickness of sand deposit at the location where maximum sand deposit occurs downstream of Cape Horn Dam (blue line), and mass of sand deposit between Cape Horn Dam and Middle Fork Eel River confluence (red line), Run T15(W).

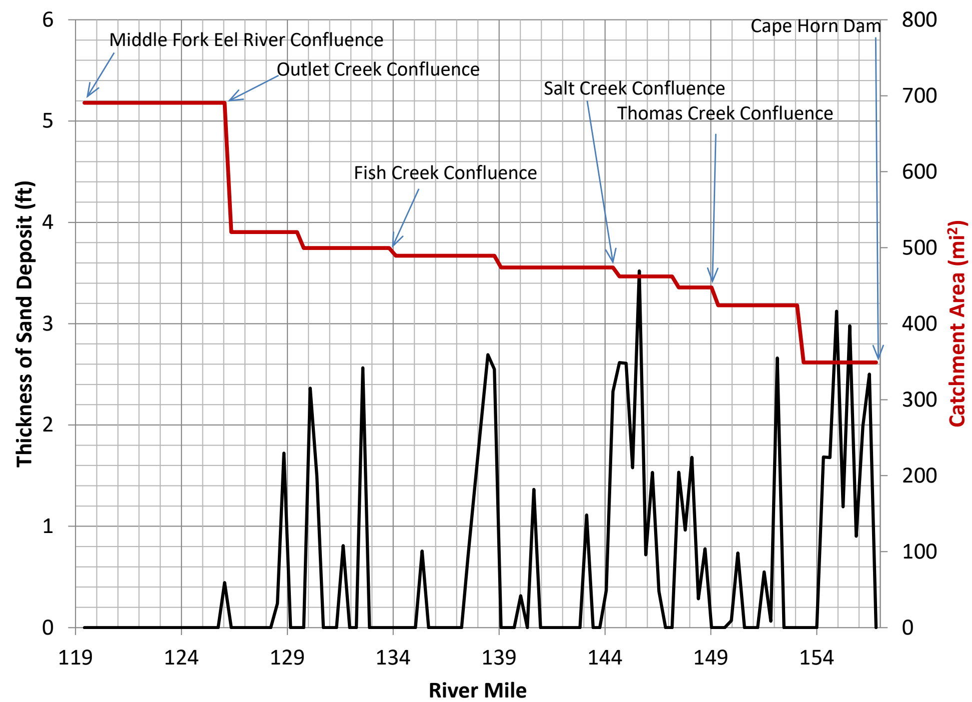

Figure C-18. Simulated thickness of sand deposit between Cape Horn Dam and Middle Fork Eel River confluence on the day maximum sand deposition occurred, Run T15(W). Catchment area and tributary locations are provided for reference.

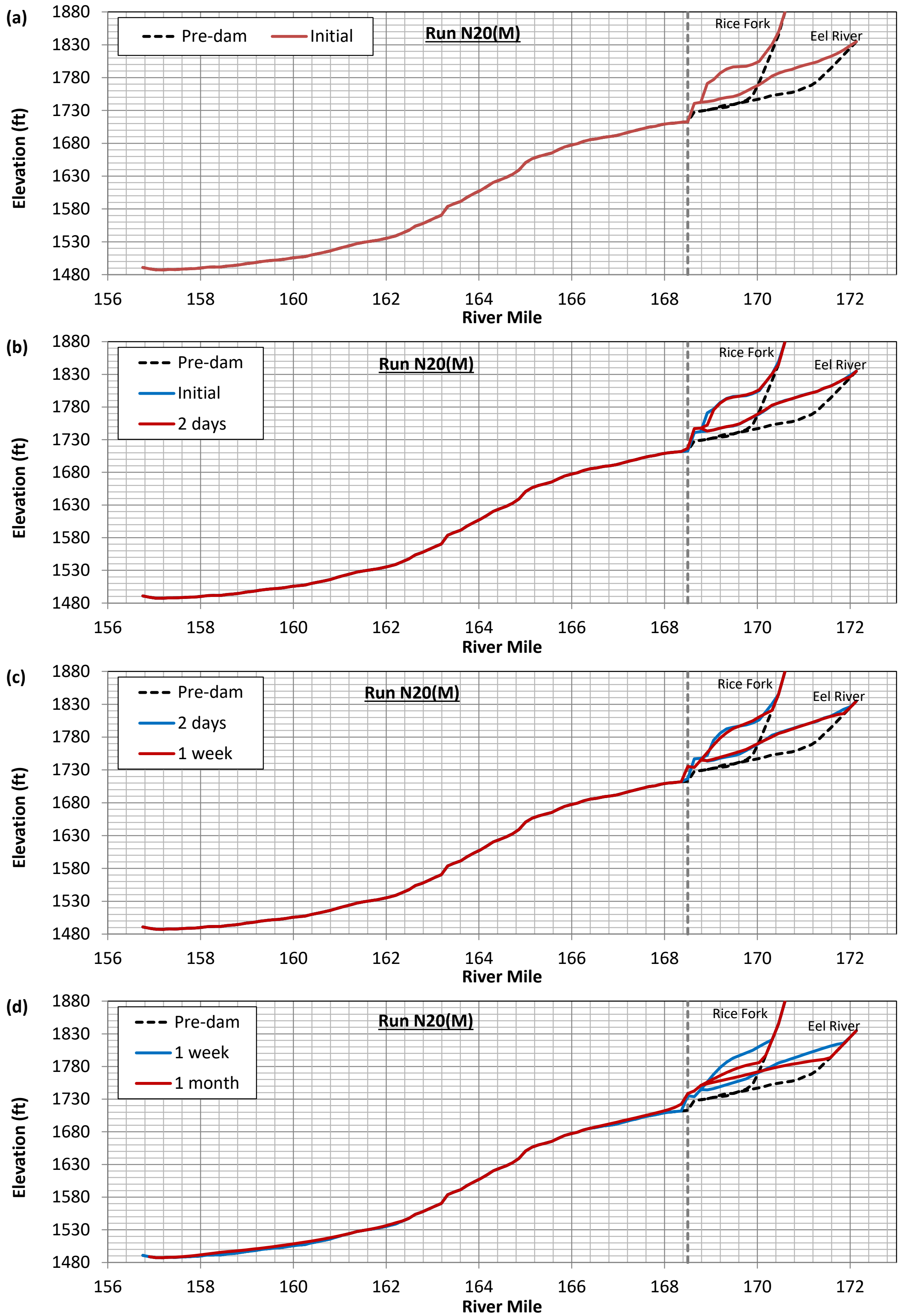

Figure C-19 continues on the next page

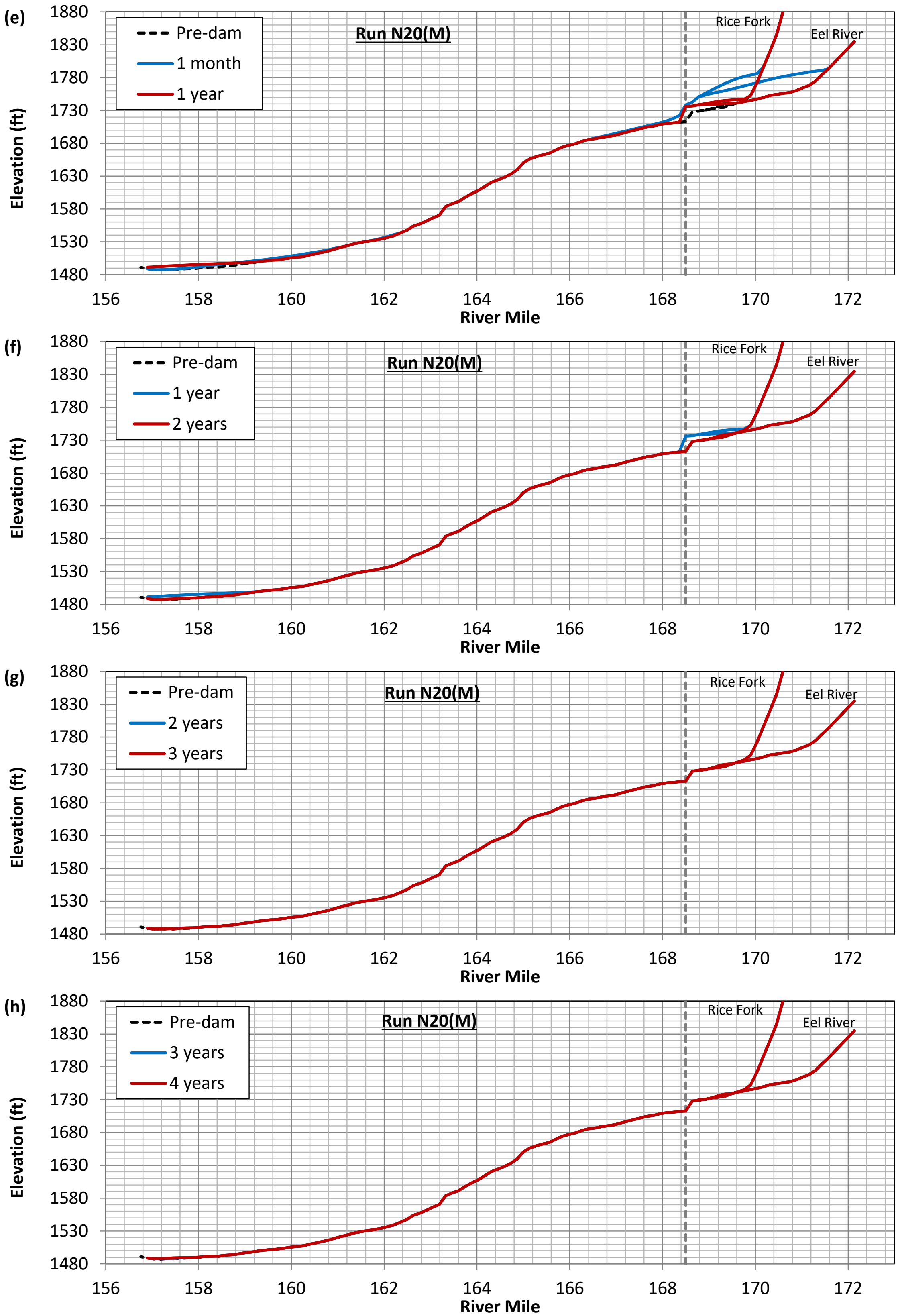

Figure C-19. Bed profile following Scott Dam removal for vertical notching alternative with 20 ft notch width, dam removal starts in a median year [Run N20(M)].

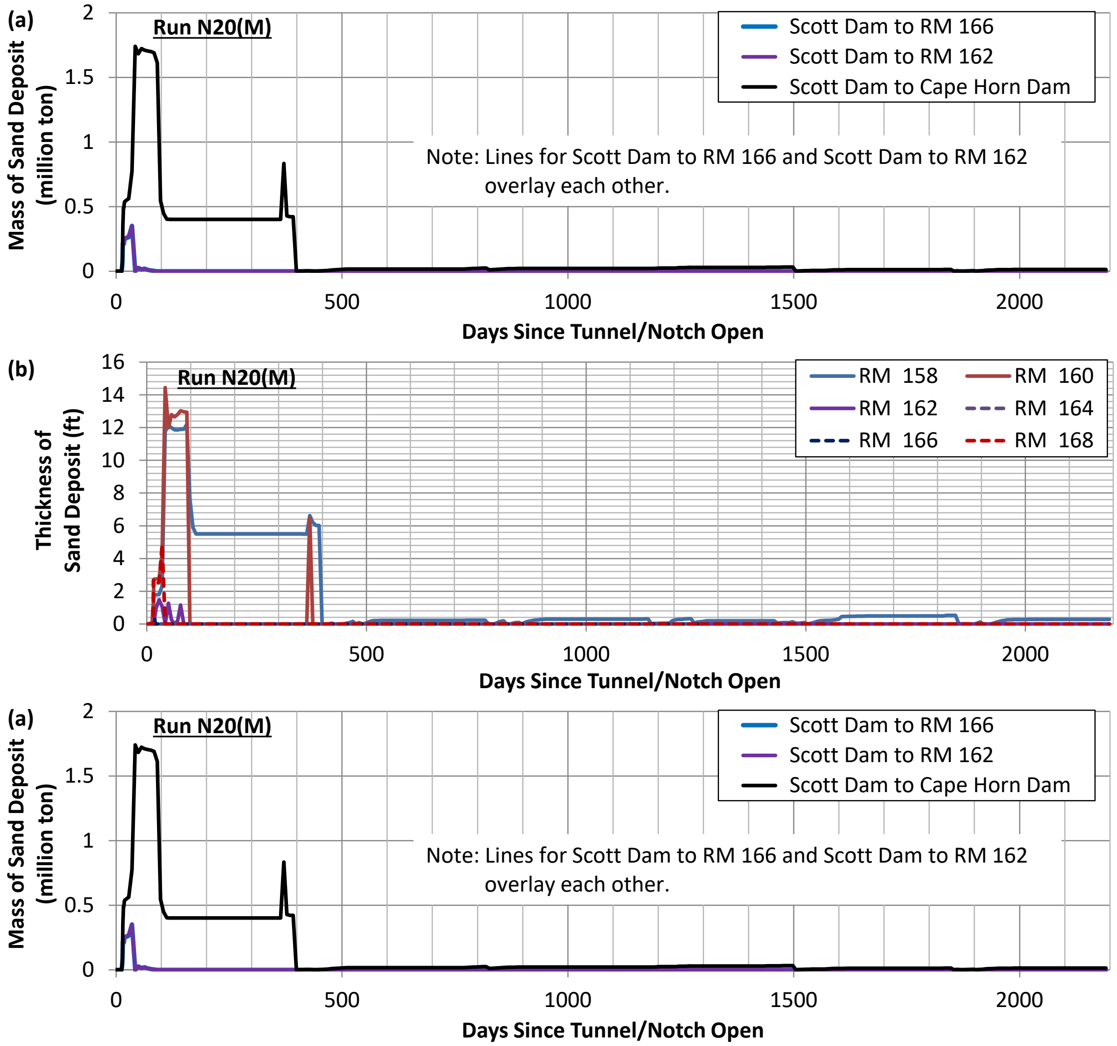

Figure C-20. Simulated mass of sand deposition in selected reaches upstream of Cape Horn Dam (a) and thickness of sand deposition in selected locations upstream of Cape Horn Dam (b), along with water discharge at Scott Dam for reference (c), Run N20(M).

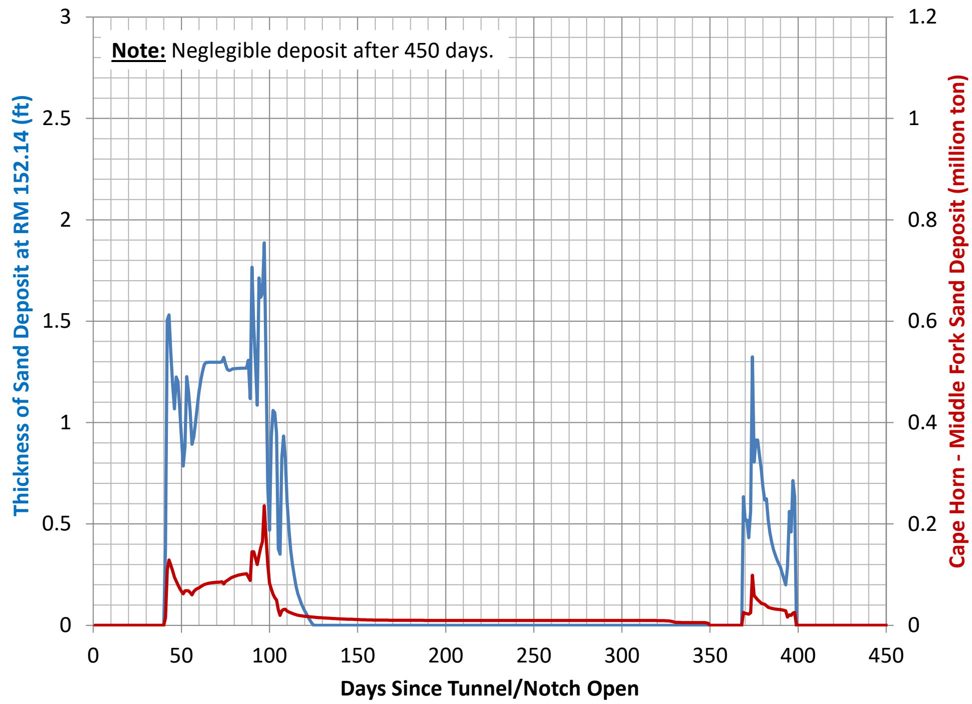

Figure C-21. Simulated thickness of sand deposit at the location where maximum sand deposit occurs downstream of Cape Horn Dam (blue line), and mass of sand deposit between Cape Horn Dam and Middle Fork Eel River confluence (red line), Run N20(M).

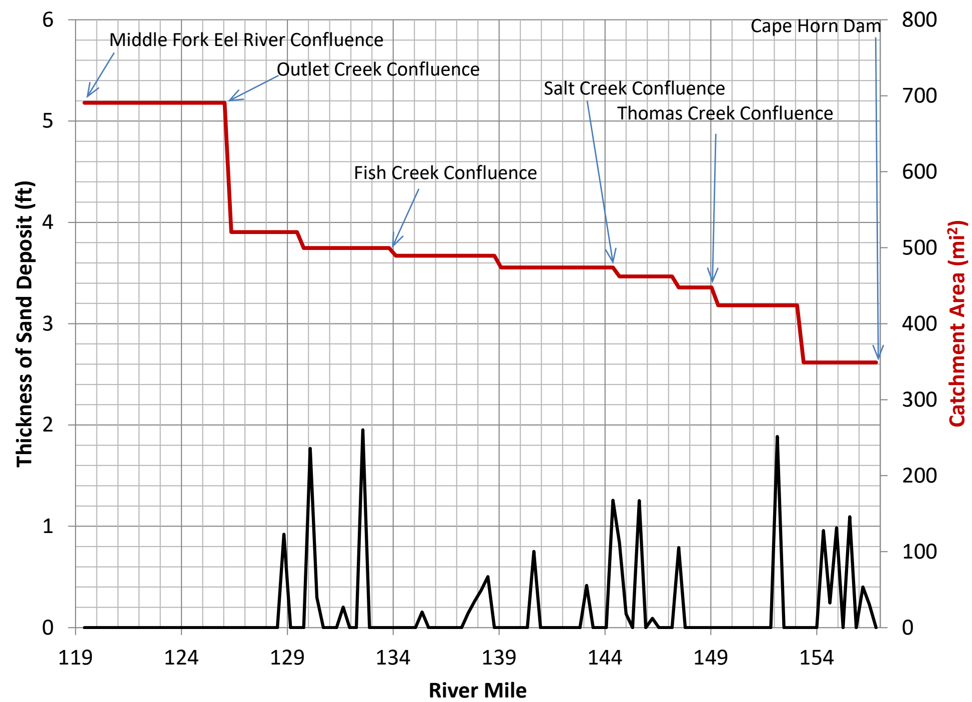

Figure C-22. Simulated thickness of sand deposit between Cape Horn Dam and Middle Fork Eel River confluence on the day maximum sand deposition occurred, Run N20(M). Catchment area and tributary locations are provided for reference.

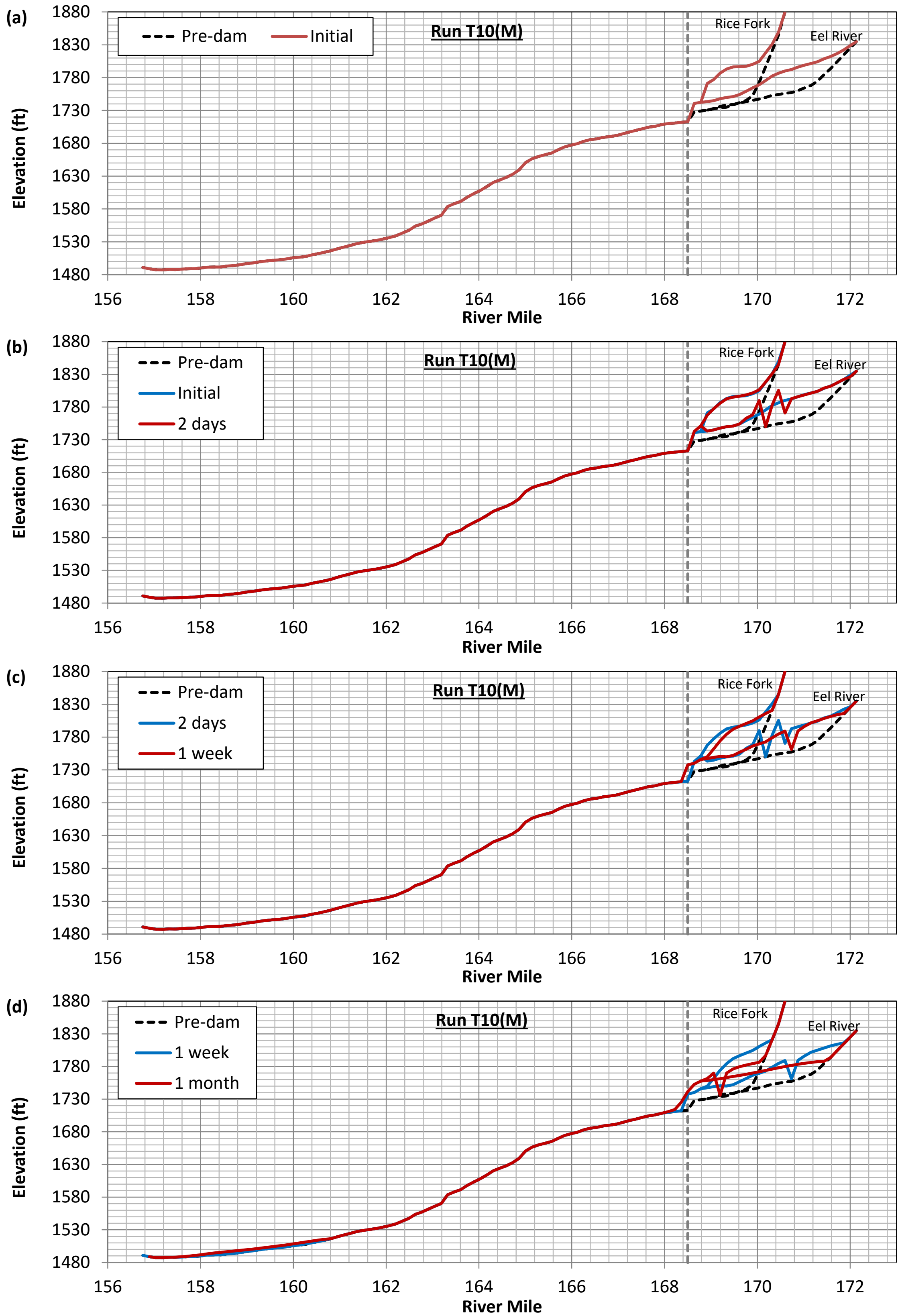

Figure C-23 continues on the next page

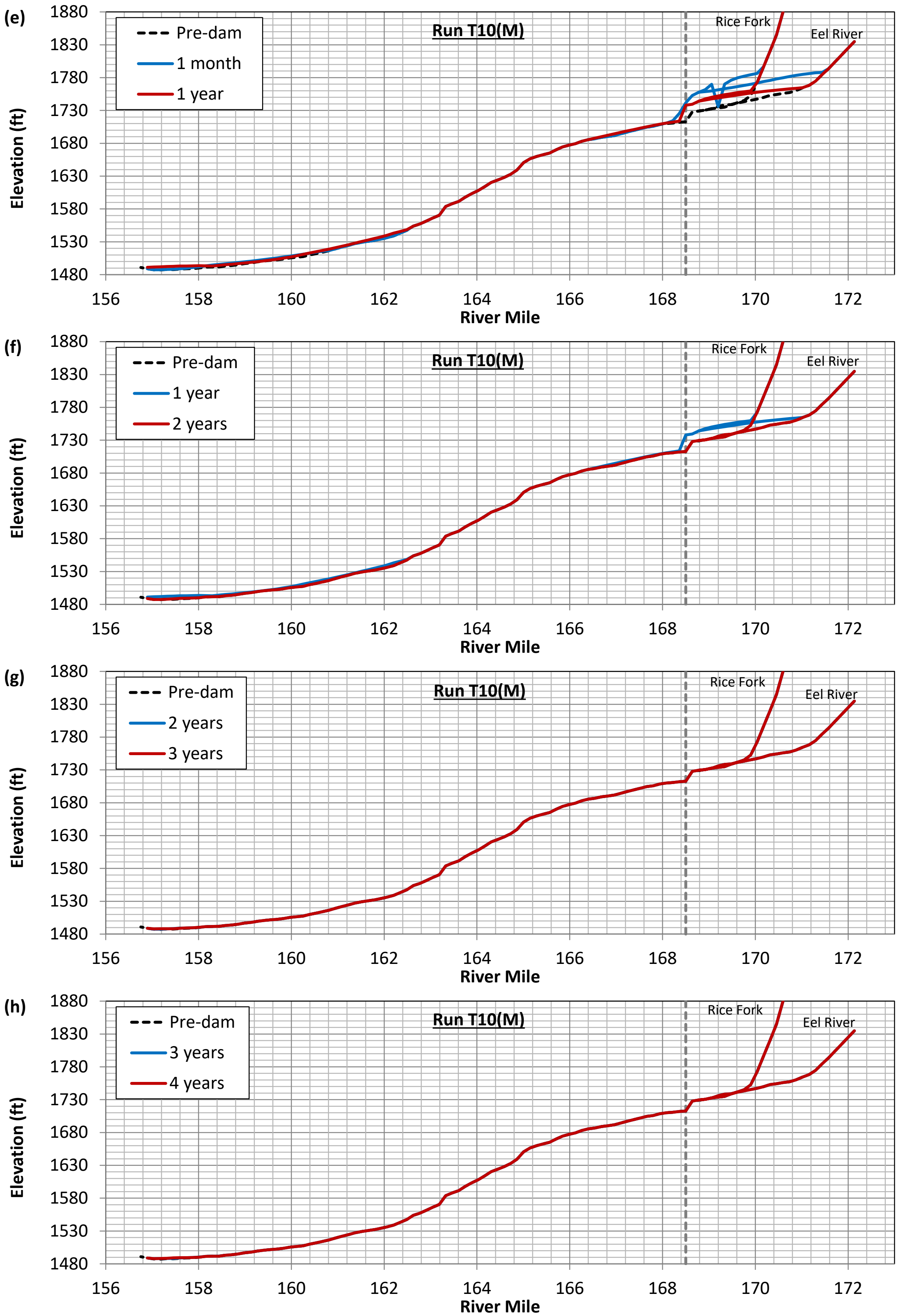

Figure C-23. Bed profile following Scott Dam removal for tunneling alternative with 10 ft tunnel diameter, dam removal starts in a median year.

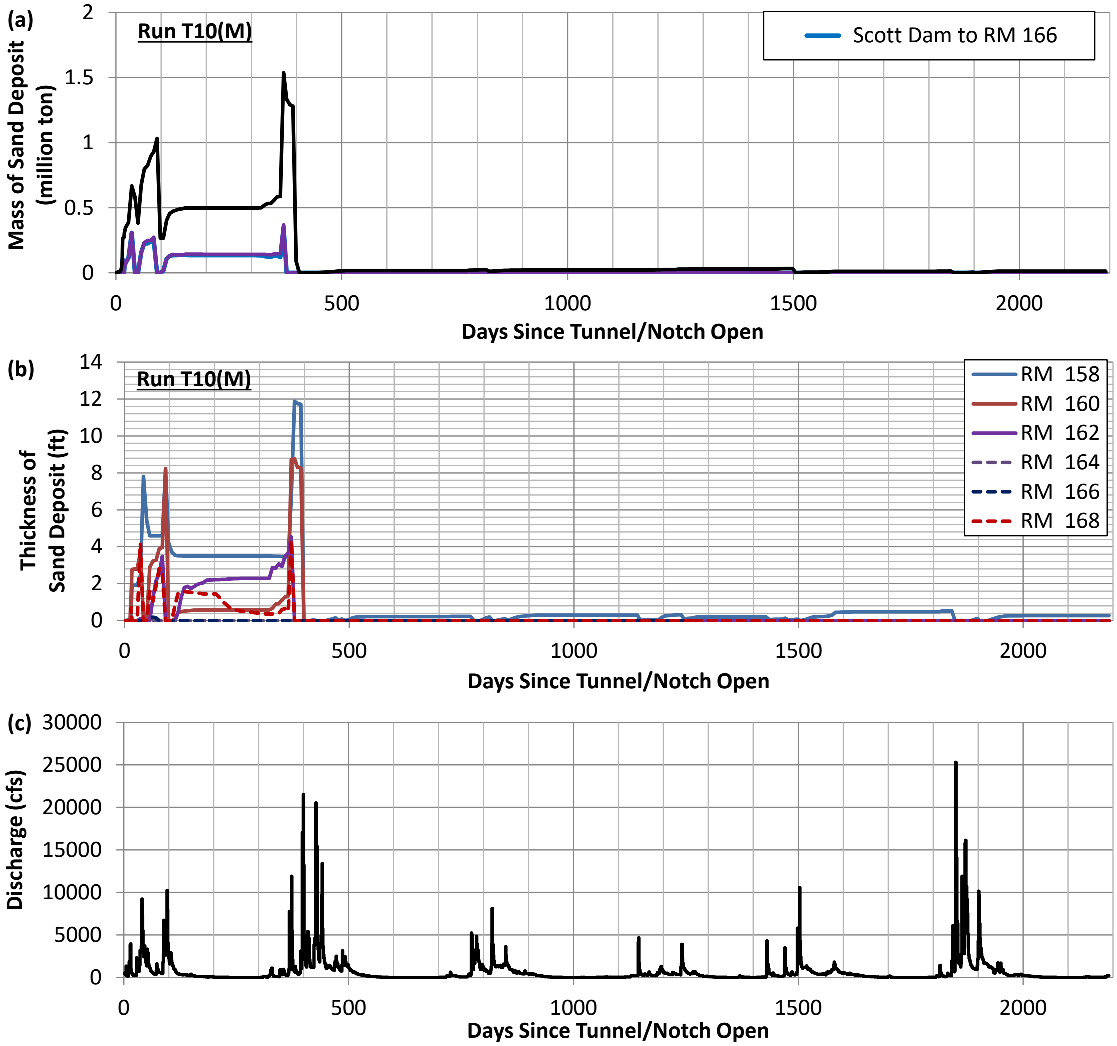

Figure C-24. Simulated mass of sand deposition in selected reaches upstream of Cape Horn Dam (a) and thickness of sand deposition in selected locations upstream of Cape Horn Dam (b), along with water discharge at Scott Dam for reference (c), Run T10(M).

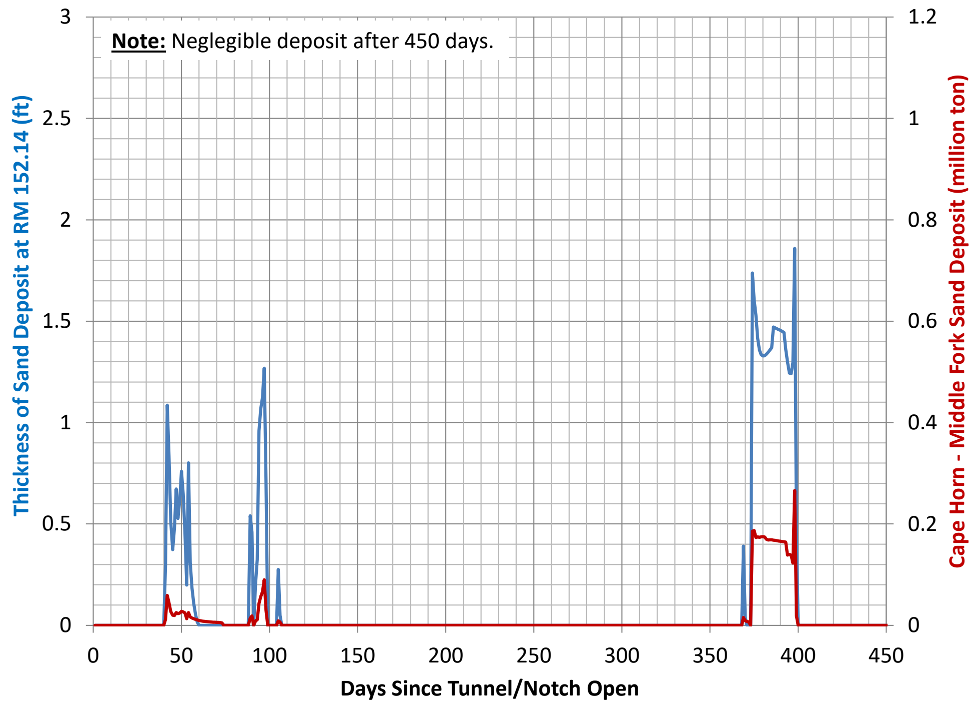

Figure C-25. Simulated thickness of sand deposit at the location where maximum sand deposit occurs downstream of Cape Horn Dam (blue line), and mass of sand deposit between Cape Horn Dam and Middle Fork Eel River confluence (red line), Run T10(M).

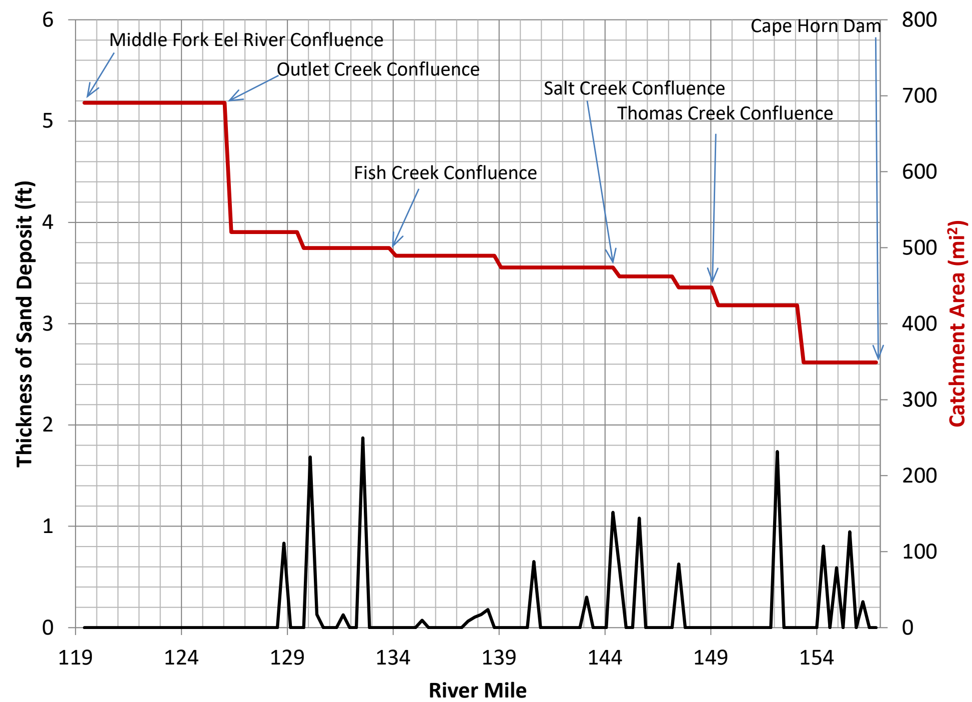

Figure C-26. Simulated thickness of sand deposit between Cape Horn Dam and Middle Fork Eel River confluence on the day maximum sand deposition occurred, Run T10(M). Catchment area and tributary locations are provided for reference.

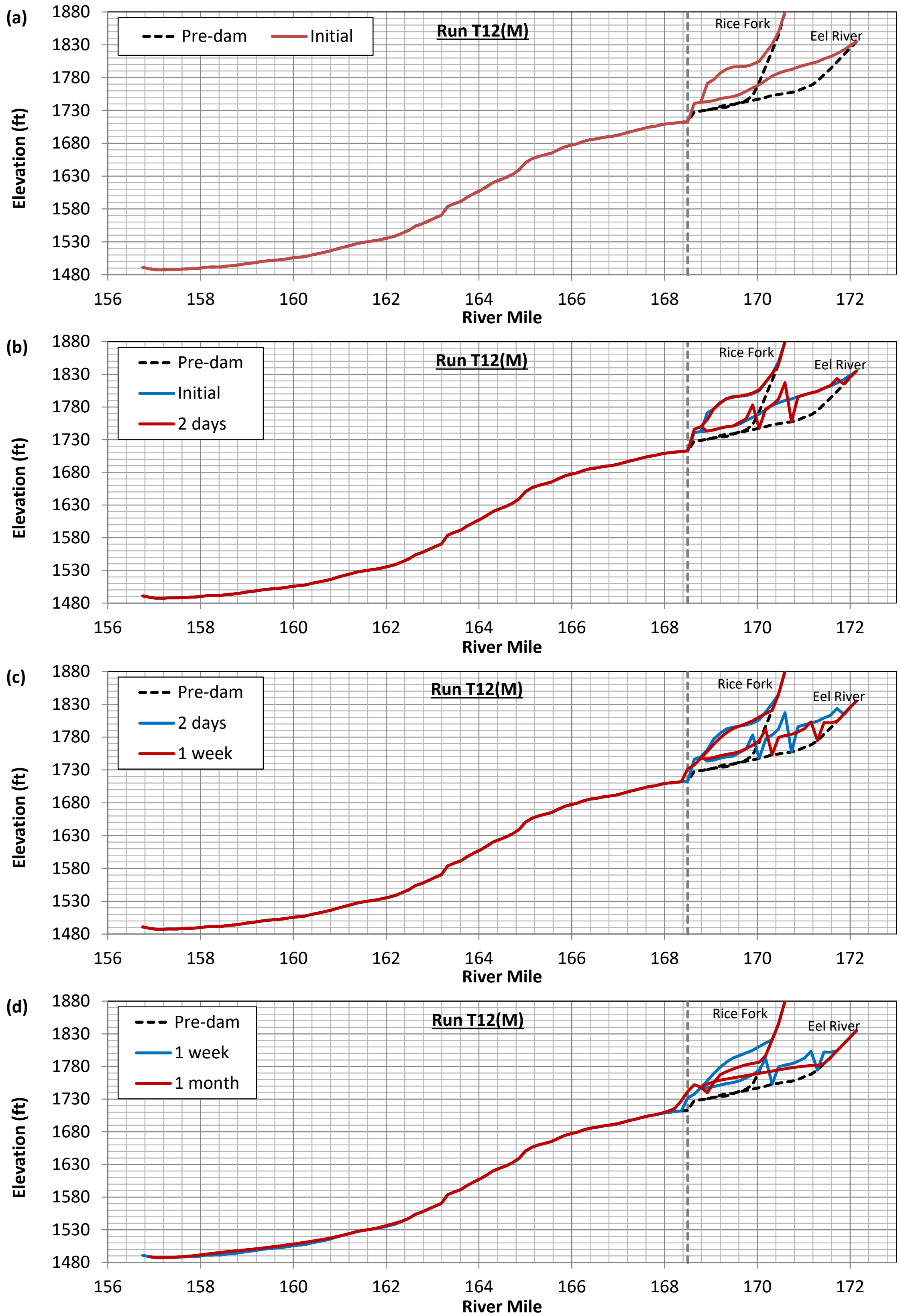

Figure C-27 continues on the next page

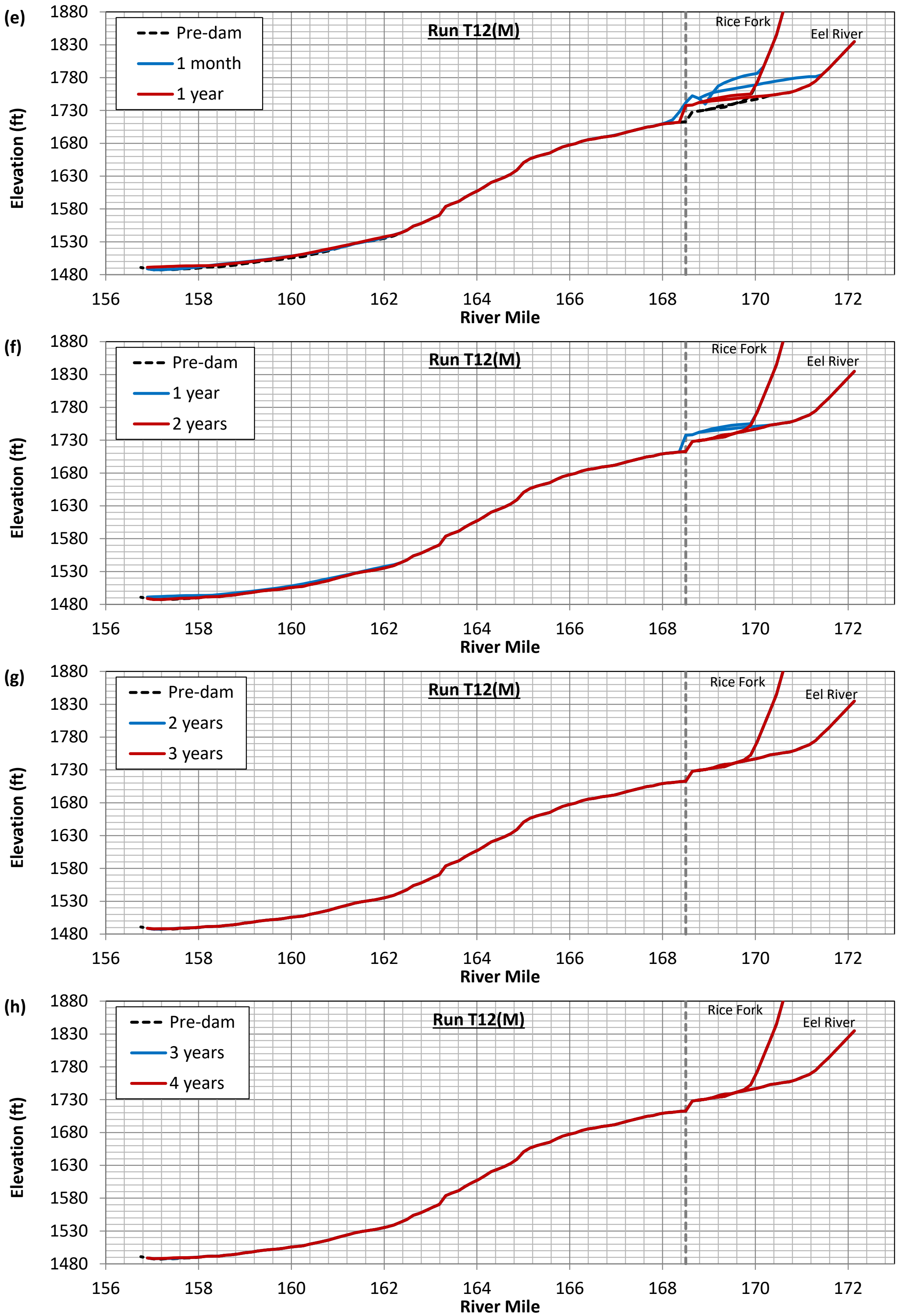

Figure C-27. Bed profile following Scott Dam removal for tunneling alternative with 12 ft tunnel diameter, dam removal starts in a median year [Run T12(M)].

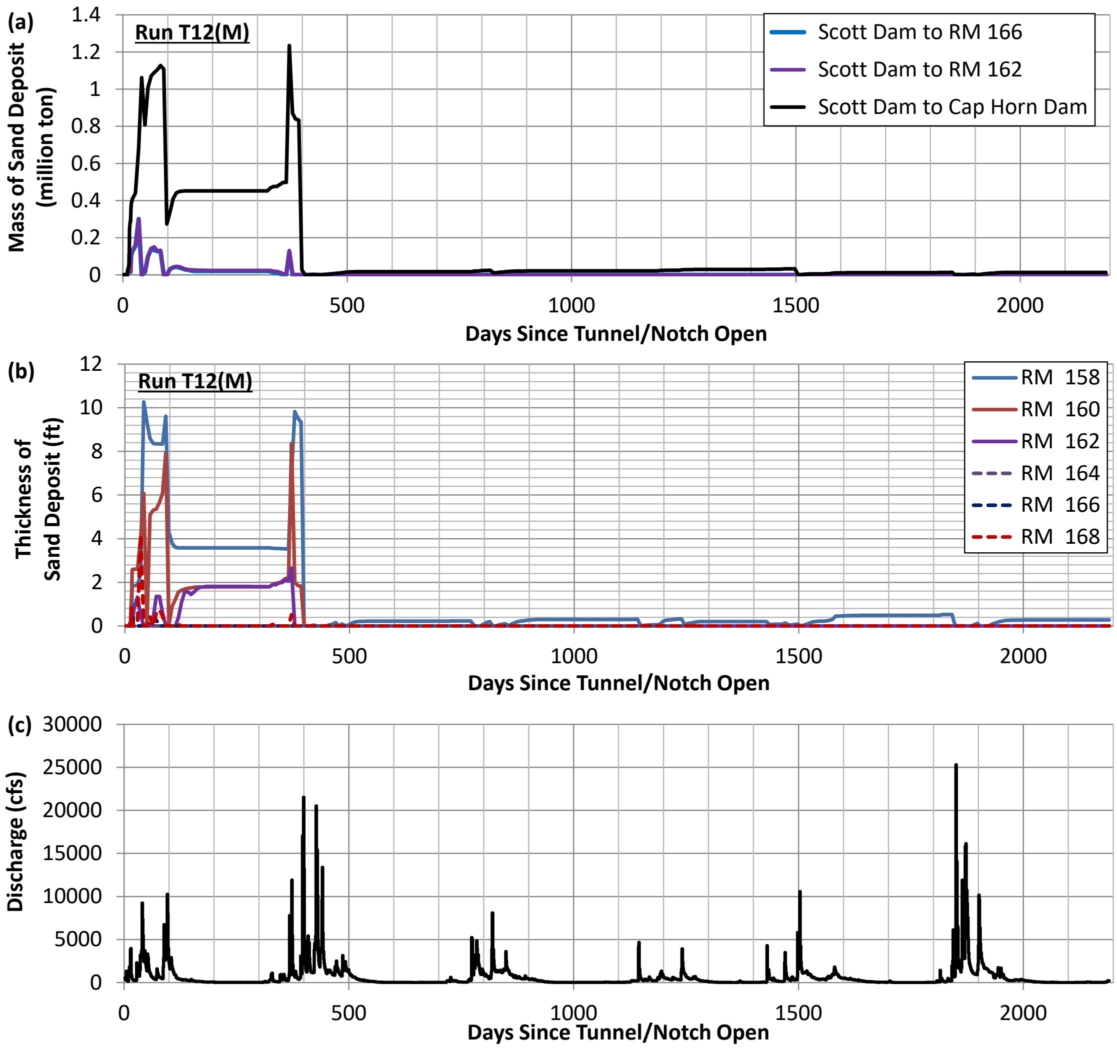

Figure C-28. Simulated mass of sand deposition in selected reaches upstream of Cape Horn Dam (a) and thickness of sand deposition in selected locations upstream of Cape Horn Dam (b), along with water discharge at Scott Dam for reference (c), Run T12(M).

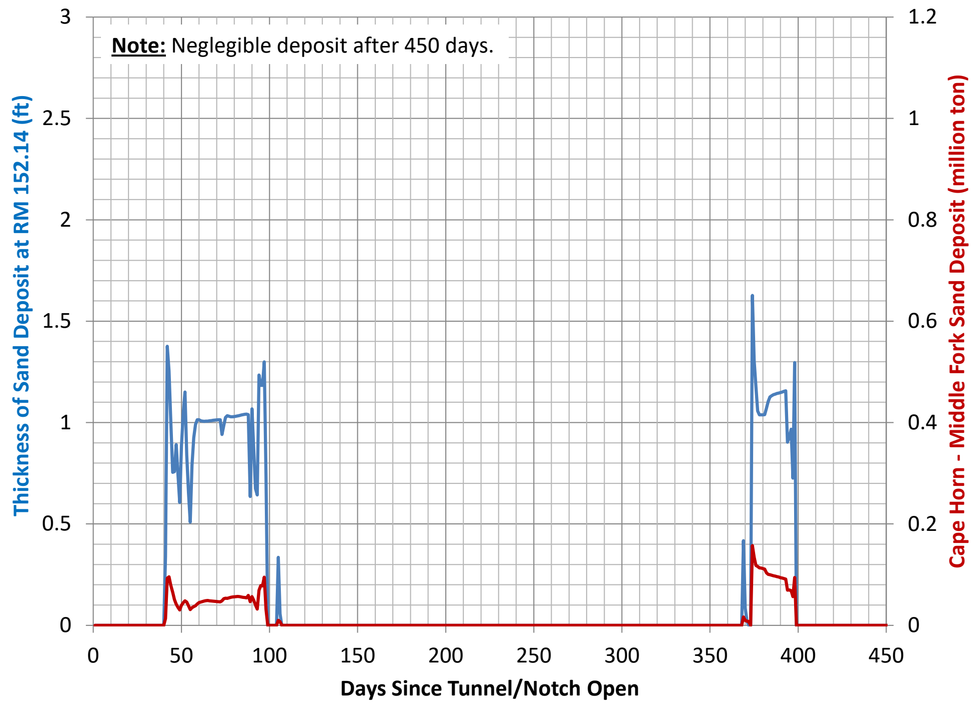

Figure C-29. imulated thickness of sand deposit at the location where maximum sand deposit occurs downstream of Cape Horn Dam (blue line), and mass of sand deposit between Cape Horn Dam and Middle Fork Eel River confluence (red line), Run T12(M).

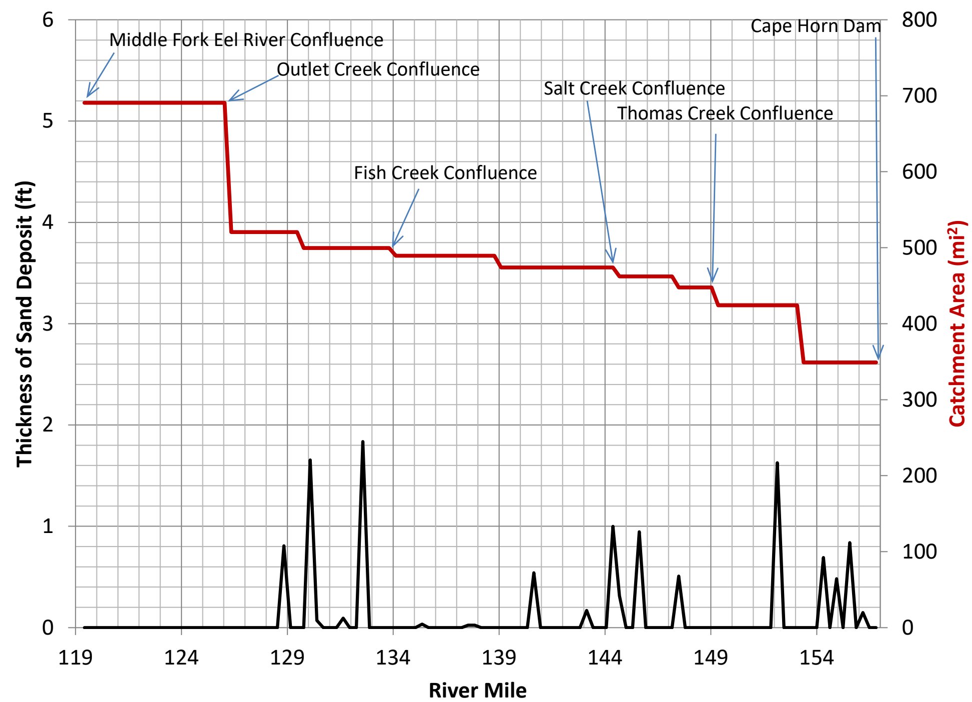

Figure C-30. Simulated thickness of sand deposit between Cape Horn Dam and Middle Fork Eel River confluence on the day maximum sand deposition occurred, Run T12(M). Catchment area and tributary locations are provided for reference.

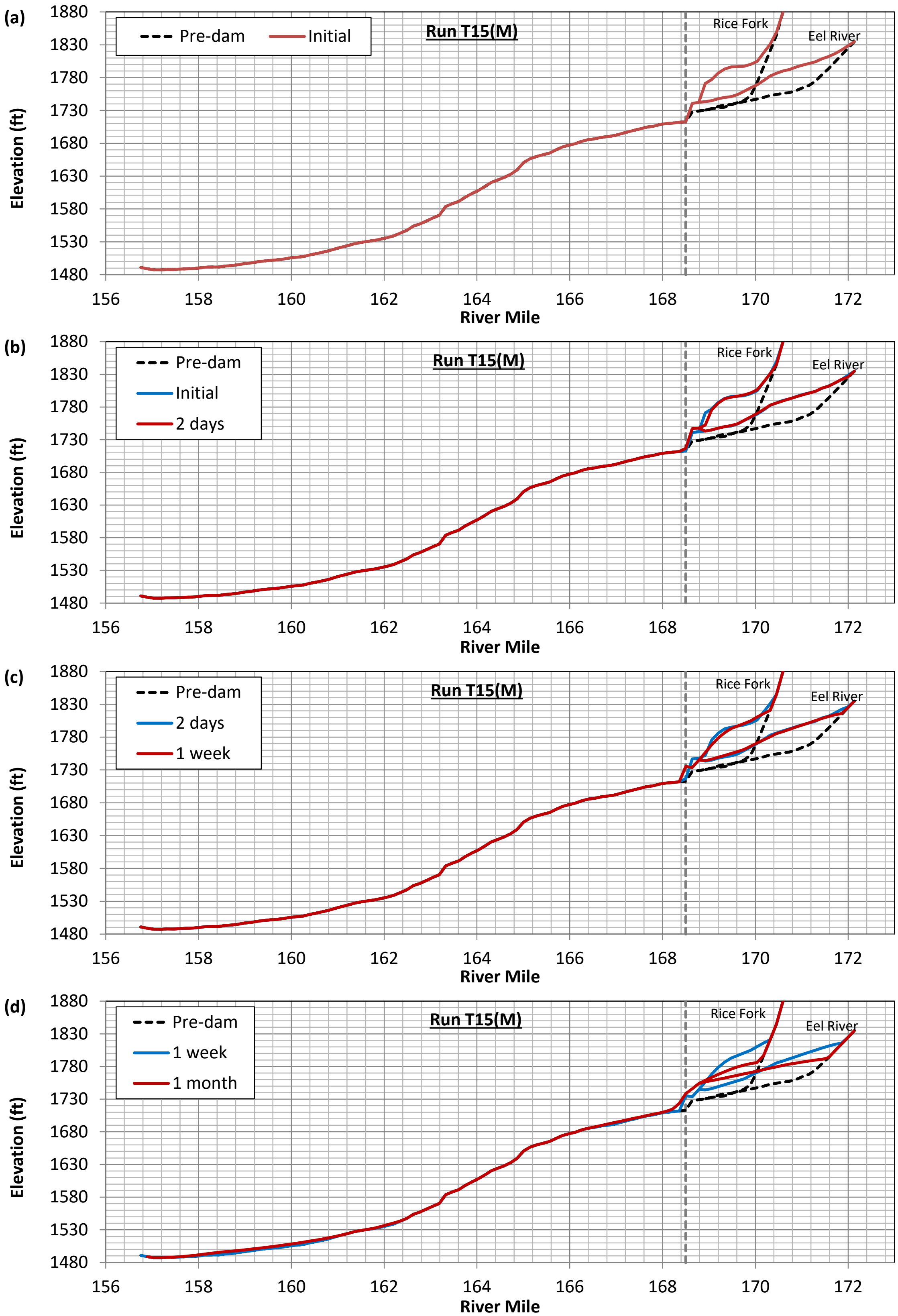

Figure C-31 continues on the next page

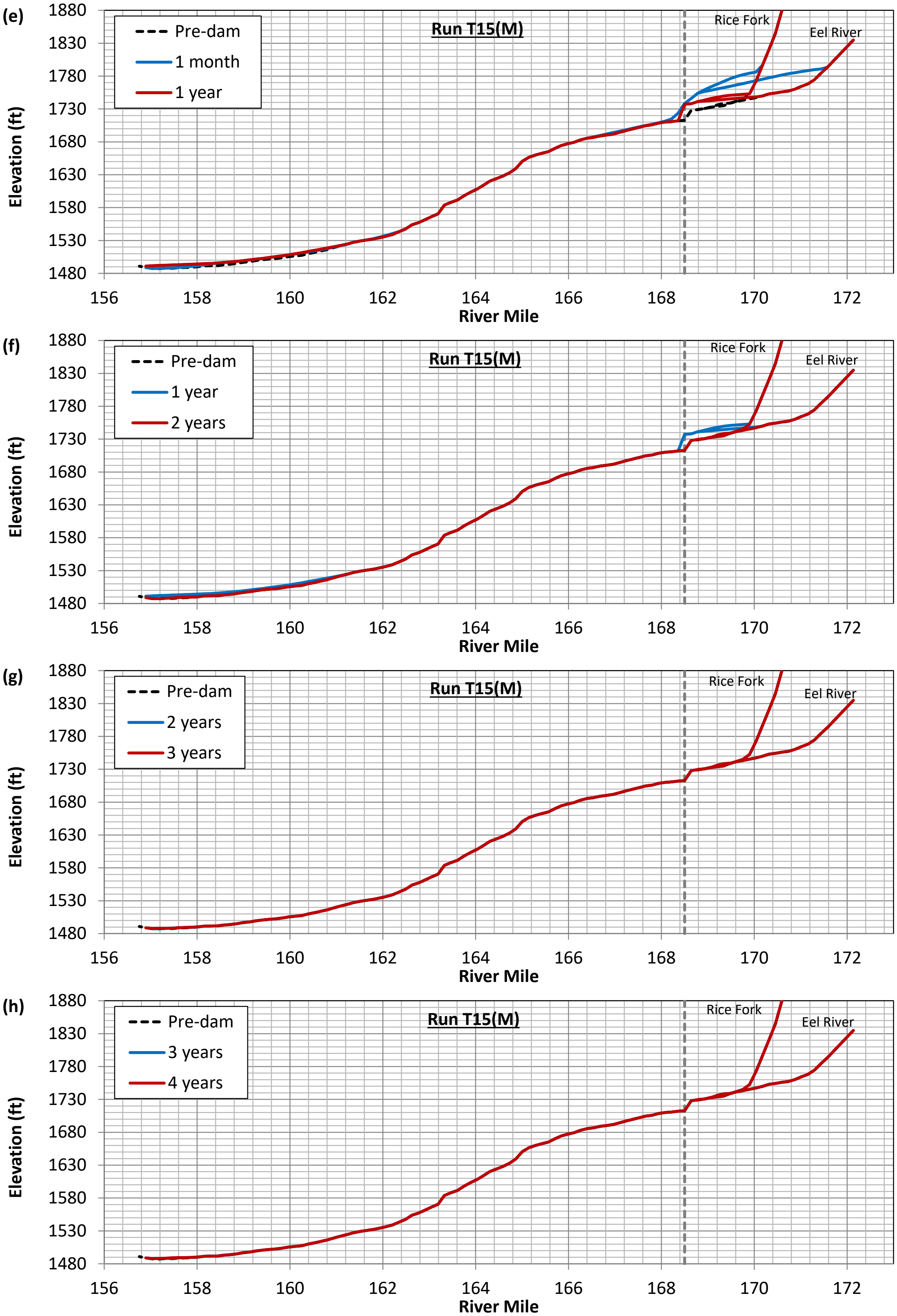

Figure C-31. Bed profile following Scott Dam removal for tunneling alternative with 15 ft tunnel diameter, dam removal starts in a median year [Run T15(M)].

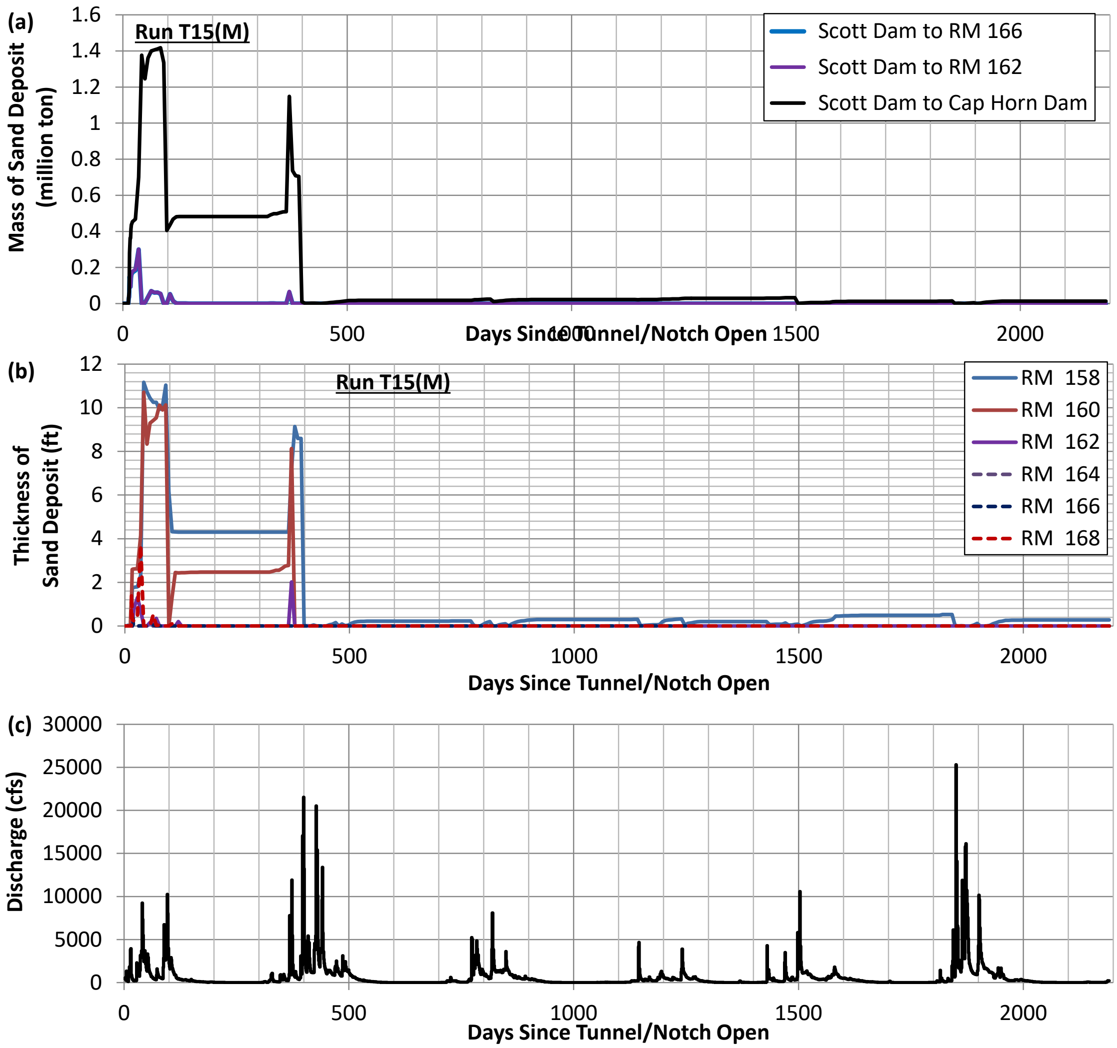

Figure C-32. Simulated mass of sand deposition in selected reaches upstream of Cape Horn Dam (a) and thickness of sand deposition in selected locations upstream of Cape Horn Dam (b), along with water discharge at Scott Dam for reference (c), Run T15(M).

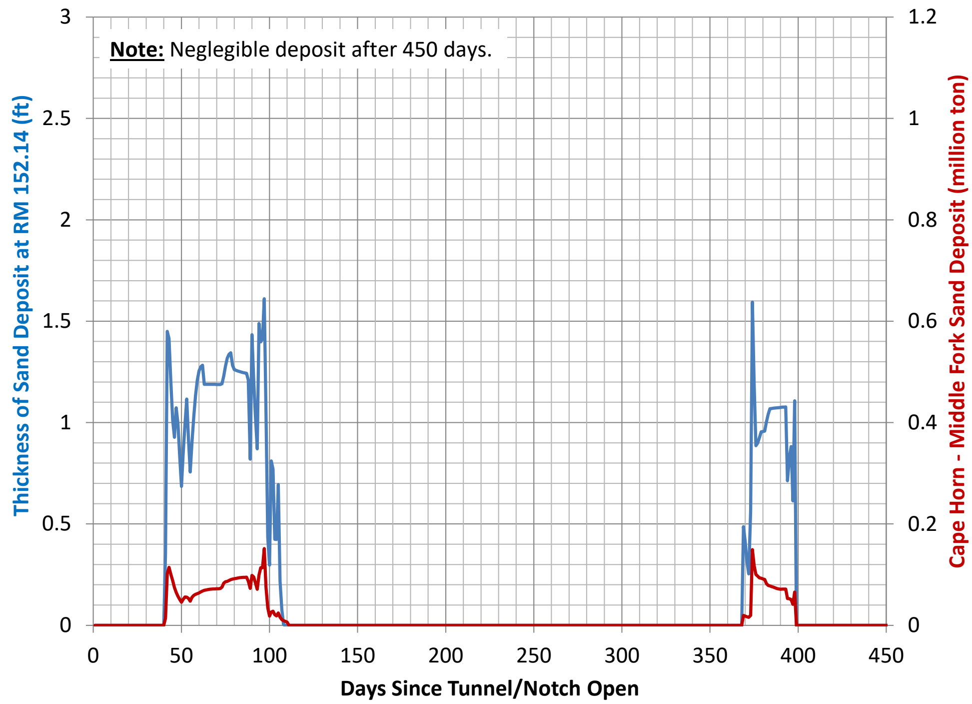

Figure C-33. Simulated thickness of sand deposit at the location where maximum sand deposit occurs downstream of Cape Horn Dam (blue line), and mass of sand deposit between Cape Horn Dam and Middle Fork Eel River confluence (red line), Run T15(M).

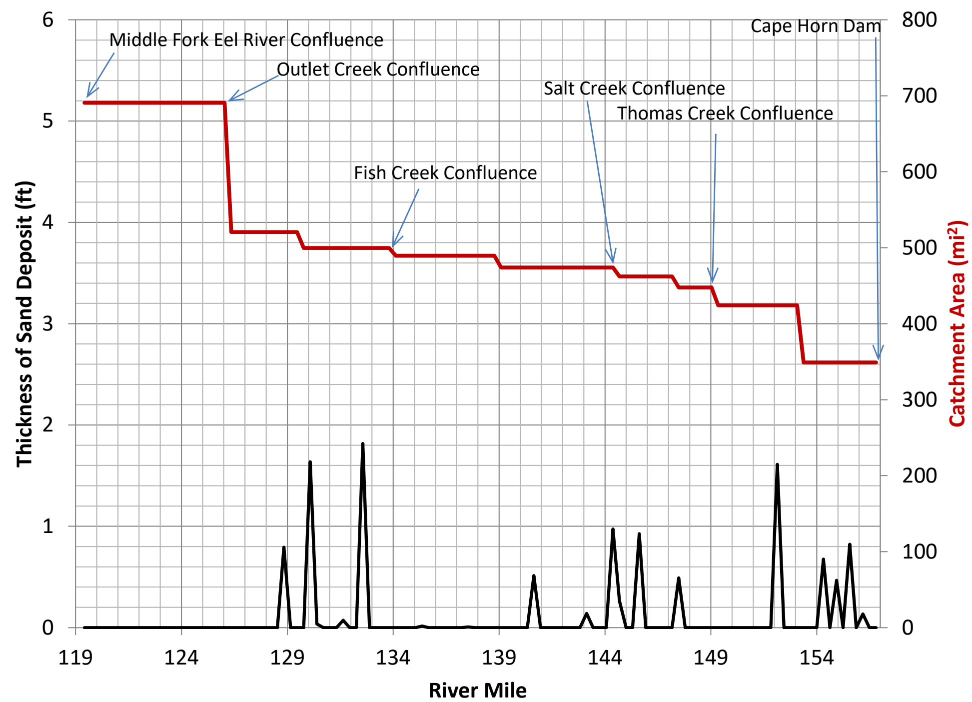

Figure C-34. Simulated thickness of sand deposit between Cape Horn Dam and Middle Fork Eel River confluence on the day maximum sand deposition occurred, Run T15(M). Catchment area and tributary locations are provided for reference.

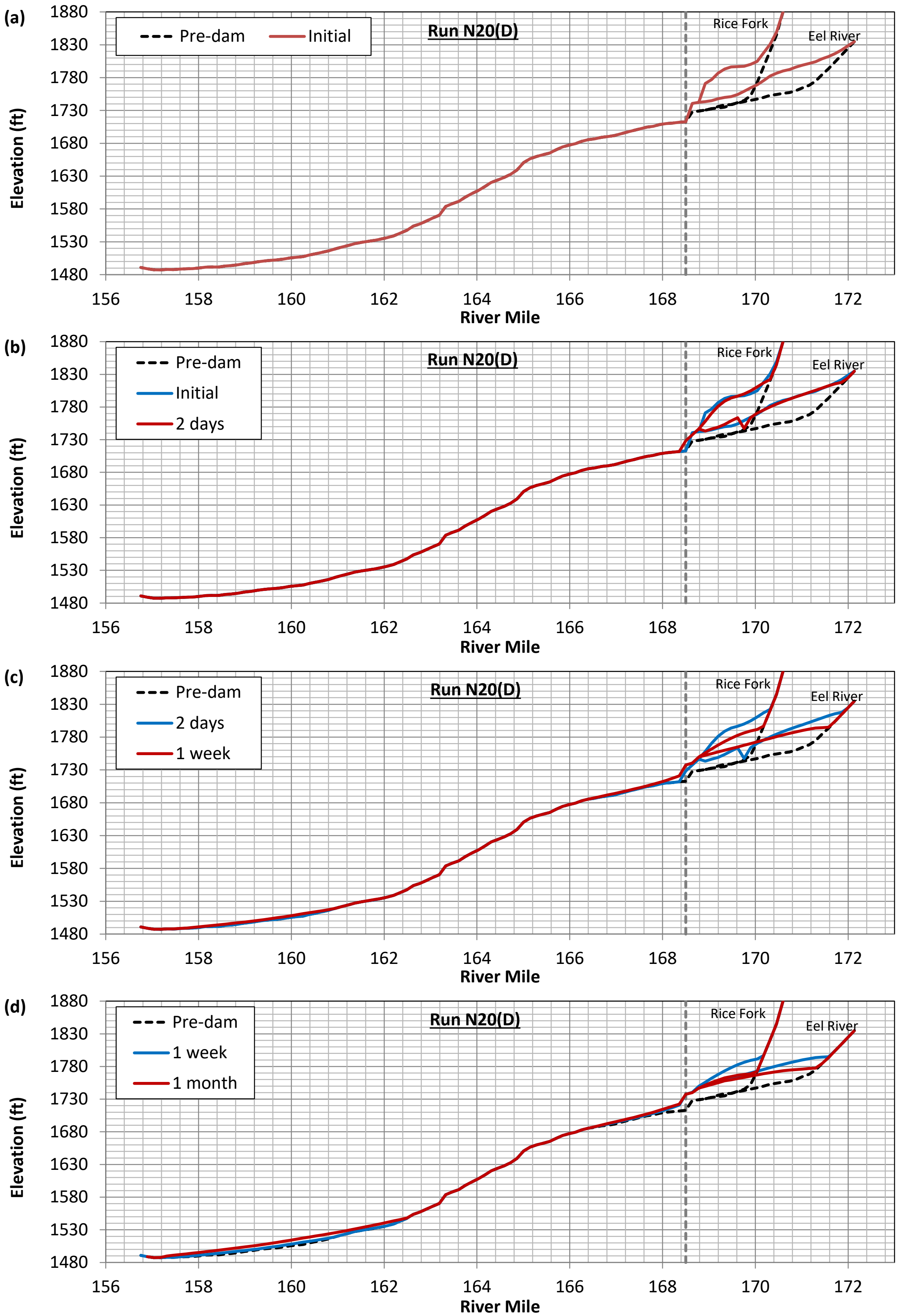

Figure C-35 continues on the next page

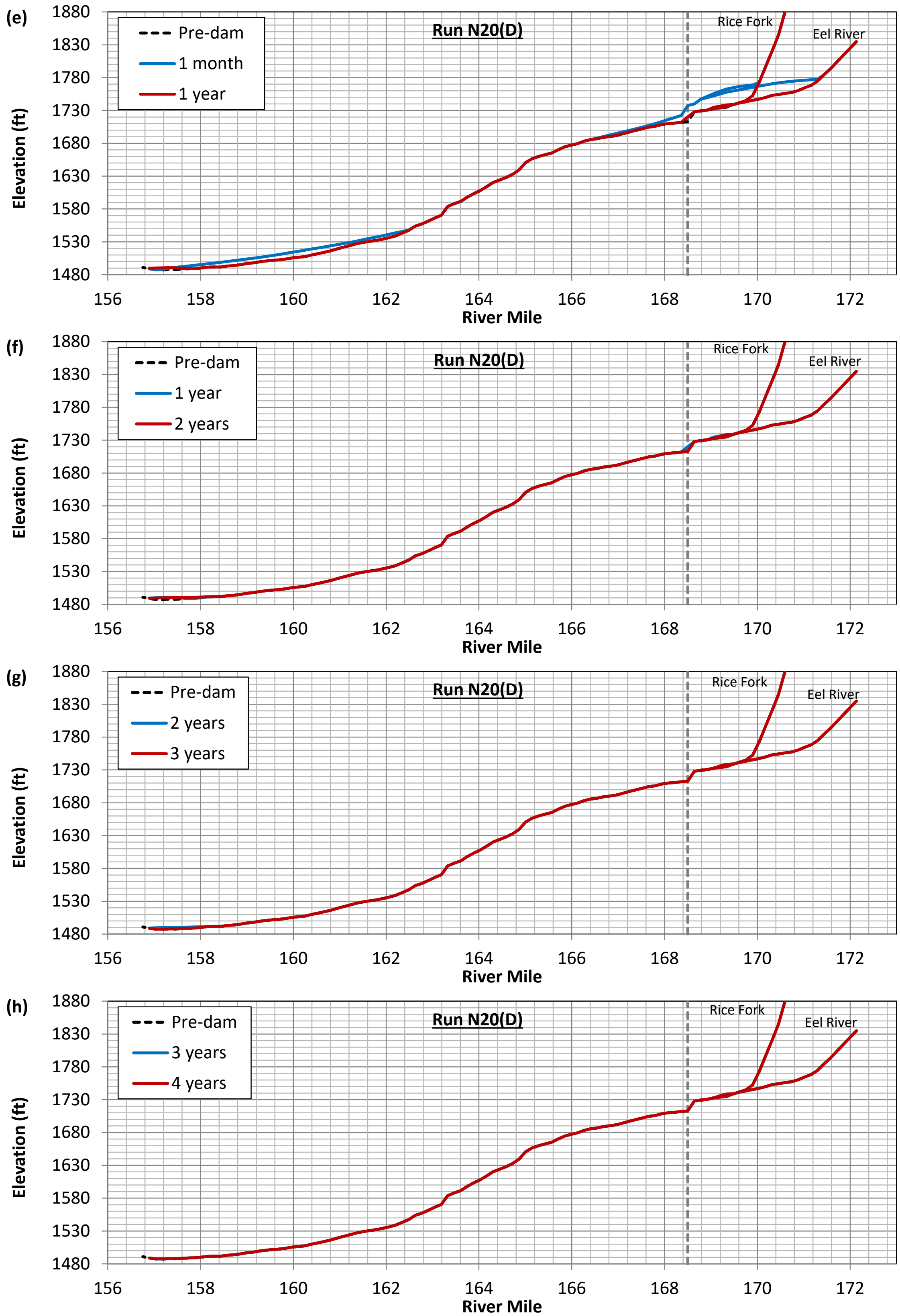

Figure C-35. Bed profile following Scott Dam removal for vertical notching alternative with 20 ft notch width, dam removal starts in a dry year [Run N20(D)].

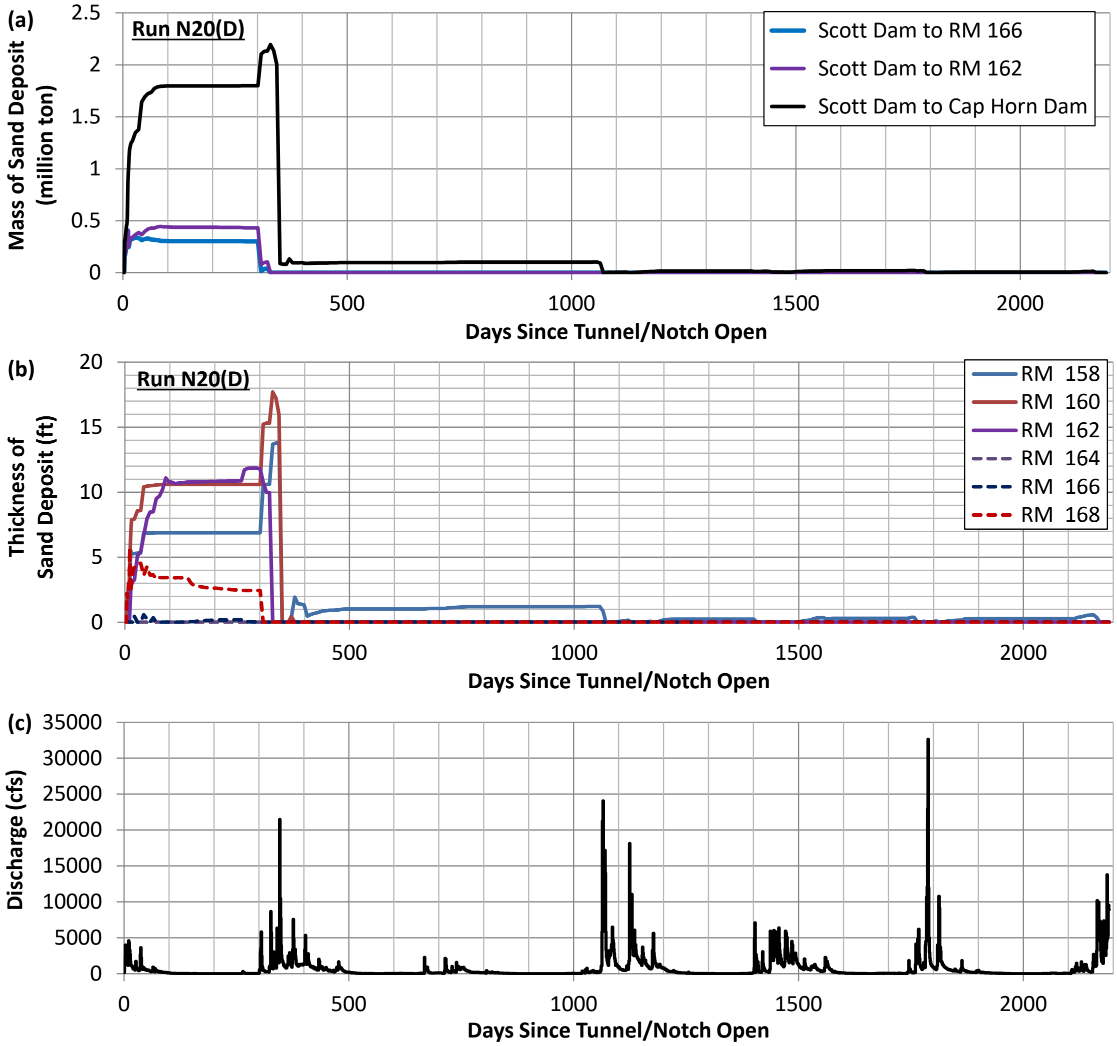

Figure C-36. Simulated mass of sand deposition in selected reaches upstream of Cape Horn Dam (a) and thickness of sand deposition in selected locations upstream of Cape Horn Dam (b), along with water discharge at Scott Dam for reference (c), Run N20(D).

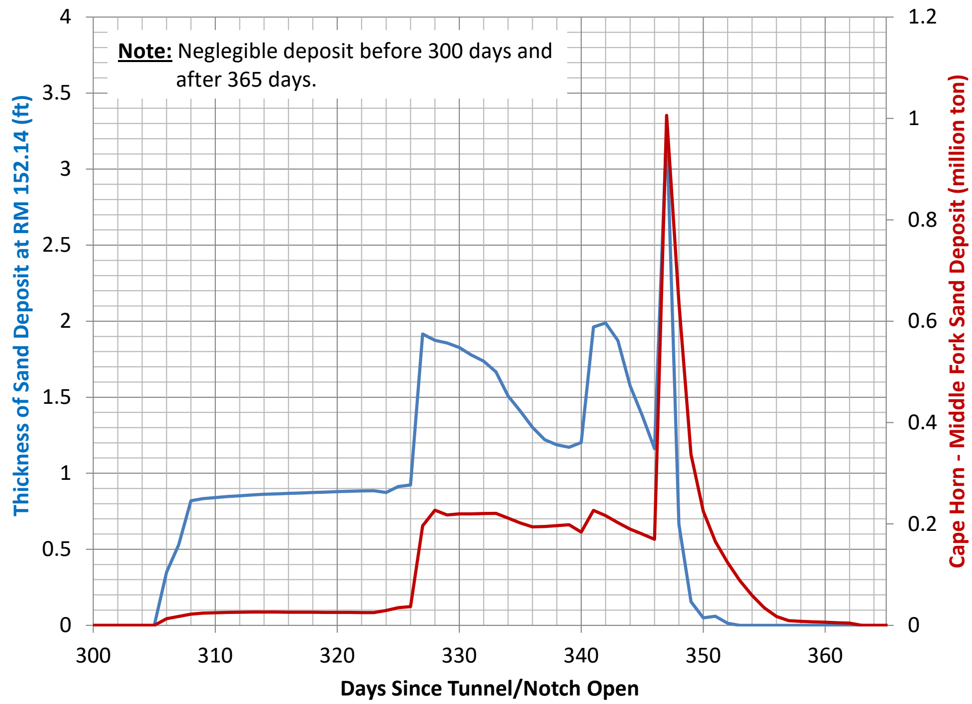

Figure C-37. Simulated thickness of sand deposit at the location where maximum sand deposit occurs downstream of Cape Horn Dam (blue line), and mass of sand deposit between Cape Horn Dam and Middle Fork Eel River confluence (red line), Run N20(D).

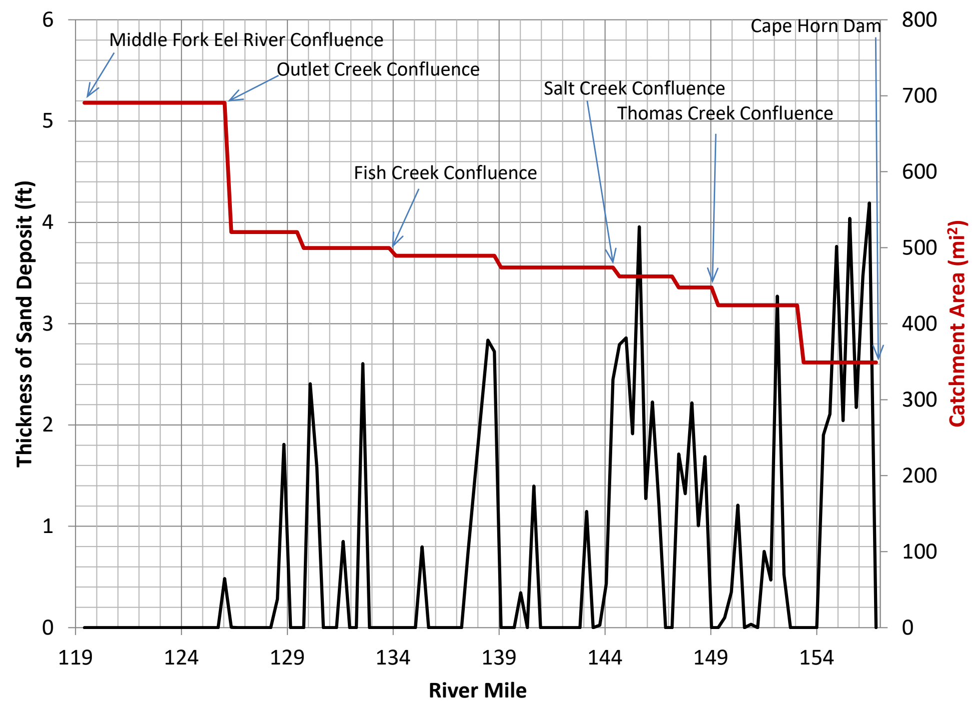

Figure C-38. Simulated thickness of sand deposit between Cape Horn Dam and Middle Fork Eel River confluence on the day maximum sand deposition occurred, Run N20(D). Catchment area and tributary locations are provided for reference.

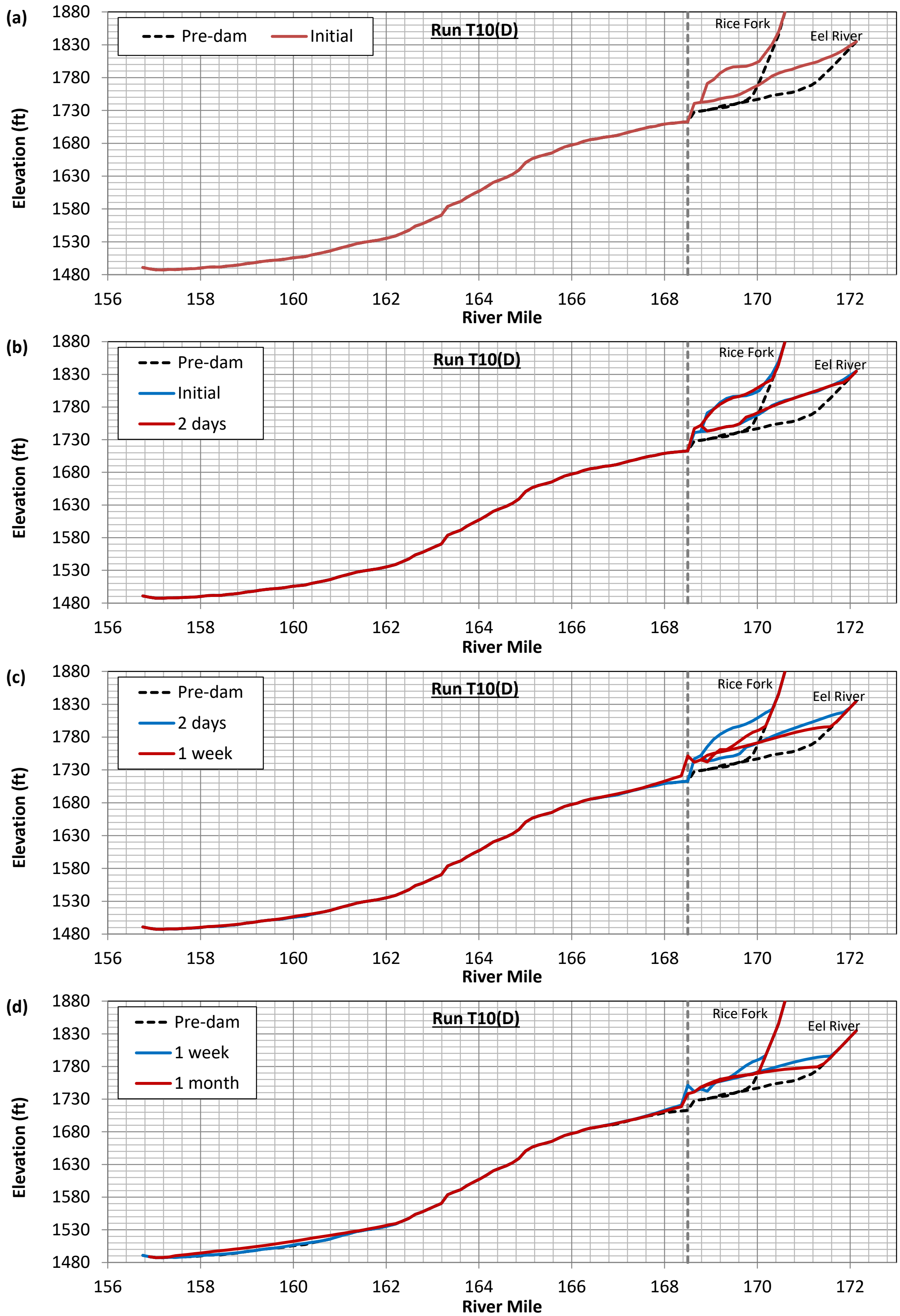

Figure C-39 continues on the next page

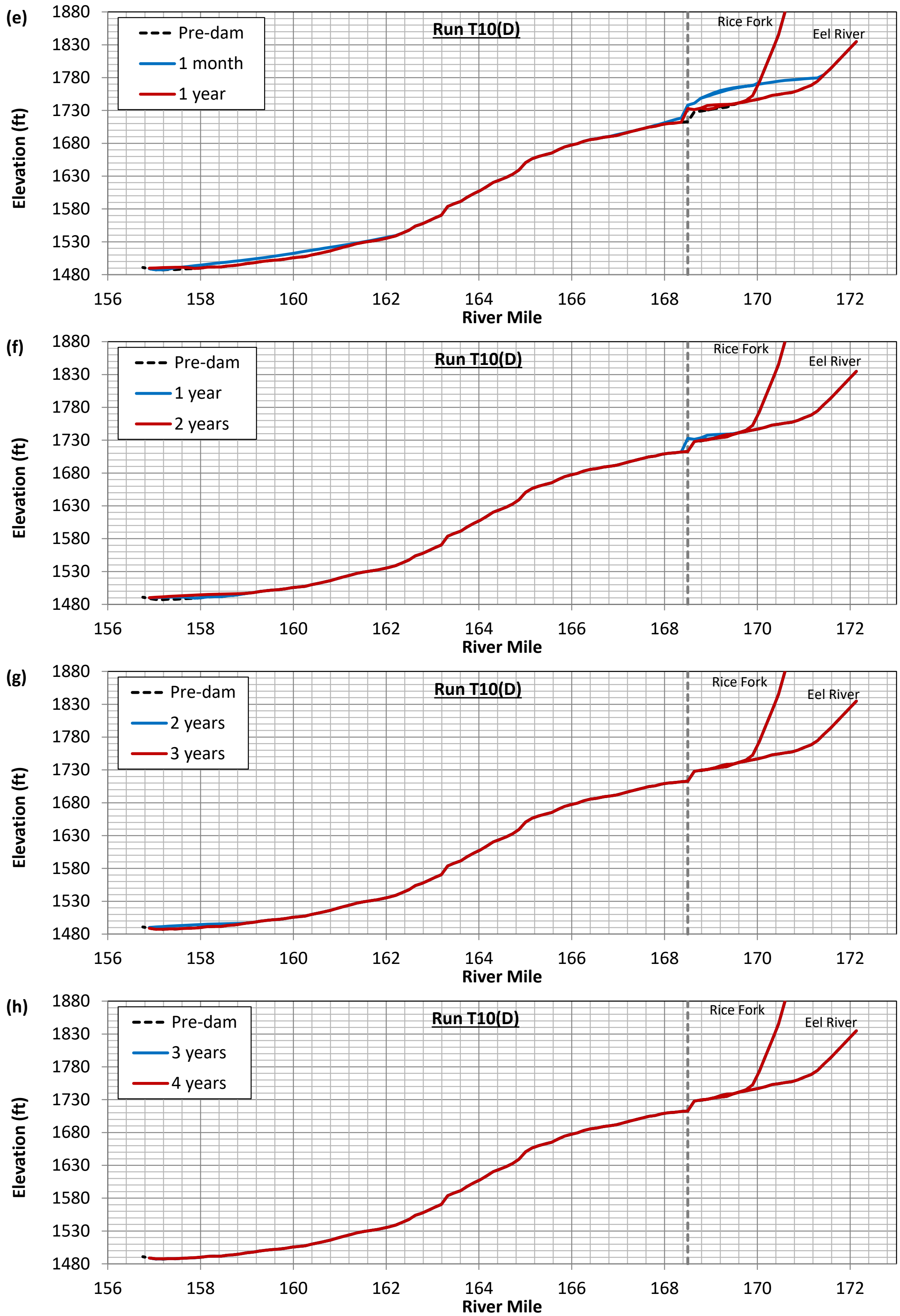

Figure C-39. Bed profile following Scott Dam removal for tunneling alternative with 10 ft tunnel diameter, dam removal starts in a dry year [Run T10(D)].

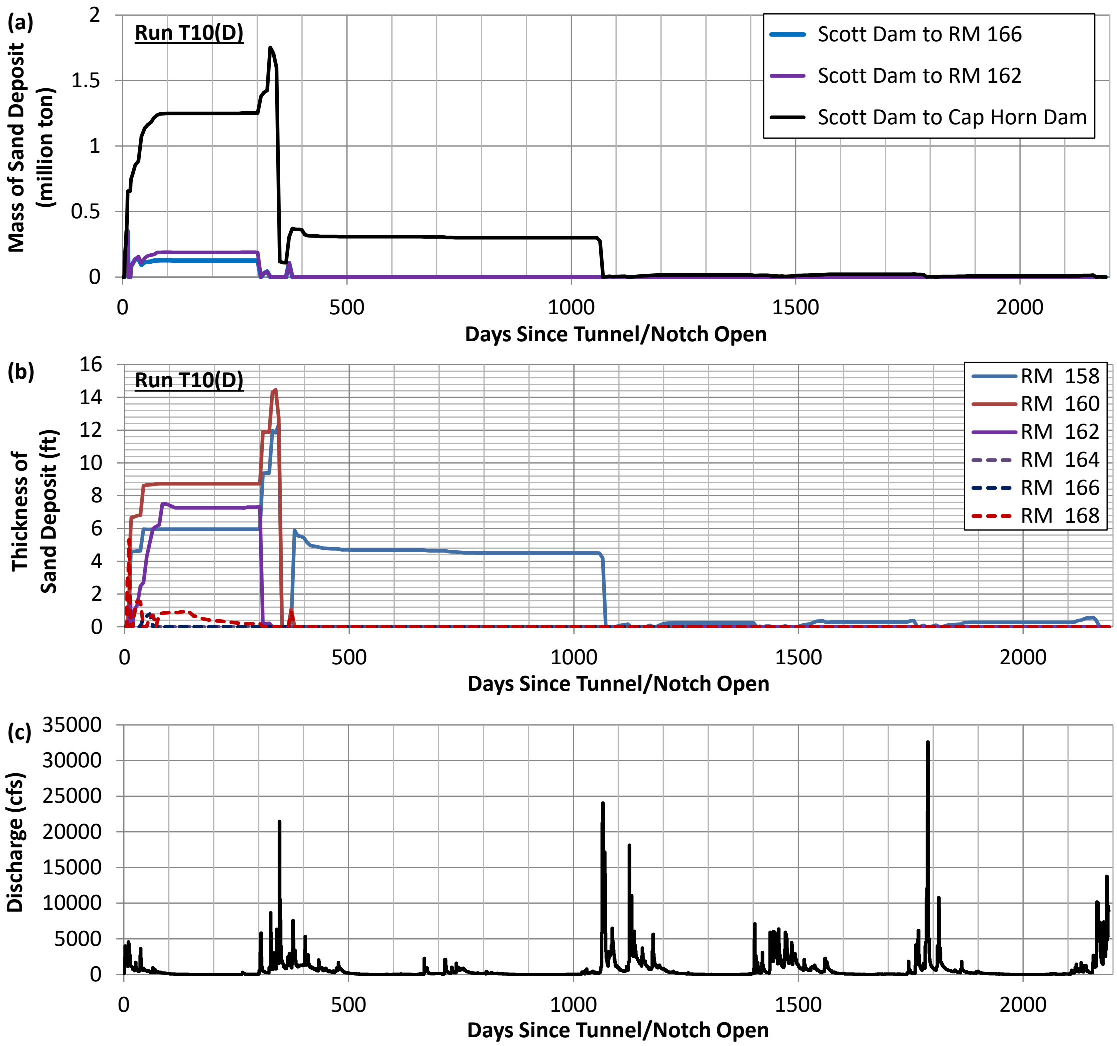

Figure C-40. Simulated mass of sand deposition in selected reaches upstream of Cape Horn Dam (a) and thickness of sand deposition in selected locations upstream of Cape Horn Dam (b), along with water discharge at Scott Dam for reference (c), Run T10(D).

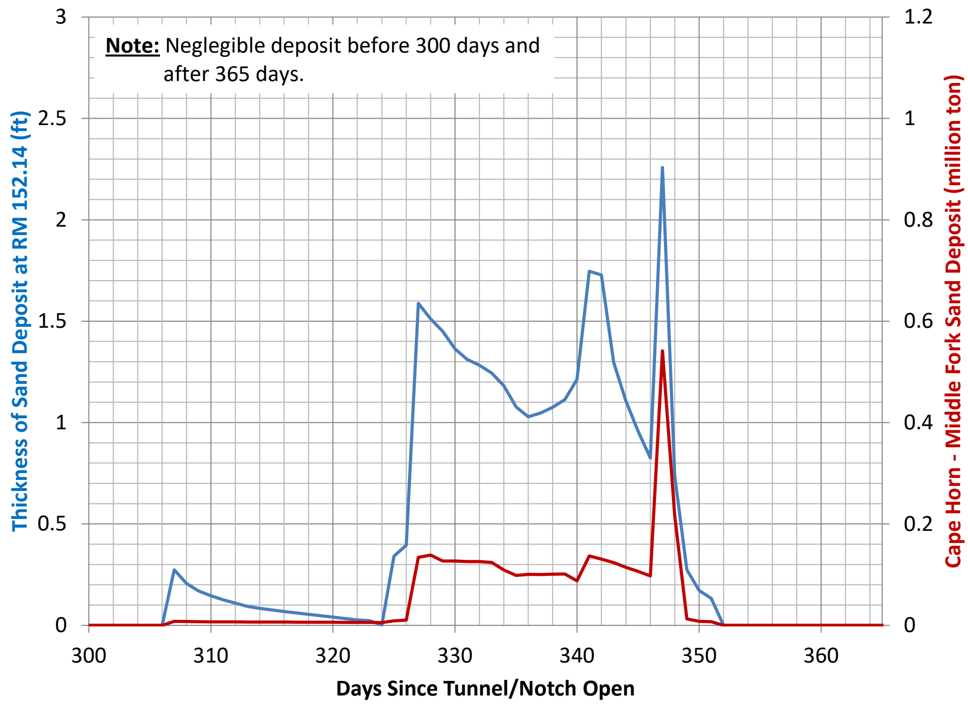

Figure C-41. Simulated thickness of sand deposit at the location where maximum sand deposit occurs downstream of Cape Horn Dam (blue line), and mass of sand deposit between Cape Horn Dam and Middle Fork Eel River confluence (red line), Run T10(D).

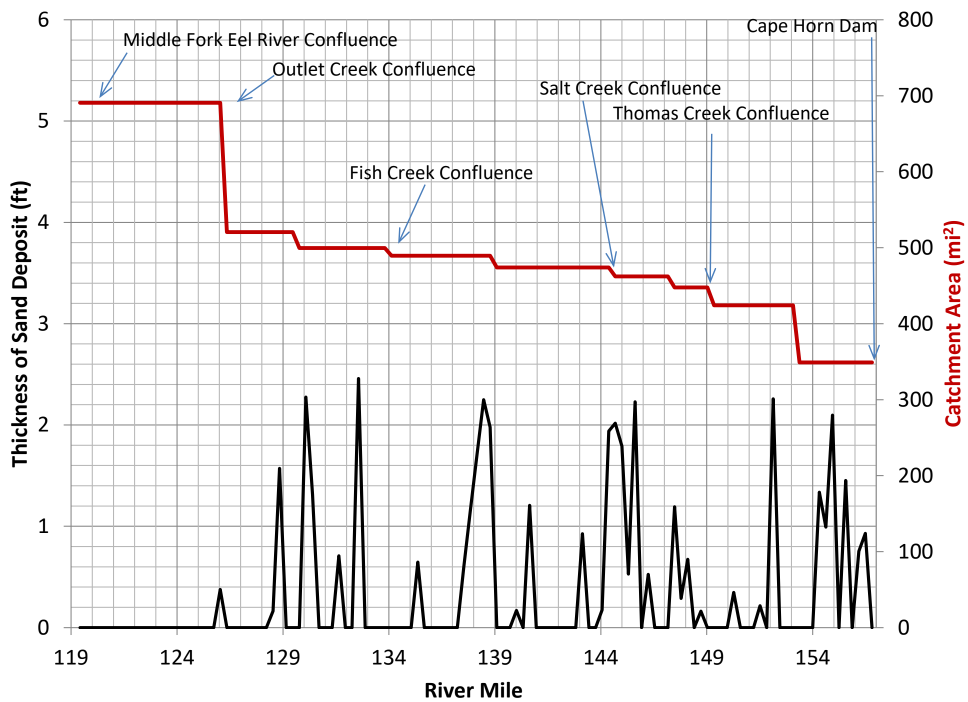

Figure C-42. Simulated thickness of sand deposit between Cape Horn Dam and Middle Fork Eel River confluence on the day maximum sand deposition occurred, Run T10(D). Catchment area and tributary locations are provided for reference.

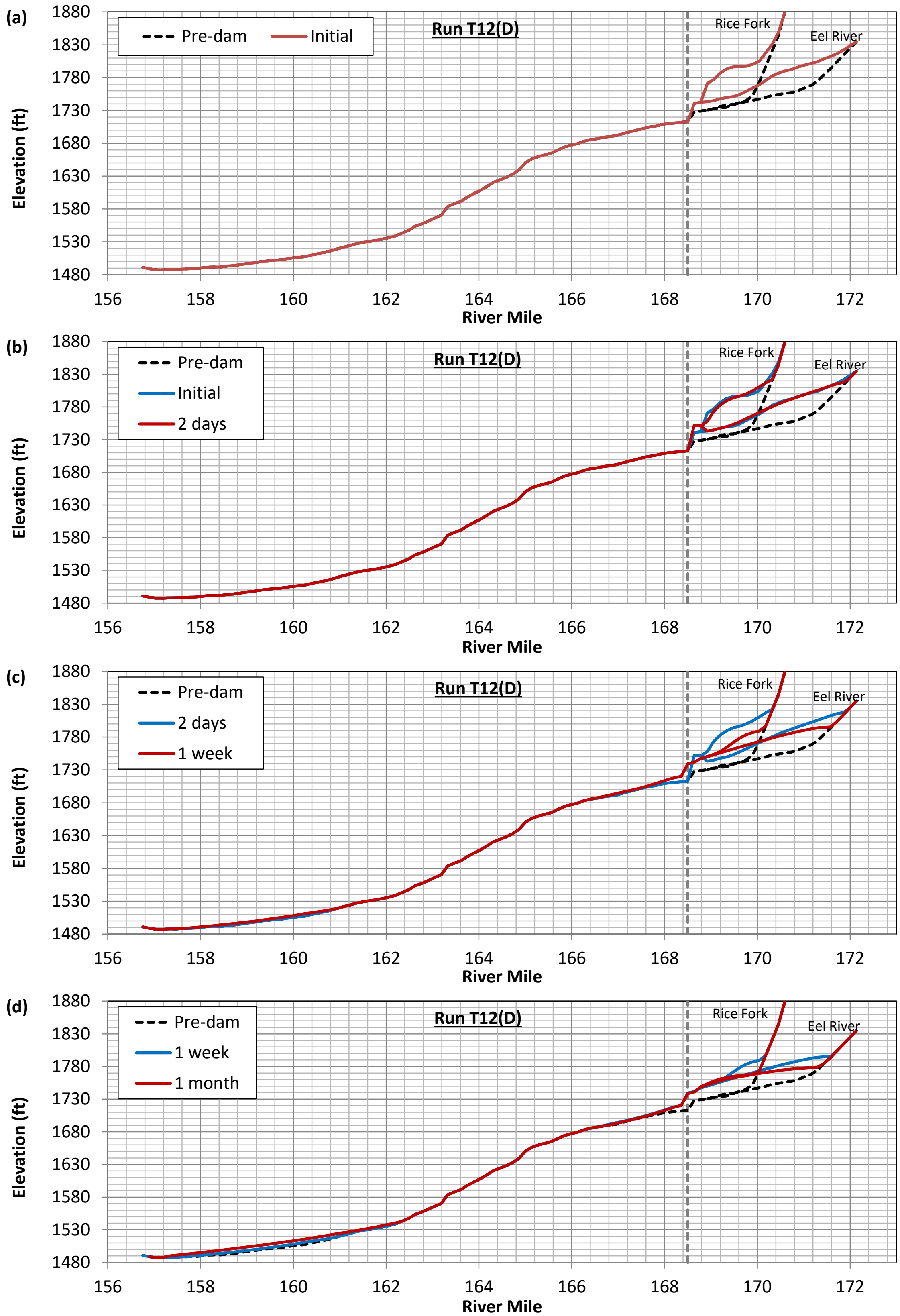

Figure C-43 continues on the next page

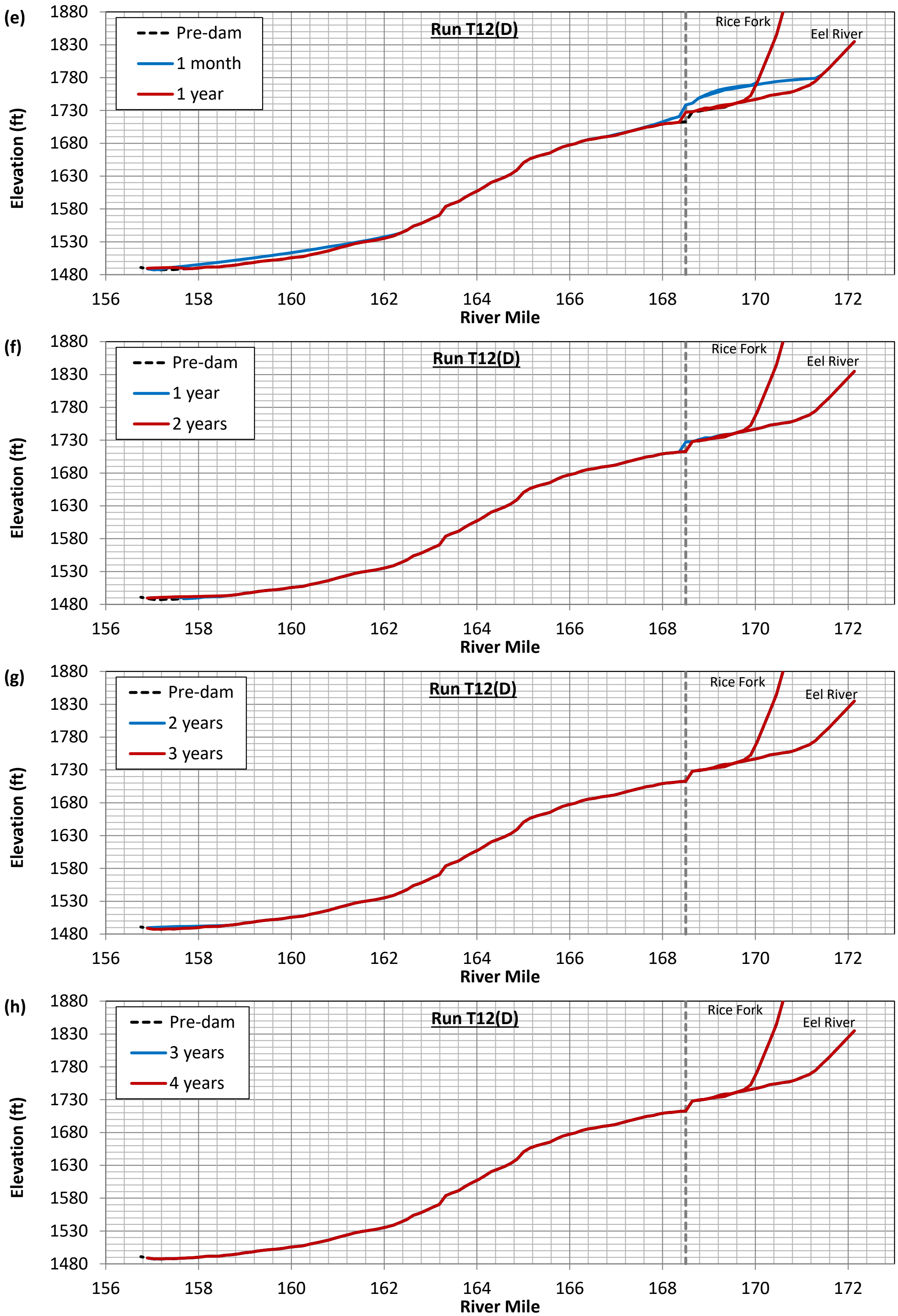

Figure C-43. Simulated profile following Scott Dam removal for tunneling alternative with 12 ft tunnel diameter, dam removal starts in a dry year [Run T12(D)].

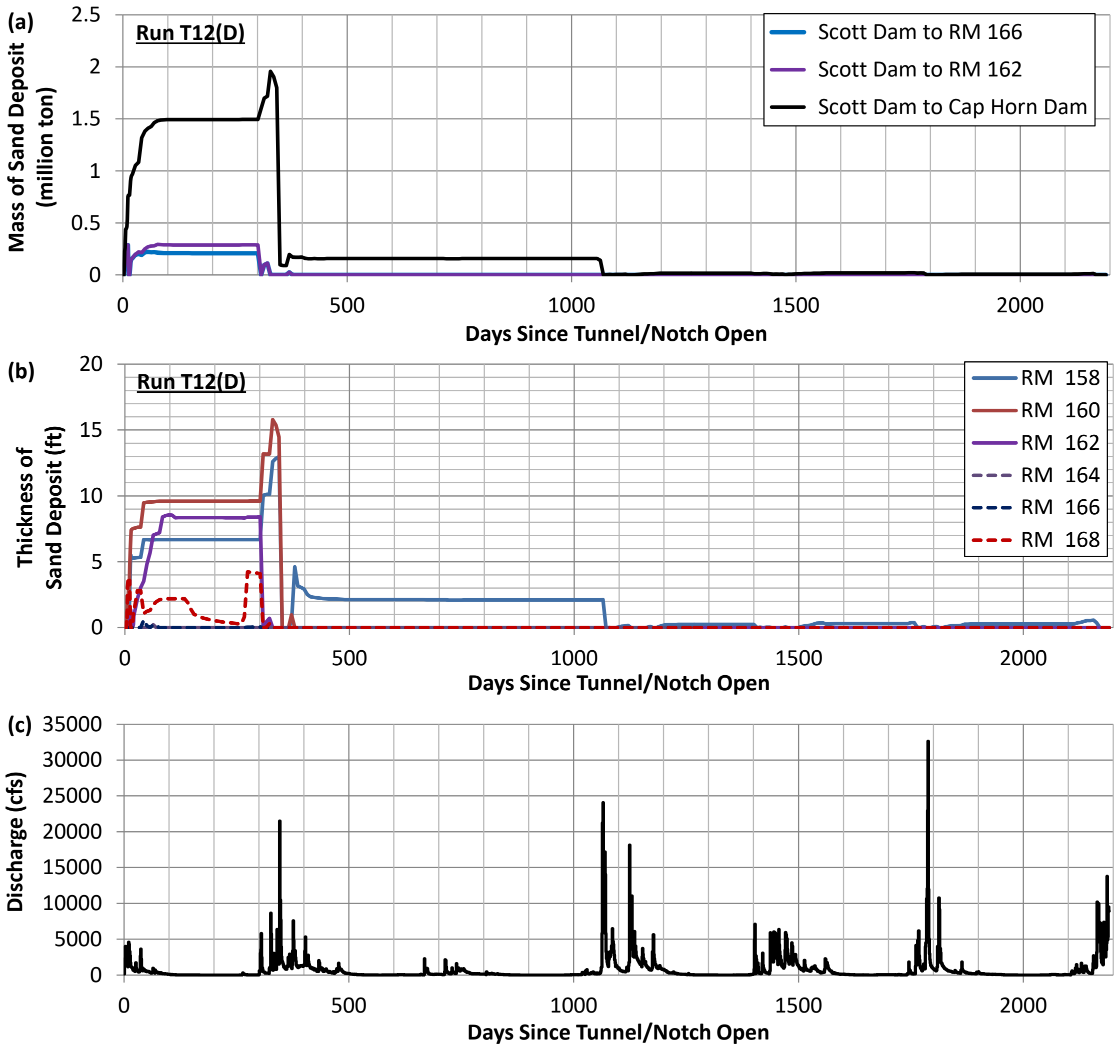

Figure C-44. Simulated mass of sand deposition in selected reaches upstream of Cape Horn Dam (a) and thickness of sand deposition in selected locations upstream of Cape Horn Dam (b), along with water discharge at Scott Dam for reference (c), Run T12(D).

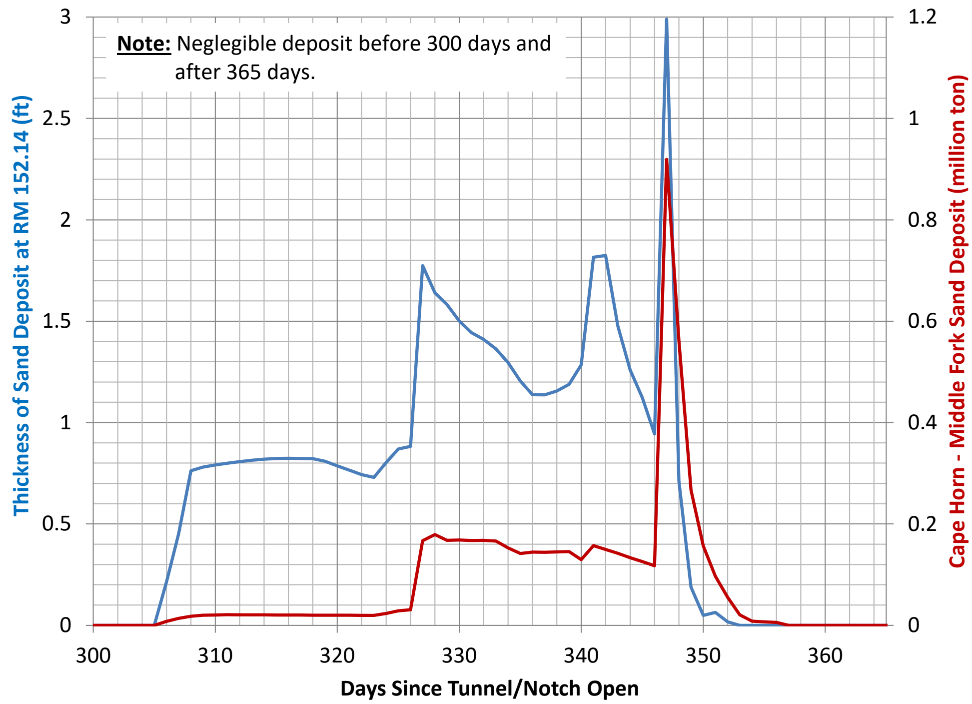

Figure C-45. Simulated thickness of sand deposit at the location where maximum sand deposit occurs downstream of Cape Horn Dam (blue line), and mass of sand deposit between Cape Horn Dam and Middle Fork Eel River confluence (red line), Run T12(D).

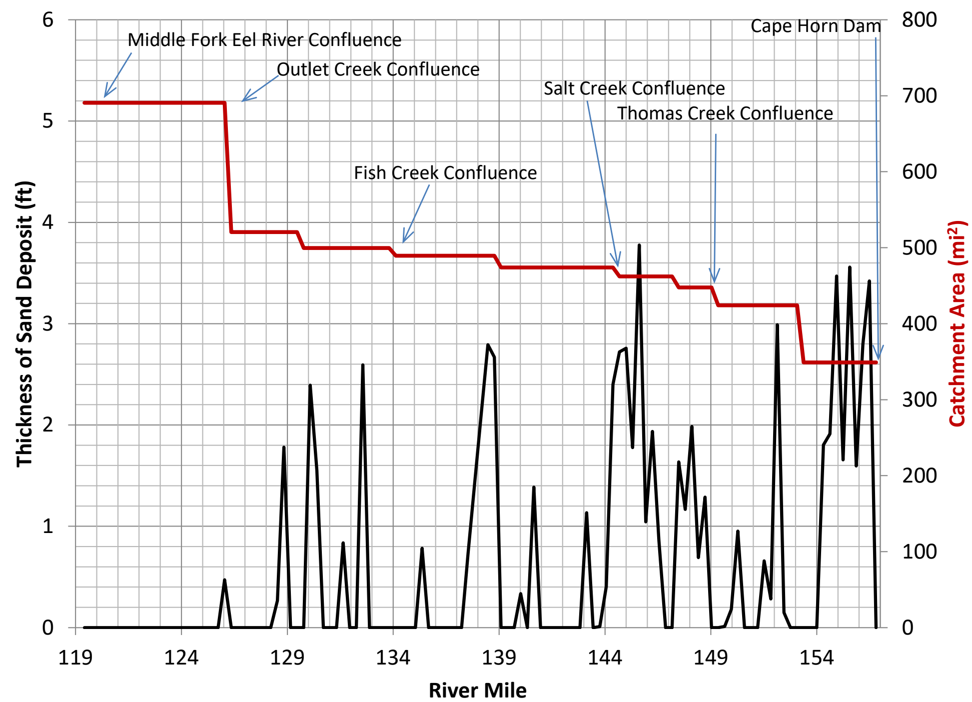

Figure C-46. Simulated thickness of sand deposit between Cape Horn Dam and Middle Fork Eel River confluence on the day maximum sand deposition occurred, Run T12(D). Catchment area and tributary locations are provided for reference.

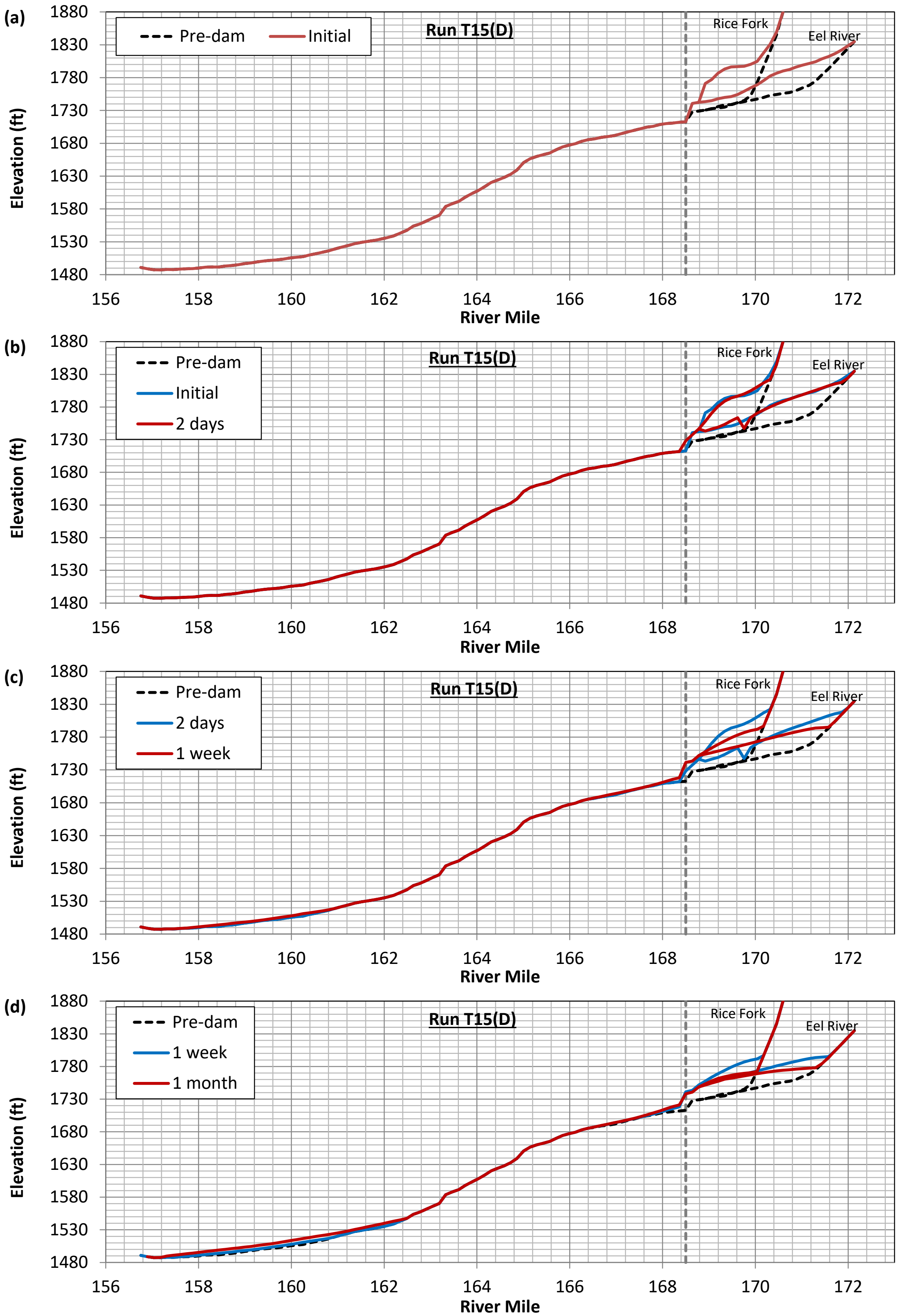

Figure C-47 continues on the next page

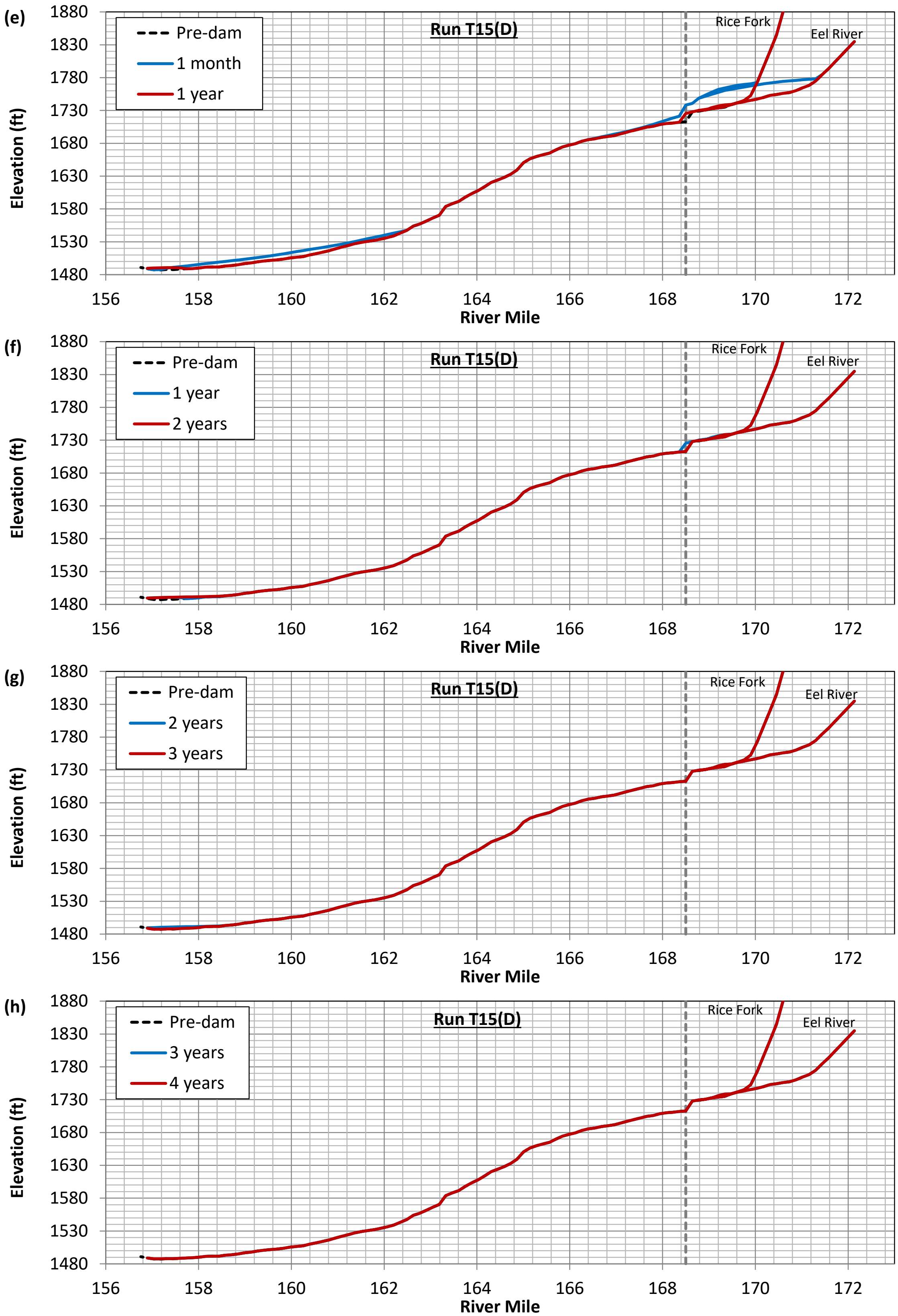

Figure C-47. Bed profile following Scott Dam removal for tunneling alternative with 15 ft tunnel diameter, dam removal starts in a dry year.

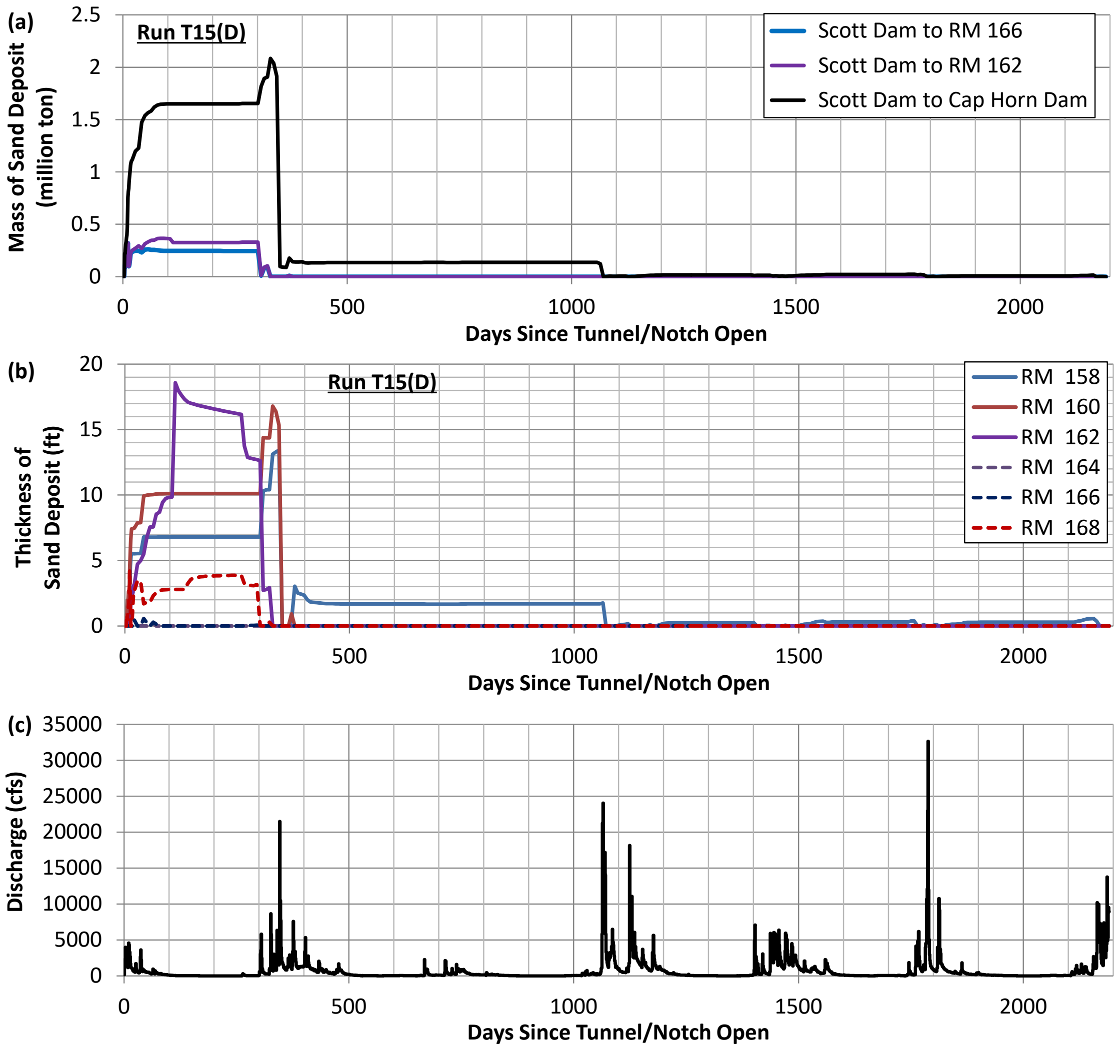

Figure C-48. Simulated mass of sand deposition in selected reaches upstream of Cape Horn Dam (a) and thickness of sand deposition in selected locations upstream of Cape Horn Dam (b), along with water discharge at Scott Dam for reference (c), Run T15(D).

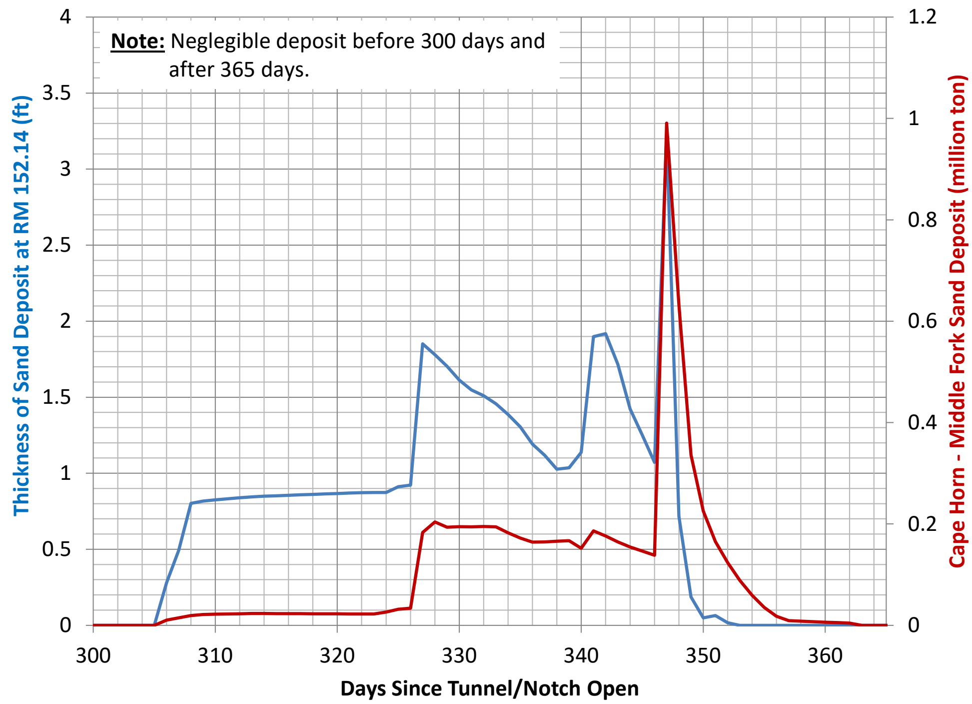

Figure C-49. Simulated thickness of sand deposit at the location where maximum sand deposit occurs downstream of Cape Horn Dam (blue line), and mass of sand deposit between Cape Horn Dam and Middle Fork Eel River confluence (red line), Run T15(D).

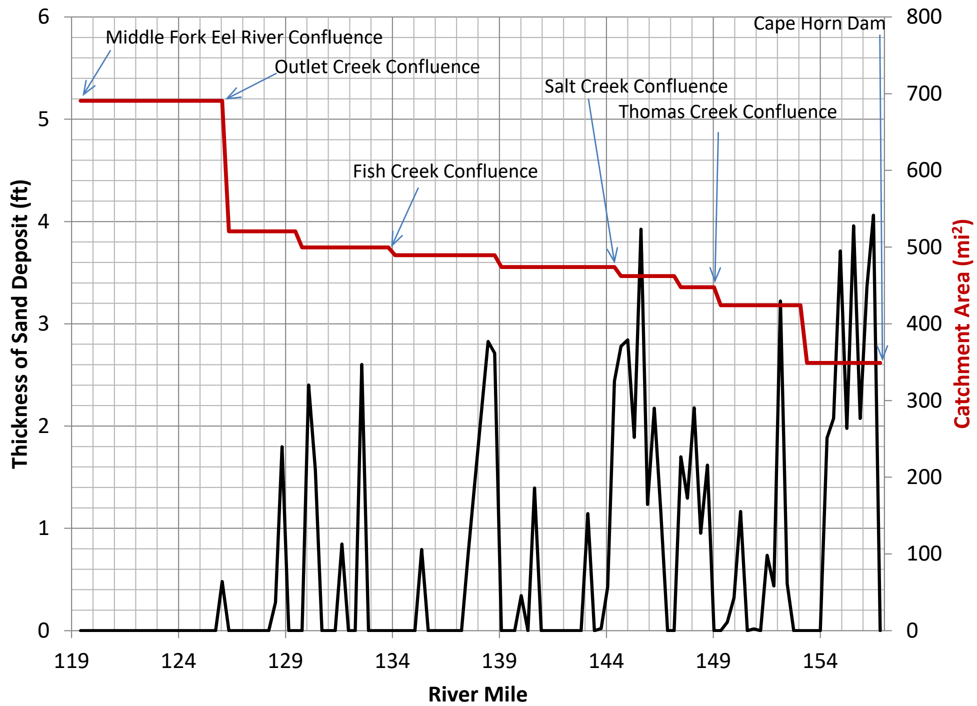

Figure C-50. Simulated thickness of sand deposit between Cape Horn Dam and Middle Fork Eel River confluence on the day maximum sand deposition occurred, Run T15(D). Catchment area and tributary locations are provided for reference.

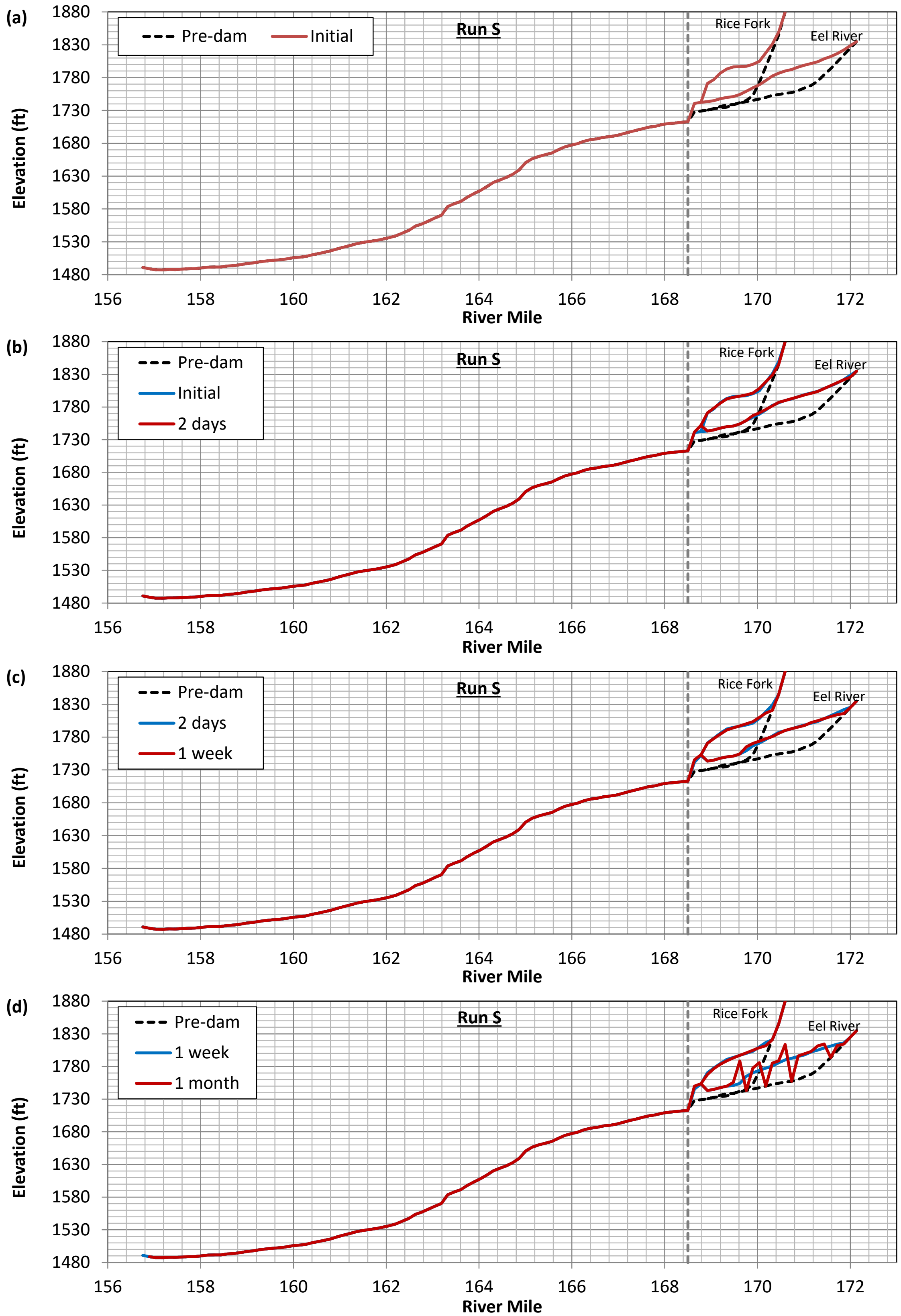

Figure C-51 continues on the next page

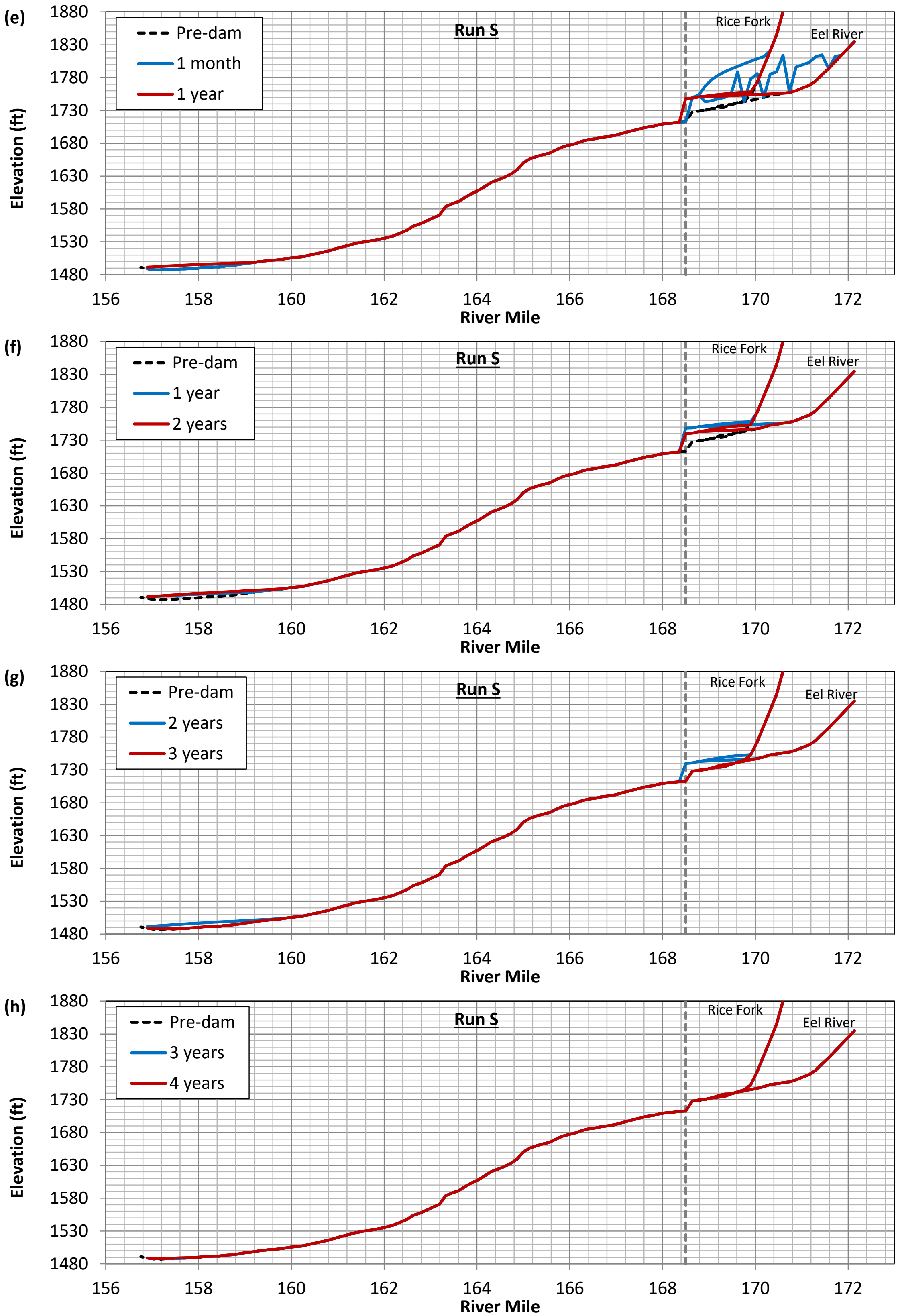

Figure C-51. Bed profile following Scott Dam removal for staged removal alternative (Run S). Day 0 of the simulation is the day the second stage removal started.

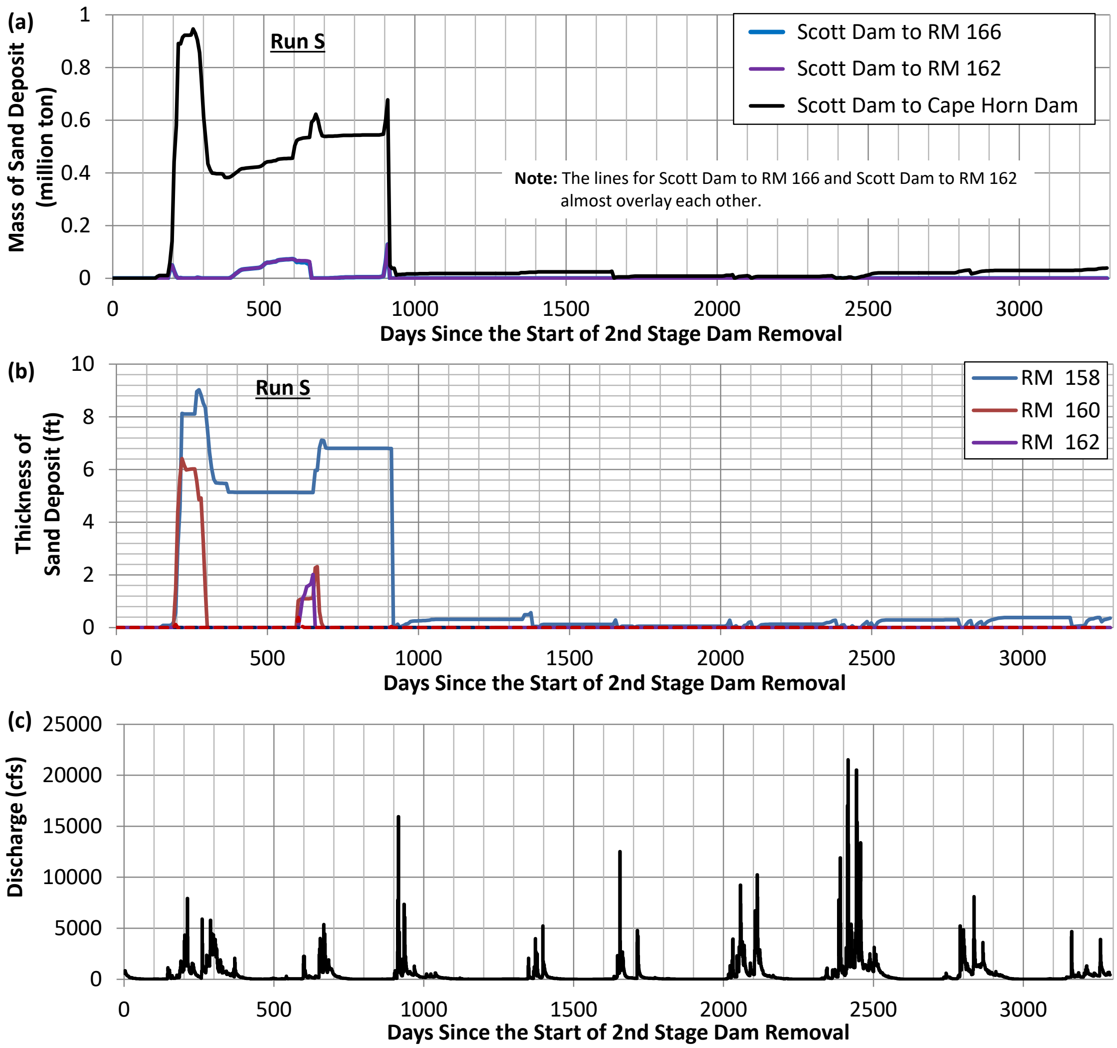

Figure C-52. Simulated mass of sand deposition in selected reaches upstream of Cape Horn Dam (a) and thickness of sand deposition in selected locations upstream of Cape Horn Dam (b), along with water discharge at Scott Dam for reference (c), Run S.

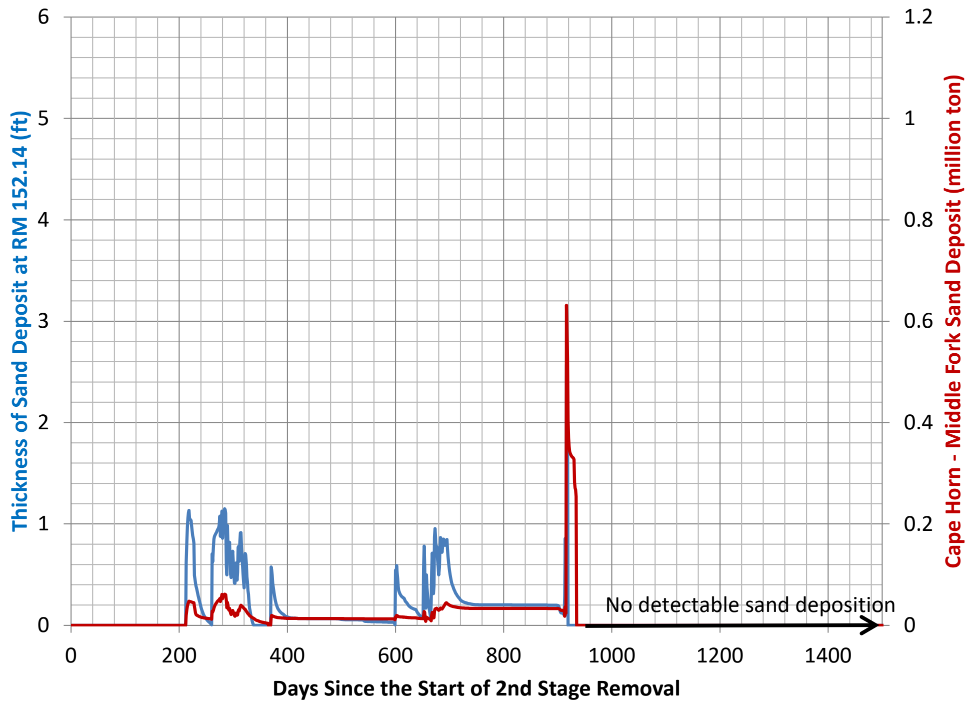

Figure C-53. Simulated thickness of sand deposit at the location where maximum sand deposit occurs downstream of Cape Horn Dam (blue line), and mass of sand deposit between Cape Horn Dam and Middle Fork Eel River confluence (red line), Run S.

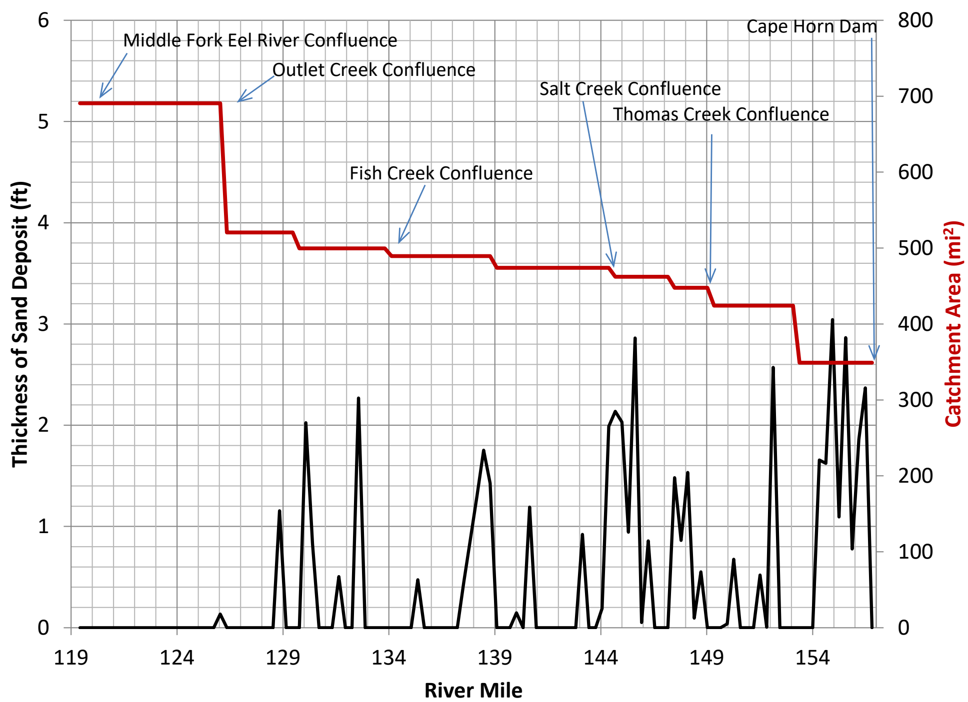

Figure C-54. Simulated thickness of sand deposit between Cape Horn Dam and Middle Fork Eel River confluence on the day maximum sand deposition occurred, Run S. Catchment area and tributary locations are provided for reference.